信州大学審査学位論文

Development of Functional Polyvinyl Alcohol Nanofibers by Electrospinning Technology

Interdisciplinary Graduate School of Science and Technology

(Department of Bioscience and Textile Technology)

Shinshu University

March 2012

LIU FAN

Contents

Abstract

Polyvinyl alcohol (PVA) is an important water-soluble synthetic polymer produced industrially by the hydrolysis of polyvinyl acetate. Electrospinning is a relatively simple and inexpensive method to produce fibers with diameters in the nanometer range. PVA is one of the most popular polymers used for ultrafine electrospun fiber production. Especially, fully hydrolyzed PVA (FH-PVA) is frequently described as a good material for producing nano-scale electrospun fibers with more universal and practical application; however, the high viscosity and tendency to gelation of FH-PVA aqueous solution make the electrospinning processing very problematic. This thesis focuses on the modification of FH-PVA spinning solution and the development of functional electrospun nanofibers based on FH-PVA. The most significant result achieved in this dissertation is given as follows:

(1) We reported the fabrication of FH-PVA electrospun fibers with uniform diameters of less than 200 nm were fabricated by reducing the viscosity of FH-PVA aqueous solutions. In this process, a novel viscosity-modifier (hydrazine monochloride, HMC) was used and gradually reduced the viscosity of FH-PVA aqueous solution over a period of several days. This phenomenon is counter to the usual effect of salt addition. After being stored for several days, the viscosity decreased by up to 60% compared to that of an equivalent pure FH-PVA solution. From SAXS and ^{1}H NMR spectra observations it is evident that this effect results from the reconfiguration of hydrogen bonding. The viscosity control of FH-PVA solutions with HMC were used to electrospin highly uniform ultrafine (<200nm) fibers.

(2) Fully hydrolyzed ultra-high-molecular-weight PVA electrospun fibers with uniform diameters of about 200 nm were fabricated by reducing the viscosity of PVA in aqueous solution. A novel viscosity-modifier HMC gradually reduces the viscosity of PVA aqueous solution over a period of several days. After being stored for several days, the viscosity decreased by up to 50% compared to

that of an equivalent pure PVA solution. Using HMC to control the viscosity of the PVA solution made it possible to fabricate ultrafine electrospun fibers. In addition, by simple annealing treatment, the electrospun fibers can remains their structure even in 60 °C water for 30 days.

(3) Magnetic nanoparticles (MNPs)/polymer composite nanofibers were prepared via electrospinning of polyacrylic acid (PAA)/polyvinyl alcohol (PVA) aqueous solutions with homogenously dispersed magnetite Fe_3O_4 nanoparticles (NPs). Experiment results showed that the diameters of Fe_3O_4 NPs were in a range of 10 nm to 40 nm under all of our synthesis conditions; and Fe_3O_4 NPs can homogenously disperse in PVA composite nanofibers when they were stabilized by PAA; the crystallinity of PAA/PVA nanofibers increased along with the increase in Fe_3O_4 NPs content. The magnetic property of Fe_3O_4 NPs/PAA/PVA composite nanofibers was also investigated and the results showed that the composite nanofibers show a soft ferromagnetic behavior which is the same as Fe_3O_4 at room temperature. In addition, the water resistance of Fe_3O_4 NPs/PAA/PVA composite nanofibers was dramatically enhanced by heat treatment. Therefore, in our process to preparing magnetic Fe_3O_4 NPs/PVA composite nanofibers, PAA acts not only as a dispersant but also as a cross-linking agent.

(4) High-strength uniaxially-aligned electrospun nanofibers were prepared from PVA reinforced by modified hydrophilic multi-walled carbon nanotubes (MWCNTs). In order to get a homogeneous spinning solution, a one-step process using ammonium persulfate (APS) as oxidant was employed to fabricate water-soluble MWCNTs, and then they were dispersed in a 10 wt% PVA aqueous solution. We utilized this macroscopically homogeneous dispersion to produce nanofibers mat by electrospinning with an ultra-high-speed rotating cylinder as a collector. SEM image shows that the aligned degree of the fibers increases along with the increase in rotating speed. When the speed is up to 2000 rpm, the electrospun nanofibers are nearly uniaxially aligned. The tensile test results suggest that a small amount of MWCNTs dramatically enhanced the tensile strength of PVA fibers.

CHAPTER ONE

General Introduction

1 General Introduction

1.1 Introduction

Polyvinyl alcohol (PVA) is one of the most important synthetic polymers, which is water soluble and have been commercially manufacturing in bulk [1,2]. Electrospinning is a relatively simple and inexpensive method to produce fibers with diameters in the nanometer range [3-7]. PVA is one of the most popular polymers used for ultrafine electrospun fiber production due to the excellent chemical resistance, physical properties and biodegradability. In recent year, many different kinds functional composite nanofibers were produced based on PVA.

1.2 Electrospinning technology

1.2.1 Basic principle

Electrospinning is a straight forward method to fabricate fibers with diameters as small as several tens of nanometers [6]. In electrospinning, a high electrostatic voltage is imposed on a drop of polymer solution held by its surface tension at the end of a capillary, as shown in Figure 1. The surface of the liquid is distorted into a conical shape known as the Taylor cone. Once the voltage exceeds a critical value, the electrostatic force overomes the solution surface tension and a stable liquid jet is ejected from the cone tip. Solvent evaporates as the jet travels through the air, leaving behind ultrafine polymeric fibers collected on an electrically grounded target. The jet often follows a bending or a spiral track resulting from the interaction between the external electric field and the surface charge of the jet. Bending instability of jets not only results in the electrospinning jet being elongated up to

ultrafine fibers but also leads to the formation of randomly deposited nonwoven electrospun fiber mats [8–10].

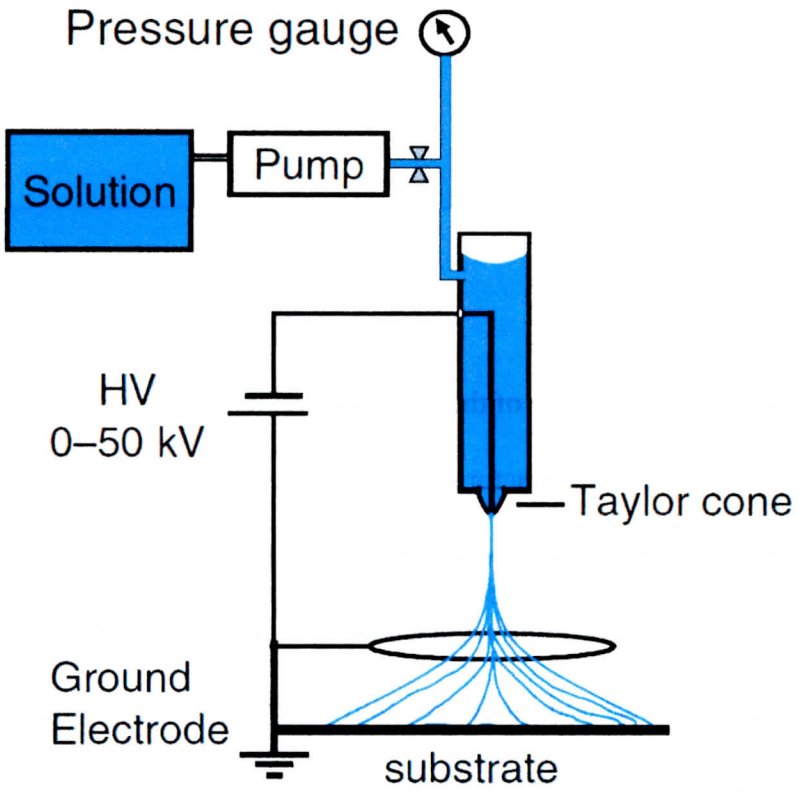

Figure 1.1 Setup for electrospinning from polymer solutions [11].

Electrospun mats have a larger specific surface area and small pore size compared to commercial nonwoven fabrics. They are of interests in a wide variety of applications including semi-permeable membranes, nanocomposites, filters, protection clothing and biomedical applications such as wound dressings, tissue engineering scaffolds and drug delivery systems [12–15]. The fiber diameter of fibers formed during electrospinning is influenced by:

System parameters

1. Polymer properties such as molecular weight, structure and poly-dispersity of the polymer, on centration, and melting point and glass transition point.

2. Solution properties such as solvent, volatility, viscosity, conductivity, surface tension, presence of

other additives.

Process parameters

1. Ambient parameters such as Solution temperature, humidity, atmosphere, air velocity in the electrospinning chamber

2. Equipment parameter including voltage, field strength, electrode distance and arrangement, flow rate, delivery volume and needle diameter.

3. The formation of fibers in the electrospinning process is mainly influenced by the following forces:

Surface tension, electrical-repellent force derived from electrical charged polymer, and droplets visco-elastic force coming from the polymer.

A further advantage of electrospinning compared to conventional solvent-spinning is that water can be used as solvent. Water-soluble fibers have to be cross-linked, e.g. by thermal or by chemical cross-linking [16, 19, 24]. These advantages result in great application potentials of nanofibers in broad fields such as separation, adsorption, filtration, catalysis, fiber reinforced composites, tissue engineering, wound dressings, drug delivery systems, sensors, cleaning tissues, protective textile and other [16–27]. Nano-fibers can be spun from polymer solutions or from polymer melts. Larrondo and Manley [29–31] were the first to carry out and report on melt electrospinning experiments. Working with PE and PP in the early 1980s, they successfully formed fibers with diameters only as small as the tens of microns range. Electrospinning from polymer melts has the advantage that no solvents are needed which have to be removed by evaporation. However, the melting temperature of the polymers is an important influencing factor for the applicability of the procedure to produce nanofibers.

1.2.2 Practical process

Typical electrospinning equipment consists of three components: a high voltage source, a spinneret (or nozzle) and a collector (as shown in Figure 2). The polymer solution or melt is applied into a syringe which is equipped with a piston and a stainless steel capillary serving as electrode and

pushed through by a pump with a defined flow rate. The spinneret is connected with the high-voltage source and applies high voltage to the polymer. This results in the formation of a polymer drop at the end of the spinneret. Under higher voltage the drop changes its shape and turns into a conic form (Taylor cone) (Figure 1 and Figure 2) [29–31, 33, 34]. At a defined voltage, the surface tension of the polymer cone at the tip of the spinneret starts to elongate and stretch so that a charged jet is formed. The jet moves in loops bending and whipping towards the electrode with opposite polarity or to the grounded target (Figure 2).

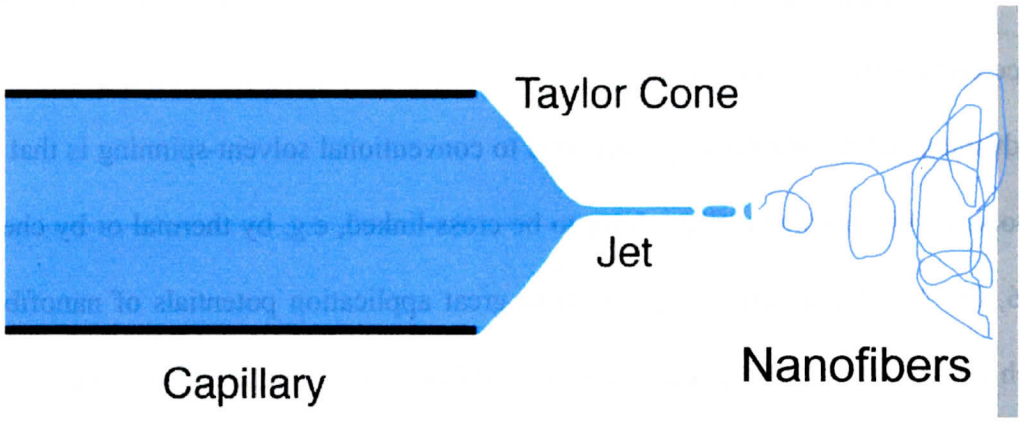

Figure 1.2 Taylor cone in electrospinning process

Recent experiments demonstrate that the rapidly whipping fluid jet is an essential mechanism of electrospinning [35, 36]. Different collection systems are known [32]. For the usually produced nonwoven mats metal plates are used as counter electrode and collection system of the nano-fibers or nano-webs. However, for special applications further grounded collectors were developed.

1.2.3 Morphologies and structure of electrospun nanofibers

Electrospinning can be used to produce novel fibers with the diameters in the range from 100 nm to 10 μm. As the solvent evaporates, the polymer molecules can come together by either a phase separation through a spinodal reaction or through classic nucleation and growth of the crystalline phase [37]. As a result, the structure in the polymer deposited on the collector can consist of a totally

amorphous, an oriented, a spherulitic or a textured fibrillar structure. In electrospinning, jets are stretched along their axis by the external electrical field and are elongated further by the repulsive force between charges on adjacent segments. The resulted area reduction rate and the associated high longitudinal strain rate imply that the macromolecules in the fibers should be stretched and axially oriented [38]. It is generally recognized that electrospinning may lower the degree of crystallinity in the polymer [39-41]. The exact reasons for this behavior are not clear. It has been suggested that the development of structure in electrospinning occurs much more rapidly than other processes and this kinetic effect may result in lower crystallinity [41]. A high degree of orientation may also be observed in the fibrils. The degree of orientation of the molecules in the amorphous regions is directly proportional to the amount of extensional flow. In summary, electrospinning is a novel technique that can be used to produce nano-scale porous structures with a variety of morphologies. The fiber size and distribution, and inter-fiber spacing (i.e. porosity) and distribution can be varied significantly by controlling the process parameters. Drugs and growth factors can be incorporated easily into the structure for biomedical applications.

1.3 Polyvinyl alcohol

1.3.1 General properties

PVA as a hydrophilic polymer is water soluble and is the largest volume synthetic resin produced in the world [42]. The excellent chemical resistance, physical properties and Commercial PVA is typically made by the hydrolysis of poly (vinyl acetate) or PVAC in the reaction as shown in Figure 3. Biodegradability of PVA has led to the development of many commercial products based on this polymer. PVA is used as an emulsifier and as a stabilizer for colloid suspensions, as a sizing agent and coating in the textile and paper industries, and as an adhesive. PVA is a truly biodegradable polymer with the degradation products being water and carbon dioxide. Hence, it is used in many biomedical and pharmaceutical applications, due to its advantages such as: nontoxic, noncarcinogenic, and

bioadhesive characteristics with the ease of processing [43].

Molecular structure of PVA

Commercial PVA is typically made by the hydrolysis of poly (vinyl acetate) or PVAC in the reaction as shown in Figure 3.

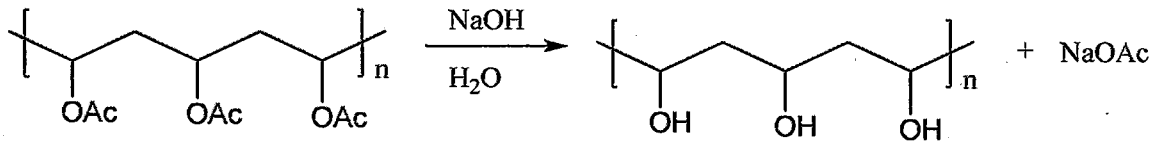

Figure 1.3 Hydrolysis of PVAC to produce PVA

As seen from Figure 3, there is a great amount of –OH groups on PVA chain. The hydroxyl groups could be a source of hydrogen bonding, which readily formed between PVA chains in aqueous solutions [44]. The percentage of hydroxyl groups is so called hydrolysis degree, which is simply defined as the following:

$$\text{Degree of hydrolysis} = \frac{x}{x+y} \times 100\,\%$$

where x and y are the molar fractions of the hydroxyl and the acetate groups, respectively, specified in the following stoichiometric formula:

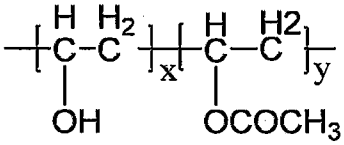

Crystallinity of PVA

The degree of hydrolysis of PVA affects the degree of polymer crystallinity [45]. For high hydrolysis PVA, the hydroxyl groups on one polymer chain can form hydrogen bonding with hydroxyl

groups of another chain as illustrated in Figure 4 (a). Consequently, the polymers will line up with each other and produce orientation. The acetyl groups in PVA with partial hydrolysis PVA act as spacers, which limit the crystallinity by preventing molecular chains from close approach as illustrated in Figure 4 (b) [44]. Due to the difficulty of carrying the reaction to completion without more drastic treatment, there is always a appreciable proportion of residual acetate groups from the parent poly (vinyl acetate) [46].

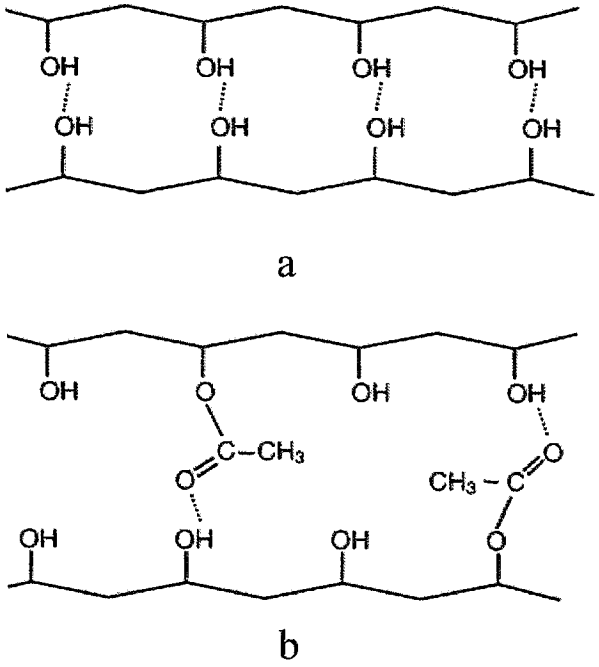

Figure 1.4 Hydrogen bonding in commercial PVA (a) at high hydrolysis many secondary hydrogen bonds can be established. (b) at low hydrolysis, acetate groups act as spacers and restrict the level of hydrogen bonding. [44]

Thermo property of PVA

PVA is a polymer with good hydrogen bonding and a high degree of crystallinity. The melting point of PVA depends on Mw, degree of hydrolysis, crystallinity and tacticity of the polymer. Typical melting points are on the order of 228 to 240°C for atactic, 212 to 235°C for isotactic and 230 to 267°C

for syndiotactic structures [45]. The glass transition temperature is 85°C for highly hydrolyzed PVA and 58°C for 87%-89% hydroxylation [46].

1.3.2 Solution behavior

Because of the said hydroxyl groups, in PVA aqueous solution, there is a great amount of hydrogen bonding not only inter- and intra-PVA molecules, but also between PVA/water molecules [47,48]. So it is important to understand the role of hydrogen bonding in controlling the properties of aqueous solutions of polymers, such as solubility, phase behaviour and viscosity. In aqueous PVA solutions, a part of the inter-chain hydrogen bonding remains, in addition to the hydrogen bonding between the PVA chains and the water molecules formed newly upon dissolution [48]. The extent of both inter- and intra chain hydrogen bonding and solute–solvent hydrogen bonding is mainly determined by the degree of hydrolysis in the PVA chains. Thus viscosity, surface tension and other solution properties can be related to the degree of hydrolysis. The effect of the degree of hydrolysis on solution viscosity and solubility are schematically illustrated in Figure 5.

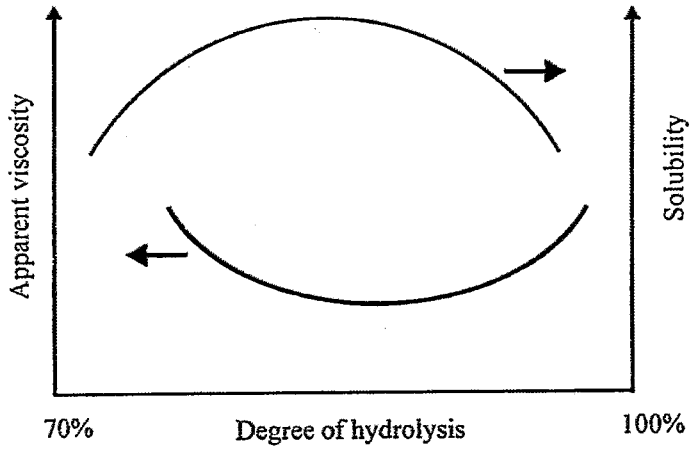

Figure 5 Schematic diagram of the interrelationship between apparent viscosity and degree of hydrolysis, and between solubility and degree of hydrolysis for aqueous PVA solutions; other conditions are fixed [49].

In addition, PVA solutions are generally shear thinning and may exhibit significant thixotropy

[50]. The viscosity of aqueous PVA solutions increases along with the increase molecular weight and concentration [51]. The dependence of solution viscosity on degree of polymerization (DP), concentration, hydrolysis, and temperature is as shown in Figs. [52, 53]

1.3.3 Applications of PVA

Fiber application –"Vinylon"

The PVA industry has grown hand in hand with the fiber "Vinylon". "Vinylon" was first developed in Japan before the Second World War, but was not commercialized until after the War, when it is extensively studied by academic and commercial laboratories; must of the research was directed towards the synthesis of polyvinyl alcohol as a raw material for "Vinylon" and towards the education of the properties of polyvinyl alcohol. Later, two firms (Kurary Company Limited and Nichibo Company Limited) successfully started commercial production of the fiber. The major emphasis in research was placed on the improvement of "Vinylon" fiber, including a research for polymers with higher degree of polymerization, more uniform distribution, and higher degree of crystallinity, to obtain the improvements of mechanical strength and water resistance needed for fiber application.

Non-fiber applications

With the gradual reduction in cost, various other end uses began to be exploited. As a result, grades of PVA suitable for particular applications have become increasingly available with the impetus of growing demand.

Applications of PVA can be classified into five groups (Table 1). These are papercoating, warp sizing, adhesives (including protective colloids), and films. Other applications have gradually increased, of which the most important are laminating film between safety glass and printing plates.

Table 1.1 Production of PVA for non-fiber applications in Japanese domestic use

Year	Warp sizing	Paper coating	Adhesives[a]	Film	Other	Total
1955	240	200	300	60	50	850
1960	1900	900	1500	200	200	4700
1965	10500	3700	5400	3000	4400	27000
1970	16100	8500	16400	9200	5400	55600
1980	15400	12800	19500	11700	9600	69000
1985	18100	13800	21100	13500	14300	80800

[a] Including protective colloids.

1.4 PVA nanofibers by electrospinning

1.4.1 Properties of PVA effect on electrospinning

Depending on the polymer properties and characteristics of the solution, electrospinning can produce a variety of structures, most of which including beads, beaded fibers and fibers. Various solution parameters affecting the morphology and diameter of electrospun PVA fibers, such as the solution concentration, molecular weight, pH,[54] salt,[55] surfactant molecules[56] and so on.

Effect of molecular weight

In aqueous solutions, there is inter- and intra chain bonding between the polar hydroxyl groups in the PVA molecules. In addition, hydrogen bonding between the PVA chains and the water molecules is also established after dissolution [57]. Hence, after dissolution, the molecules of semi-crystalline PVA cannot completely disperse and microgel particles containing paracrystalline regions and amorphous domains may remain. In order to improve the solubility of polymers with a high degree of hydrolysis, a temperature in excess of 80 C has to be used so as to disrupt the strong intra- and

inter-chain bonding that may exist in the polymer. This intra- and inter-chain bonding may reform upon cooling or during solvent evaporation. At a constant solution concentration, as the molecular weight of the polymer is increased in polymers with a high degree of hydrolysis, the solution viscosity increases significantly. Thus, the rate of solvent evaporation from the gel structure (created at a high degree of hydrolysis) may be reduced as the molecular weight increased. In this case, the relatively wet fibers that reach the collector will become flattened. The solution concentration plays a major role in stabilizing the fibrous structure.

It has been studied that in dilute solutions $[\eta]C < 1$, where [g] is the intrinsic viscosity and C is the concentration [57]. When $[\eta]C>4$ (semi-dilute entangled regime), the polymer chains in the solution begin to entangle with each other and the solution viscosity increases significantly. Tacx et al. [58] have obtained the following Mark–Houwink relationship for PVA in water:

$$[\eta] = 6.51 \times 10^{-4} M_w^{0.628}$$

Using this equation, $[\eta]C$ was calculated for various conditions used in this study. It was observed that a fibrous structure could not be stabilized for $[\eta]C < 4$. The calculated values of $[\eta]C$ for stable fibrous structures were typically between 5 and 12, indicating that a minimum degree of chain entanglement is needed for producing fibrous structures. At low to moderate molecular weights, structures obtained at equal values of $[\eta]C$ have proved to be similar.

Effect of degree of hydrolysis

Electrospinning occurs when the applied electrical voltage exceeds a critical electrical potential at which the electrostatic force overcomes the surface tension of the polymer solution. Therefore, a low surface tension is desirable in electrospinning, as it reduces the critical voltage needed for the ejection of the jet from the Taylor's cone.

The surface tension of aqueous PVA solutions exhibits a marked dependence on the degree of hydrolysis of the PVA, which may result in an altered spinnability. For instance, Wnek and colleagues

[59] reported that the addition of small amounts of Triton surfactant improves the Electrospinnability of fully (99%) hydrolyzed PVA, probably because of lowered surface tension and retarded PVA gelation, and therefore affords reproducible electrospinning.

1.4.2 Functional PVA nanofibers by electrospinning

Aligned PVA nanofibers

Most nanofibers obtained so far are in non-woven form, which can be useful for relatively small number of applications such as filtration, tissue scaffolds, implant coating film, and wound dressing. However, as we understand from traditional fiber and textile industry, only when continuous single nanofibers or uniaxially fiber bundles are obtained can their applications be expanded into unlimited. Nevertheless, this is a very tough target to be achieved for electrospun nanofibers, because the polymer jet trajectory is in a very complicated three-dimensional "whipping" way caused by bending instability rather than in a straight line. Efforts are believed to be being made in various research groups all over the world. To the best of our knowledge, five techniques for fabricating aligned fibers have been proposed: they are a rotating drum collector technique [60], an auxiliary electrode and electrical field technique [61, 62], a spinning thin wheel with a sharp edge technique [63], a frame collector technique [64], and a multiple field technique [65]. For single or individual nanofiber, some proposed specific applications are as sensors and nanowires. This type of electrospun fiber can be fabricated by a scanned electrospinning nanofiber deposition system that consists of an arrow-shaped tip source and a rotating counter electrode to which a deposition device is attached [64].

PVA composite nanofibers

The idea of incorporating nanoscale fillers into polymer solution to electrospin composite nanofibers has been extended to prepare a composite solution of organic and inorganic materials for

electrospinning.

CNT/PVA nanofibers

J.S. Jeong et al.[65] fabricated a non-woven sheet of PVA/MWNTs nanofibers by electrospinning process. Before dispersing the fillers in the PVA solution, the nanotubes were functionalized by thorough acid treatment. They spun the fibers for 5 h to obtain the non-woven sheets of PVA/MWNTs composite (MWNT=1 wt.%) which exhibited an enhancement in the tensile strength of ~15% as compared to the non-woven PVA sheets. As the nanotube concentration is further increased, the tensile strength is found to decrease markedly. However, a fine dispersion, a high degree of orientation/anisotropy, and weaker interfacial stresses are the main factors involved in enhancing the tensile properties at lower filler concentration.

Cellulose nanocrystals/PVA nanofibers

M. S. Peresin et al.[66] used Cellulose nanocrystals (CN) to reinforce nanofibers in composite mats produced via electrospinning of poly(vinyl alcohol) (PVA) with two different concentrations of acetyl groups with the amount of CN from 0 to 15wt%. The degree of crystallinity of PVA polymer matrix increased significantly together with a slight increase in the corresponding melting temperature. They proved the strong interaction of the PVA matrix with the dispersed CN phase, mainly via hydrogen bonding or bond network, was reduced with the presence of acetyl groups in PVA. Most importantly, the elastic modulus of the nanocomposite mats increased significantly as a consequence of the reinforcing effect of CNs via the percolation network held by hydrogen bonds. However, this organization-driven crystallization was limited as observed by the reduction in the degree of crystallinity of the CN-loaded composite fibers.[67]

Shuhong Wang et al. have presented a simple and effective technique, combining in-situ composite with electrospinning to prepare magnetic composite nanofibers with an average diameter of 231 nm and the Fe3O4 nanoparticles incorporated in the PVA matrix. The result indicated that the

Fe3O4 nanoparticles were inverse cubic spinel structure and as-prepared magnetic composite nanofibers exhibit a comparative high saturation magnetization although with 4 wt.% Fe3O4 content. The magnetic composite nanofibers would serve as ideal candidates for biomedical applications.

1.4.3 Application of PVA nanofibers

PVA is a popular polymer used for ultrafine electrospun fiber production. Nano-scale PVA fibers have several interesting characteristics, such as high surface area to mass ratio, significant possibilities for surface functionalization, and high mechanical performance due to an improvement in the molecular organization of the spun fiber. These properties make electrospun PVA fibers excellent candidates for many applications, such as filtration, reinforcing materials, wound dressings, tissue scaffolding, and drug releasing carriers. [68-72]

In addition, PVA composite nanofibers can also be used as an intermediary-structure to facilitate the preparation of inorganic nano structures. For an example, Dai H-Q used sol-gel processing and electrospinning technique to prepare alumina-borate/PVA composite nanofibers. These fibers were then calcined at above 1000 °C into alumina-borate ultrafine fibers. [73]

1.5 The purpose, method and significance of our research

Although PVA nanofibers have great potential applications in various fields, there are several unneglectable problems:

(1) The extremely high viscosities of PVA aqueous solutions which usually make them difficult to implement electrospinning to get ultrafine fibers.

(2) The poor water resistance of PVA nanofibers also limits their applications.

(3) The weakness in strength of PVA electrospun nanofibers mat extremely reduces the probability of their practical applications.

In order to overcome these issues, we use a novel viscosity-modifier (hydrazine monochloride, HMC) to reduced the viscosity of PVA aqueous solution and readily fabricated fully hydrolyzed

polyvinyl alcohol (FH-PVA) electrospun fibers with uniform diameters of less than 200 nm and ultra-high-molecular-weight PVA electrospun fibers with uniform diameters of about 200 nm; we prepared a magnetic PVA composite nanofibers with homogenously dispersed nanoparticles and high water resistance based on polyacrylic acid (PAA) stabilized Fe3O4 nanoparticles (NPs); we fabricated a high-strength uniaxially-aligned PVA composite nanofibers by electrospinning with an ultra-high-speed rotating cylinder as a collector, using modified hydrophilic multi-walled carbon nanotubes (MWCNTs) as a reinforcement filler.

1.6 Organization of this dissertation

This dissertation is organized to provide snapshots of development of electrospun PVA functional nanofibers.

In chapter 1, I reviewed references and provided brief summary of electrospinning technology and the application of PVA electrospun nanofibers.

In chapter 2, we reported the fabrication of FH-PVA electrospun fibers with uniform diameters of less than 200 nm were fabricated by viscosity control.

In chapter 3, we successfully prepared fully hydrolyzed ultra-high-molecular-weight PVA electrospun fibers with uniform diameters of about 200 nm reducing the viscosity of PVA in aqueous solution.

In chapter 4, we proposed a facile process to prepare magnetic nanoparticles (MNPs)/polymer composite nanofibers via electrospinning of polyacrylic acid (PAA)/polyvinyl alcohol (PVA) aqueous solutions with homogenously dispersed magnetite Fe3O4 nanoparticles (NPs).

In chapter 5, we prepared high-strength uniaxially-aligned electrospun nanofibers from PVA reinforced by water-soluble multi-walled carbon nanotubes (MWNTs).

In chapter 6, we did a conclusion of this dissertation.

Reference

[1] C. Shao, H. Kim, J. Gong, B. Ding, D. Lee, S. Park, *Mater Lett*, 57, 1579 (2003).

[2] M. Krumova, D. Lo´pez, R. Benavente, C. Mijangos, J.M. Peren, *Polymer*, 41, 9265 (2000).

[3] S. H. Tan, R. Inai, M. Kotaki, S. Ramakrishna, *Polymer*, 46, 6128 (2005).

[4] K. H. Lee, O. Ohsawa, S. Lee, J. C. Park, K. W. Kim, H. Y. Kim, *Sen'i Gakkaishi*, 64, 306 (2008).

[5] J. H. Park, B. S. Kim, Y. C. Yoo, M. S. Khil, H. Y. Kim, *J Appl Polym Sci* 107, 2211 (2007).

[6] J. Doshi, D. H. Reneker, *J Electrostat*, 35, 151 (1995).

[7] K. Wei, T. Ohta, B. S. Kim, K. H. Lee, M. S. Khil, H. Y. Kim, I. S. Kim. *Polym Adv Technol*, 21, 746 (2010).

[8] H. Fong, I. Chun, D. H. Reneker, *Polymer*, 40, 4585 (1999).

[9] Y. M. Shin, M. M. Hohman, M. P. Brenner, G. C. Rutledge, *Polymer*, 42, 9955 (2001).

[10] H. Fong, W. Liu, C. S. Wang, R. A. Vaia, *Polymer*, 43, 775 (2002).

[11] K. Schaefer, H. Thomas, P. Dalton, M. Moeller, Vol 97, *Chapter 7, Nano-Fibers for Filter Materials, Multifunctional Barriers for Flexible Structure: Textile, Leather and Paper* (Springer Series in Materials Science) .

[12] P. P. Tsai, H. Schreuder-Gibson, P. Gibson, *J Electrostat*, 54, 333 (2002).

[13] P. Gibson, H. Schreuder-Gibson, D. Rivin, *Colloid Surface A*, 187–188, 469 (2001).

[14] E. R. Kenawy, G. L. Bowlin, K. Mansfield, J. Layman, D. G. Simpson, E. H. Sanders, G. E. Wnek. *J Control Release*, 81, 57 (2002).

[15] Y. K. Luu, K. Kim, B. S. Hsiao, B. Chu, M. Hadjiargyrou, *J Control Release*, 89, 341 (2003).

[16] R. Dersch, A. Greiner, M. Steinhart, J. H. Wendorff, *DWI Rep.*, 8, 127 (2003).

[17] T. Grafe, K. Graham, *Proceedings of the International Nonwovens Technical Conference (Joint INDA-TAPPI Conference)*, 24–26 September, Atlanta, (2002).

[18] T. H. Grafe, K. M. Graham, *Nonwovens in Filtration, 5th International Conference,Stuttgart*, Germany, March (2003).

[19] A. Greiner, Lecture on "Electrospinning for Biomedical Applications" at DWI Aachen, Germany (2005).

[20] H. Schreuder-Gibson, P. Gibson, K. Senecal, M. Senett, J. Walker, W. Yeomans, D. Ziegler, P. P. Tsai, *Adv. Mater.*, 34, 44 (2002).

[21] L. Huang, R. A. McMillan, R. P. Apkarian, B. Pourdeyhimi, V. Conticello, E.L. Chaikof, *Macromolecules*, 33, 2989 (2000).

[22] G. Verreck, I. Chun, J. Rosenblatt, J. Peeters, A. Van Dijck, J. Mensch, M. Noppe, M. E. Brewster, *J. Control. Release*, 92, 349 (2003).

[23] A. Frenot, I. S. Chronakis, *Colloid Interf. Sci.*, 8, 64 (2003).

[24] H. Thomas, E. Heine, R. Wollseifen, C. Cimpeanu, M. M¨oller, *Int. Nonwovens, J.* , 14(3), 12 (2005).

[25] P. Gibson, H. Schreuder-Gibson, D. Rivin, *Colloids Surf. A: Physicochem. Eng. Asp.*, 187–188, 469 (2001).

[26] M. Jacobsen, *Nonwovens Industry*, 36 (1991). cf. also: Chemiefasern/ Textilindustrie 39/91, 868 (1989).

[27] E. R. Kenawy, G. L. Bowlin, K. Mansfield, J. Layman, D. G. Simpson, E. H. Sanders, G. E. Wnek, *J. Control. Release*, 81, 57 (2002).

[28] J. Zeng, *Ph.D. Thesis, University Marburg*, 30 (2003).

[29] L. Larrondo, R. St. John Manley, *J. Polym. Sci.: Polym. Phys. Ed*, 19, 909 (1981).

[30] L. Larrondo, R. St. John Manley, *J. Polym. Sci.: Polym. Phys. Ed*, 19, 921 (1981).

[31] L. Larrondo, R. St. John Manley, *J. Polym. Sci.: Polym. Phys. Ed*, 19, 933 (1981).

[32] P. Dalton, T. Kuenzel, D. Klee, M. Moeller, *J. Mey, Eur. Cell Mater.*, 7(1), 52 (2004).

[33] G. I. Taylor, *Proc. R. Soc. Lond. Ser. A*, 280, 383 (1964).

[34] G. I. Taylor, *Proc. R. Soc. Lond. Ser. A*, 313, 453 (1969).

[35] M. Shin, M. M. Hohman, M. P. Brenner, G. C. Rutledge, *Appl. Phys. Lett.*, 78, 1149 (2001).

[36] M. M. Hohman, M. Shin, G. Rutledge, M. P. Brennera, *Phys. Fluids*, 13(8), 2201 (2001).

[37] A Weghmann, *Schriftenreihe des Deutschen Wollforschungsinstitutes*, 85, 314 (1981).

[38] K. Schmidt, *Melliand Textilber*, 61(6), 495 (1980).

[39] D. Luzhansky, *INDA/TAPPI*, Baltimore, MD, 16–18 September (2003).

[40] http://www.hovo.com.

[41] http://www.elmarco.cz and http://www.nanospider.c z/aplikace.php? kategorie =1&h.

[42] B. Briscoe, P. Luckham, S. Zhu, *Polymer*, 41, 3851 (2000).

[43] W. Cai, B. G. Ram, *Kirk-Othmer Encyclopedia of Chemical Technology*, 2002.

[44] J. Feng, F. Dogan, *Microstructure and Processing*, 283, 56 (2000).

[45] Philip Molyneux, *Water-soluble synthetic polymers, CRC, Boca Raton, FL*, 1, 119 (1983).

[46] F. L. Marten, *Vinyl Alcohol Polymers, Kirk-Othmer Encyclopedia of Chemical Technology, Wiley, New York, NY* (2002) Online.

[47] M. Shibayama, M. Uesake, S. Inamoto, H. Mihara, S. Nomura, *Macromol*, 29, 885 (1996).

[48] H. Maeda, T. Kawai, S. Sekii, *J Polym Sci*, 35, 288 (1959).

[49] B. Briscoe, P. Luckham, S. Zhu, *Polymer*, 41, 3851 (2000).

[50] N. A. Hebeish, M. H. Ibrahim, S. Abo, H. M. Fahmy, *Polymer-Plastics Technology and Engineering*, 35, 517 (1996).

[51] P. Molyneux, *Water-soluble synthetic polymers, CRC, Boca Raton, FL*, 1, 119 (1983).

[52] F. L. Marten, *Vinyl Alcohol Polymers, Kirk-Othmer Encyclopedia of Chemical Technology, Wiley, New York, NY* (2002).

[53] *Vinyl Alcohol Polymers, Encyclopedia of Polymer Science and Technology, John Wiley & Sons,*

New York, NY, 14, 149 (1971).

[54] P. Hong, C. Chou, C. He, *Polymer*, 42, 6105 (2001).

[55] J. C. J. F. Tacx, H. M. Schoffeleers, A. G. M. Brands, L. Teuwen, *Polymer*, 41, 947 (2000).

[56] L. Yao, T. W. Hass, A. Guiseppi-Elie, G. L. Bowlin, D. G. Simpson, G. Wnek, *Chem.Mater.*, 15, 1860 (2003).

[57] J. Doshi, D. H. Renek er, *J. Electrost.*, 35, 151 (1995).

[58] A. Bornat, *US Patent 4689186*, (1987).

[59] J. P. Berry, *US Patent 4965110*, (1990).

[60] A. Theron, E. Zussman, A. L.Y arin, *Nanotechnology*, 12, 384(2001).

[61] R. Dersch, T. Liu, A. K. Schaper , A. Greiner, J. H. W endorff, *J. Polym. Sci.—A: Polym. Chem.* , 41, 545 (2003).

[62] J. M. Deitzel, J. Kleinme yer, J. K. Hirv onen, T. N. C. Beck, *Polymer*, 42, 8163 (2001).

[63] J. Kameoka, D. Czaple wski, H. Liu, H. G. Craighead, *J. Mater.Chem.*, 14, 1503 (2004).

[64] J. S. Jeong , J. S. Moon, S. Y. Jeon, J. H. Park, P. S. Alegaonkar , J. B. Yoo, Thin *Solid Films*, 515, 5136 (2007).

[65] M. S. Peresin, Y. Habibi, J. O. Zoppe, J. J. Pawlak, O. J. Rojas, *Biomacromolecules*, 11, 674 (2010).

[66] S. Wang, C. Wang, B. Zhang, Z. Sun, Z. Li, X. Jiang, X. Bai. *Mater. Lett.*, 64, 9 (2010).

[67] H. Q. Dai, J. Gong, H. Kim, D. Lee, *Nanotechnology*, 13 (5), 674 (2002).

[68] J. M. Deitzel, J. Kleinmeyer, D. Harris, N. C. Beck Tan, *Polymer*, 42, 261(2001).

[69] C. Chen, Y. H. Zhu, H. Bao, X. L. Yang, C. Z. Li, *Appl. Mate. Interfaces*, 2, 1499 (2010).

[70] B. E. B. Jensen, A. A. A. Smith, B. Fejerskov, A. Postma, P. Senn, E. Reimhult, M. Pla-Roca, L. Isa, D. S. Sutherland, B. Stadler, A. N. Zelikin, *Langmuir*, 27, 10216 (2011).

[71] A. D. Ossipov, J. Hilborn, *Macromolecules*, 39, 1709 (2006).

[72] D. A. Ossipov, S. Piskounova, J. Hilborn, *Macromolecules*, 41, 3971 (2008).

[73] F. Cavalieri, E. Chiessi, R. Villa, L. Vigano, N. Zaffaroni, M. F. Telling, G. Paradossi, *Biomacromolecules*, 9(7), 1967 (2008).

CHAPTER TWO

Preparation of fully hydrolyzed polyvinyl alcohol electrospun nanofibers with diameters of sub-200 nm by viscosity control

2 Preparation of fully hydrolyzed polyvinyl alcohol electrospun nanofibers with diameters of sub-200 nm by viscosity control

Fully hydrolyzed polyvinyl alcohol (FH-PVA) electrospun fibers with uniform diameters of less than 200 nm were fabricated by reducing the viscosity of FH-PVA aqueous solutions. A novel viscosity-modifier (hydrazine monochloride, HMC) gradually reduced the viscosity of FH-PVA aqueous solution over a period of several days. This phenomenon is counter to the effect of usual salt addition. After being stored for several days, the viscosity decreased by up to 60% compared to that of an equivalent pure FH-PVA solution. From Small angle X-ray Scattering (SAXS) and ^{1}H NMR spectra observations it is evident that this effect results from the reconfiguration of hydrogen bonding. The viscosity control of FH-PVA solutions with HMC were used to electrospin highly uniform ultrafine fibers (diameter < 200 nm).

2.1 Introduction

Polyvinyl alcohol (PVA) is a water-soluble synthetic polymer produced industrially by the hydrolysis of polyvinyl acetate.[1,2] Many different grades of PVA are commercially available, falling into two types, depending on the degrees of hydrolysis (DH), fully hydrolyzed PVA (FH-PVA) and partially hydrolyzed PVA (PH-PVA).[3-5] The higher chemical stability, water resistance, and excellent physical and mechanical properties of FH-PVA have led to its wide use, especially in the textile industry.[1]

Electrospinning is a relatively simple and inexpensive method to produce fibers with diameters in

the nanometer range.[6-10] PVA is one of the most popular polymers used for ultrafine electrospun fiber production. Nano-scale PVA fibers have several interesting characteristics, such as high surface area to mass ratio, significant possibilities for surface functionalization, and high mechanical performance due to an improvement in the molecular organization of the spun fiber. These properties make electrospun PVA fibers excellent candidates for many applications, such as filtration, reinforcing materials, wound dressings, tissue scaffolding, and drug releasing carriers.[11-16] FH-PVA is frequently described as a good material for producing nano-scale electrospun fibers;[17,18] however, it is difficult to fabricate electrospun FH-PVA fibers with diameters below about 200 nm due to the extremely high surface tension and viscosity of the solution.[19] It has been suggested that reducing the high surface tension of FH-PVA in solution will address this problem.[20,21] However, although the surface tension can be demonstrably modified, controlled production of FH-PVA electrospun fibers with uniform nano-size diameters remains a challenge. The alternative approach to controlling fiber diameter, namely by decreasing solution viscosity, has not yet been reported.

This paper describes the fabrication of uniform electrospun FH-PVA fibers with sub-200 nm diameters by controlling solution viscosity. Hydrazine monochloride (HMC) is widely used in organic synthesis, but until now has not been used for reducing the viscosity of FH-PVA.[22] The effect of HMC on the viscosity characteristics of the solutions was investigated and a reason for the change is investigated. Furthermore, parameters such as concentration and storage time were systematically examined and their effects on the morphology and diameter of electrospun FH-PVA fibers are described. Based on this method, the spinnability of FH-PVA aqueous solutions can be greatly improved and it is now possible to produce ultrafine FH-PVA electrospun fibers with diameters of less than 200 nm.

2.2 Experimental details

2.2.1 Materials

PVA with a degree of hydrolysis (DH) > 99% and degree of polymerization (DP) =3500, PVA with DH= 86-90% and DP= 3500 were kindly provided by Kuraray Co. Ltd, Tokyo, Japan. In this paper the abbreviation form PVA-X-Y, is used to describe polymer molecular weight and degree of hydrolysis. For example, PVA-35-99 represents a PVA with a DP of 3500 and a DH of 99%. Hydrazine monochloride (HMC, chemical formula is $N_2H_4 \cdot HCl$), sodium chloride (NaCl), sodium sulfate (Na_2SO_4), potassium chloride (KCl), ammonium sulfocyanate (NH_4SCN) and isopropanol (IPA) were obtained from Tokyo Chemical Industry Co., Ltd. Deuterium oxide (99.9%) as a NMR solvent was obtained from Wako Pure Chemical Industries, Ltd. All chemicals were of analytical grade and were used without further purification. Distilled water was used as the solvent.

2.2.2 Preparation of PVA solutions

Fully hydrolyzed PVA in aqueous solution was prepared using the method described by Briscoe et al.[23] In brief, PVA powder was dispersed in distilled water at 25 °C for 1h and then this suspension was rapidly heated to 95 °C and kept at this temperature with high speed stirring for about 2 hours. The solution was then cooled to room temperature. PVA powders with a range of degrees of hydrolysis (DH = 86-90%) were directly dissolved in hot water (95 °C) and stirred for 2 h. Various amounts of HMC were added to 6 wt% PVA solution to produce solutions with HMC concentrations of 0.05 mol/L, 0.1 mol/L and 0.3 mol/L. PVA solutions with NaCl, Na_2SO_4 and KCl (0.1 mol/L) were also prepared. These solutions were stirred for 2 h to ensure homogenization and then put into a water bath at 40 °C for several days. Samples were taken every 24 h, cooled to 25 °C. Viscosity, conductivity and surface tension were measured.

2.2.3 Electrospinning

The electrospinning experiments were performed at 25 °C. The polymer solution was placed in a 12

mL syringe with a 0.8 mm ID blunt needle, and the needle was connected to the high voltage power supply. A rotating cylinder (diameter: 12 cm; speed: 25 rpm) wrapped with aluminum foil was used as a grounded collector. The applied voltage and the tip-to-collector distance (TCD) were fixed at 10 kV and 15 cm and the syringe pump flow rate was set to 0.4 mL/h. Immediately before electrospinning, isopropanol (IPA) was added at 5 wt% to the PVA solutions to slightly decrease the surface tension.[20]

2.2.4 Measurement

The PVA solutions were stored in a recycling-water bath at constant temperature and tested every 24 h. Rheological properties were measured using a Rheologia-A300 controlled stress rheometer (Elquest) at 25 °C. A co-axial cylinder arrangement with a gap of 2.1 mm was used to measure the apparent viscosities using the Steady Flow Viscosity Testing mode. Apparent viscosities of different PVA solutions measured at a shear rate of 100 1/sec were selected as reference viscosities. Conductivity was measured using a conductivity meter (Model SC72 personal SC meter, Yokogawa Electric Corporation) and the surface tension was measured using a Wilhelm plate method tension meter (CBVP-Z, Kyowa Interface Science Co. Ltd, Saitama, Japan). Small angle X-ray Scattering (SAXS) was also used to measure molecular weights. A SAXS camera (SAXSess mc^2, Anton Paar, Austria) attached to a sealed-tube anode X-ray generator (GE Inspection Technologies, Germany) was operated at 40 kV and 50 mA. A Göbel mirror and a block collimator provided a focused monochromatic X-ray beam of Cu Ka radiation (l = 0.1542 nm) with a well-defined line-shape. The morphology of the electrospun fibers was observed using a scanning electron microscope (SEM, Hitachi S-3000N). The SEM samples were sputtered with Palladium-Platinum. ^{1}H NMR spectra of FH-PVA/D_2O solutions were recorded on a Bruker DRX-400 spectrometer, operating at 400 MHz and 40 °C.

Table 2.1 Correlation length (ξ) calculated by using the Ornstein-Zernike equation

	A	$A_{1/2}$	$A_{1/3}$	B	$B_{1/2}$	$B_{1/3}$
ξ /nm	12.1	14.0	14.2	13.0	16.5	16.2

[a](A: pure 6 wt.% PVA solutions; $A_{1/2}$: twice-diluted A solution; A1/3: 3-time-diluted A solution; B: PVA solution with HMC; $B_{1/2}$: twice-diluted B solution; $B_{1/3}$: 3-time-diluted B solution), (Storage time: 72 h)

2.3 Results and discussion

2.3.1 Effect of HMC on the viscosity of PVA solutions

PVA35-99 is nearly completely hydrolyzed, and so a preparation temperature above 95 °C is required for the complete dissolution of the solid in an acceptable time. It is believed that inter- and intra-molecule hydrogen bonding in aqueous PVA solutions is disrupted by thermal energy during the solution preparation, but upon cooling the hydrogen bonds can re-form resulting in an increase in viscosity.[24-26]

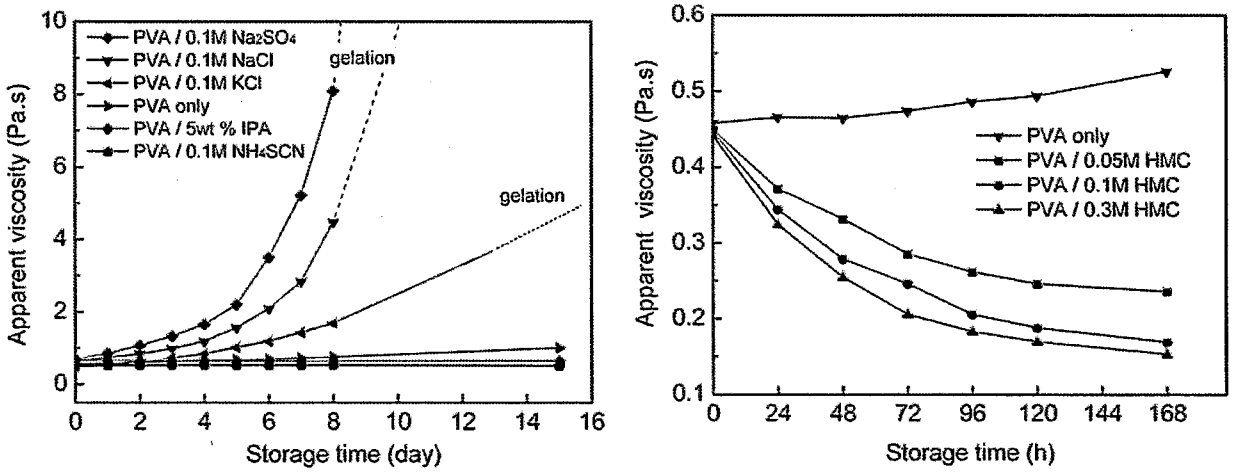

(a) (b)

Figure 2.1 The variation of apparent viscosities of FH-PVA aqueous solutions with storage time. (a) FH-PVA solutions with additives; (b) FH-PVA solutions with varying amounts of hydrazine monochloride (HMC); (Shear rate: 100 1/sec; Temperature: 25 °C).

At concentrations of ≤ 10 wt% (a typical industrial strength), aqueous solutions of high DH-PVA

undergo a viscosity increase with time and depending on temperature, concentration and additives, may ultimately gel. It is reported that several additives, such as inorganic salts and organic compounds, can affect the viscosity of PVA in solution.[27-29] We have investigated the effect of Na_2SO_4, NaCl, KCl, NH_4SCN and IPA on the viscosity of FH-PVA solutions. As seen in Figure 1(a), most of the inorganic salts have a negative effect on viscosity stability, accelerating the time dependent increase in the viscosity. However, NH_4SCN and IPA can moderate the process. HMC has an unexpected effect on the viscosity of aqueous FH-PVA, as can be seen in Figure 1(b) the apparent viscosity of PVA in solution decreased gradually with storage time in the presence of HMC with final viscosities reduced by up to 60% depending on the amount of HMC. The addition of HMC may disrupt PVA chain inter- and intra-chain hydrogen bonding resulting in a decrease in the viscosity.

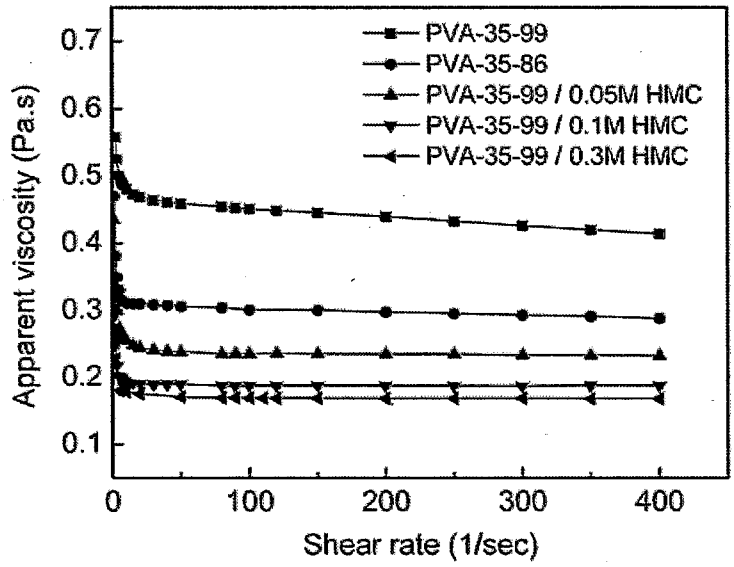

Figure 2.2 Relationship between apparent viscosity and shear rate for PVA aqueous solutions with varying concentrations of hydrazine monochloride (HMC) at 25 °C (Storage time: 120 h).

Figure 2 shows the relationship between shear rate and apparent viscosity for different PVA solutions after 120 h. Apparent viscosities of the PVA-35-99 solutions are much higher than those of the PVA-35-86 solution, and pronounced shear thinning behavior is observed in the pure PVA-35-99 solution. This is due to the higher DH causing more inter and intra chain hydrogen bonding in the

solution and hence more interaction and entanglements between the PVA chains.[23] The obvious shear thinning behavior also indicates the presence of stronger polymer chain associations. In addition, after the viscosities had decreased, the properties of the PVA-35-99 solutions with varying amounts of HMC show similar behavior to the PVA-35-86 solutions with no shear thinning. It is probable that the addition of HMC reduces inter- and intra-chain hydrogen bonding and reduces the degree of interaction and entanglement between the molecular chains in PVA-35-99.

2.3.2 Small-Angle X-ray Scattering (SAXS) of different FH-PVA solutions

SAXS was used to investigate the structural morphology of the solutions. The sample solutions were tested at original, twice-diluted and 3-time-diluted of the original solution. The scattered intensities of the aqueous solutions at 25 °C are shown in Figure 3 and all I(q) data were corrected for the background scattering from the capillary and the solvents, and the absolute scale calibration was made using water as a secondary standard. According to the Ornstein-Zernike theory, the scattering intensity near q=0 is represented by the following equation:

$$I(q) = \frac{I(0)}{1 + \xi^2 q^2} \tag{1}$$

where ξ is the Ornstein-Zernike correlation length which is believed to be related to the inter molecule coil distance.[30-33] In our experiment, the correlation lengths (ξ) were calculated from the lower q-range by using the Ornstein-Zernike model to fit our original data (the solid curves in Figure 3), which are shown in table 1. The concentration of HMC in the FH-PVA solutions is proportional to the correlation length (ξ). This indicates that the physical junction points formed by hydrogen bonding between molecules were broken, resulting that the interaction between FH-PVA molecules was weakened, which is in agreement with our inference drawn from the decrease in viscosity.

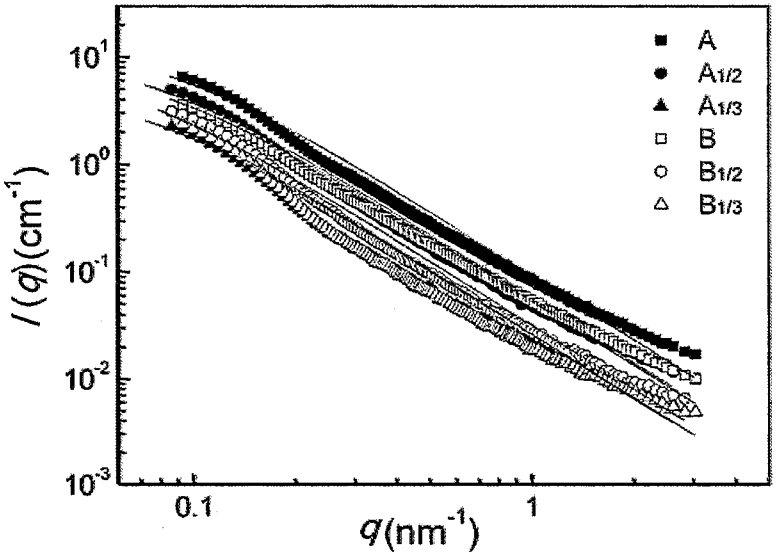

Figure 2.3 SAXS intensities, I(q) for FH-PVA aqueous solutions at 25 °C; (A: pure 6 wt% FH-PVA solutions; $A_{1/2}$ twice-diluted A solution; $A_{1/3}$: 3-time-diluted A solution; B: PVA solution with hydrazine monochloride (HMC); $B_{1/2}$: twice-diluted B solution; $B_{1/3}$: 3-time-diluted B solution.) (Storage time: 72 h).

2.3.3 NMR of different FH-PVA solutions

Our work indicates that the viscosity of FH-PVA aqueous solutions decreases related to the proportion of broken hydrogen inter- and intra-molecular bonds. To further confirm this, NMR spectroscopy, as the most direct way of investigating hydrogen bonding, was used to observe hydroxyl protons in FH-PVA solutions.[34-38] In the NMR samples, there is an extremely small residual quantity of water due to the bound water existing in FH-PVA and HMC, which is impossible to remove completely. It is known that in FH-PVA aqueous solutions, hydrogen bonding exists between the FH-PVA molecules and water, as well as the inter- and intra-molecular FH-PVA bonding, which will lead to hydroxyl protons with different hydrogen bond configurations.[27] As a result, the peak of hydroxyl protons is much wider than that of water, which has homogeneous hydrogen bonding as shown in Figure 4a and 4b. However, in the presence of HMC, the situation became more complex,

due to the strong electron supplying capacity of the imido group, which promotes the action of HMC in the formation of hydrogen bonds with protons.

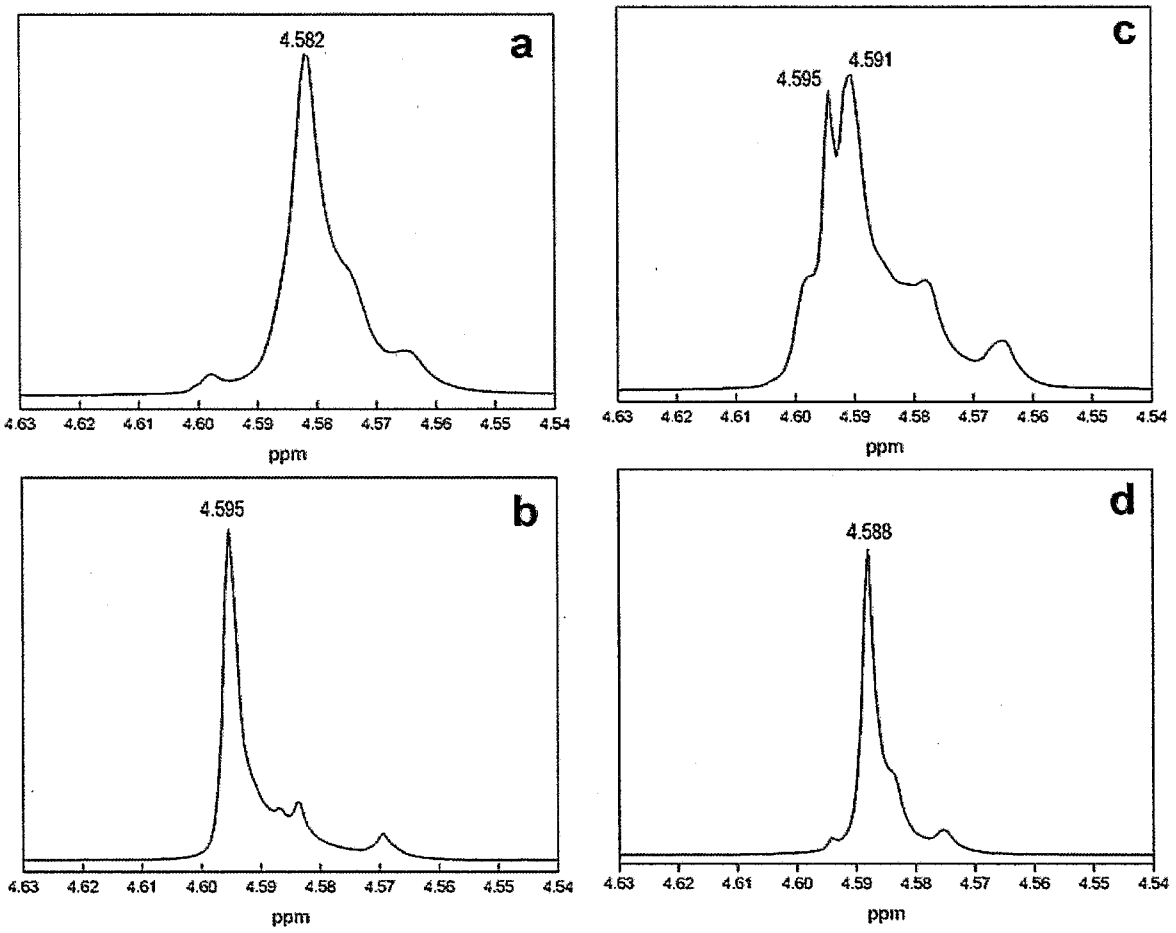

Figure 2.4 ^{1}H NMR spectra of hydroxyl protons: (a) FH-PVA/D_2O solution; (b) H_2O/D_2O solution; (c) FH-PVA/hydrazine monochloride (HMC)/D_2O immediately after solution preparation; (d) FH-PVA/HMC/D_2O solution after 72 h (Measurement temperature: 40 °C).

As seen in Figure 4c, the peak from water protons appears at 4.595 ppm. Furthermore, an up-field shift was observed for hydroxyl protons from FH-PVA (from 4.582 to 4.591 ppm) due to the weakening of inter- and intra-molecule FH-PVA hydrogen bonding and hydrogen bonds between FH-PVA and solvent molecules. After storage at 40 °C for 3 days, the peak from water protons at 4.595 ppm disappeared and the main peak of hydroxyl proton became sharp, indicating the formation of a configuration with a narrower distribution of hydrogen bonding between FH-PVA, HMC, water and solvent, which lead to a net de-shielding effect on hydroxyl protons (Figure 4d).

2.3.4 Electrical conductivity and surface tension

To investigate the spinnability of FH-PVA in detail, we examined the solution properties of electrical conductivity and surface tensions, which are important factors in electrospinning.[20] As seen in Figure 5, the surface tension was slightly reduced by adding HMC while the conductivities increased sharply with the concentration of HMC. However, both the surface tension and conductivity changed very little during the period of storage although during the same period the viscosity decreased greatly.

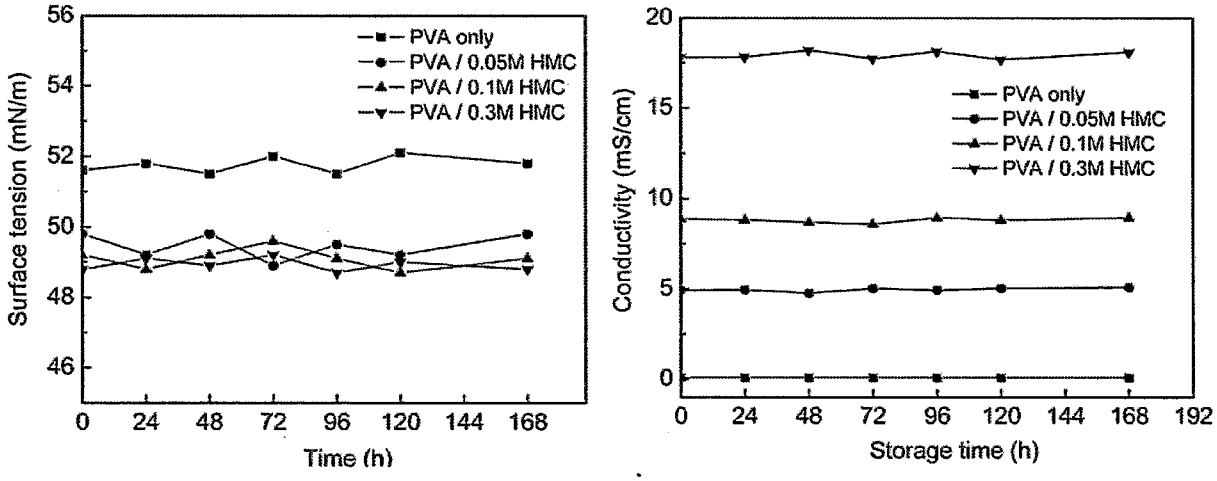

(a) (b)

Figure 2.5 Surface tension (a) and conductivity (b) of PVA in aqueous solution with different concentrations of hydrazine monochloride (HMC) and varying storage time at 25 °C.

2.3.5 Electrospinnability of FH-PVA

In the electrospinning process, as a consequence of the applied electric force, the pendant drop of solution on the tip of the nozzle forms a conical protrusion known as the Taylor cone.[39-41] When the applied electric field strength overcomes the surface tension; a straight jet is ejected from the apex of Taylor cone. This jet remains straight for some distance and then it bends and follows a looping and spiraling path the so-called instability. Solvent is evaporated from the strand surface as the jet flies to the collector. Finally, the jet solidifies and deposits on the grounded collector forming

a nonwoven fiber mat. These fundamental processes in electrospinning are related to solution viscosity and surface tension; these properties also significantly affect the morphology and diameter of the fibers.[42-46]

The surface tension and viscosity of FH-PVA in aqueous solution is much higher than PH-PVA,[19] this is the root cause of the difficulty in fabricating electrospun FH-PVA fibers with diameters below 200 nm. To make ultrafine FH-PVA fibers, previous studies concentrated in reducing the solution surface tension.[19-21] This paper describes the effects of reducing the viscosity of FH-PVA and examines the relationship between solution viscosity and the morphologies and diameters of the electrospun fiber product. Electrospun FH-PVA fibers fabricated from solutions with different viscosities, controlled by HMC addition and aging are shown in Figure 6. For the pure PVA solution (Figure 6A), long threads with irregular fiber structures like tree roots were formed from the high surface tension and viscosity precursor solutions. It is difficult to say what an ideal Taylor cone geometry formed during the spinning process.[47] However, in the presence of HMC, the diameters of electrospun fibers are significantly decreased (when the concentration of HMC is above 0.1 M and after 72 h maturation) and fibers with diameter of 140-260 nm could be fabricated. This is not only because of the decrease of surface tension and the increase in conductivity, but also because of the decrease in viscosity. It is thought to be impossible to get regular morphology ultrafine fibers without modifying these three factors. However, SEM observations show a heavily beaded morphology (Figure 6C and 6D) when the concentration of HMC was 0.3 M, which is enough to reduce the viscosity.

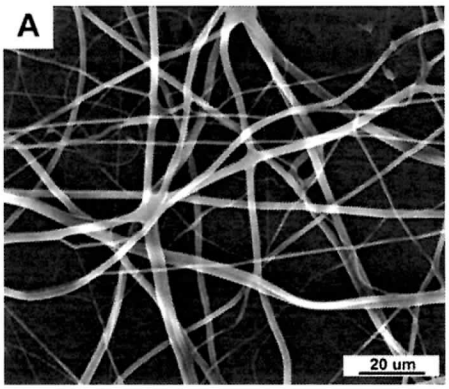
A
20 um

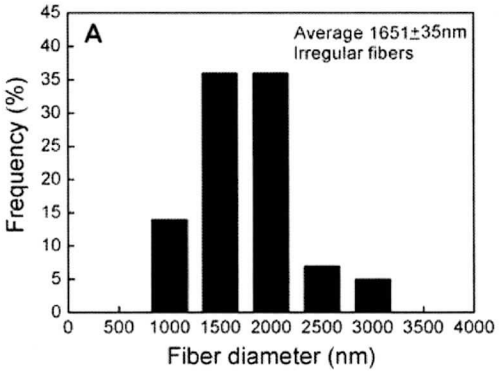
A
Average 1651±35nm
Irregular fibers
Frequency (%)
Fiber diameter (nm)

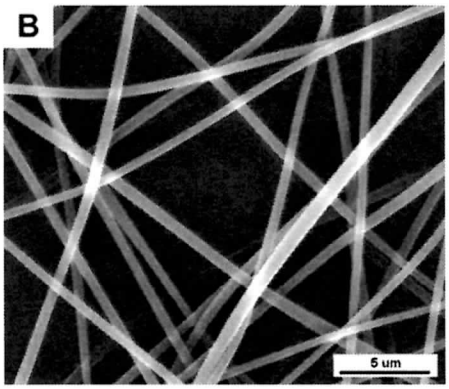
B
5 um

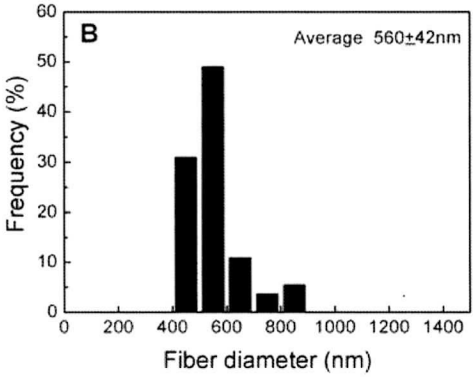
B
Average 560±42nm
Frequency (%)
Fiber diameter (nm)

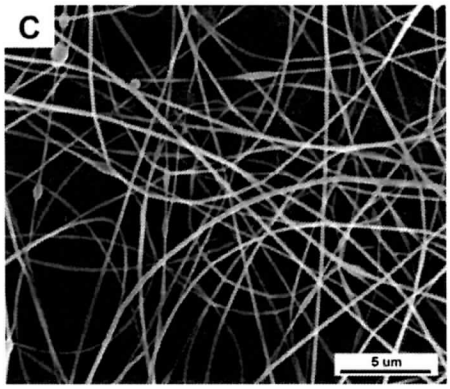
C
5 um

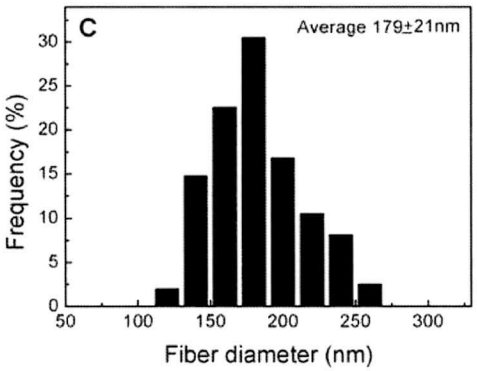
C
Average 179±21nm
Frequency (%)
Fiber diameter (nm)

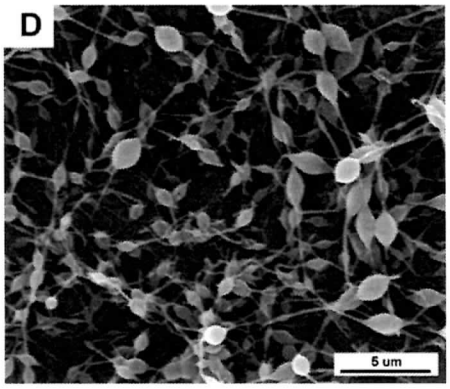
D
5 um

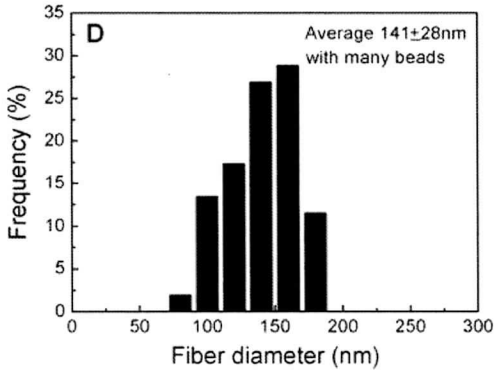
D
Average 141±28nm
with many beads
Frequency (%)
Fiber diameter (nm)

Figure 2.6 SEM images of electrospun FH-PVA fibers produced from different FH-PVA solutions: (A) pure FH-PVA solution; (B) FH-PVA solution with 0.05 M hydrazine monochloride (HMC); (C) FH-PVA solution with 0.1 M HMC; (D) FH-PVA solution with 0.3 M HMC (Storage time: 72 h).

To reveal the dependence on viscosity of fiber diameter and morphology, FH-PVA solution with 0.1 M HMC was selected as a model solution since its surface tension and conductivity remained virtually constant (shown in Figure 5), even as the viscosity gradually decreased during the storage period: electrospun fibers from this solution are shown in Figure 7. With the original solution, both the conductivity and high viscosity are high and it is difficult to form a stable jet and only some spotty deposition was observed on the aluminum foil target (Figure 7A). After several days' storage, the solution viscosity decreased to 0.25-0.35 Pa·s, and uniform electrospun fibers could be fabricated. However, when the viscosity became too low, a beaded morphology resulted. All the results indicate that viscosity is a predominant factor affecting fiber diameter. Electrospun fibers with diameter down to about 180 nm can be fabricated by this method of controlling viscosity.

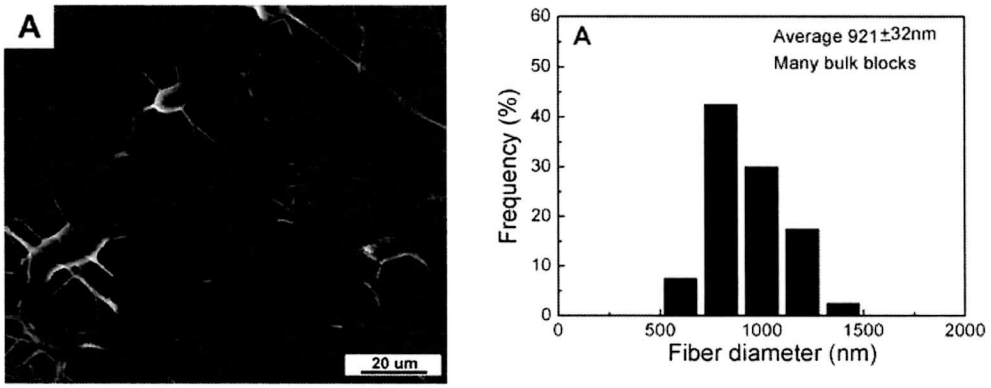

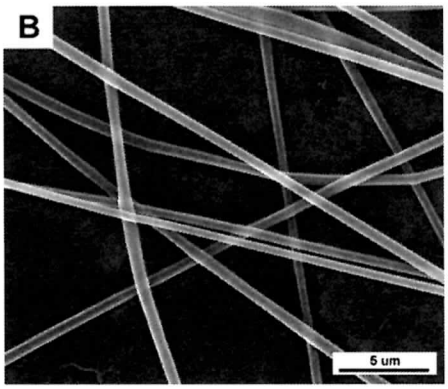
B
5 um

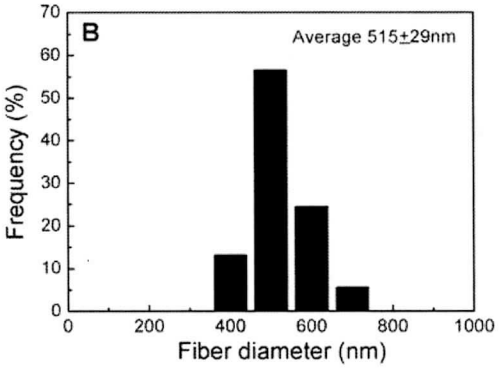
B
Average 515±29nm
Frequency (%)
Fiber diameter (nm)

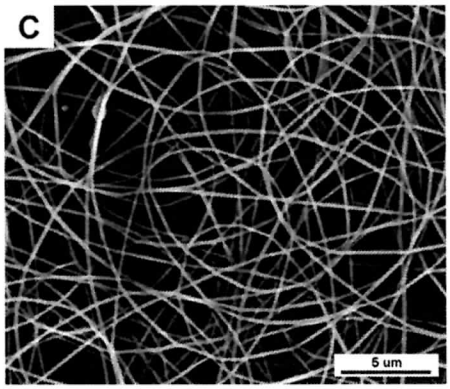
C
5 um

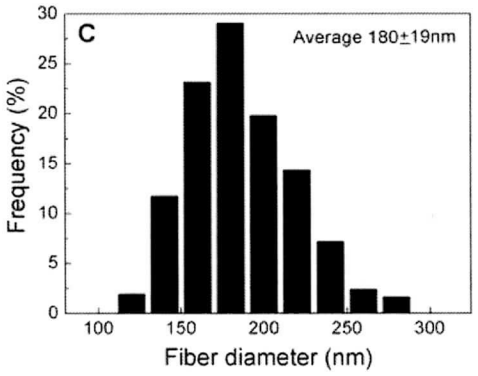
C
Average 180±19nm
Frequency (%)
Fiber diameter (nm)

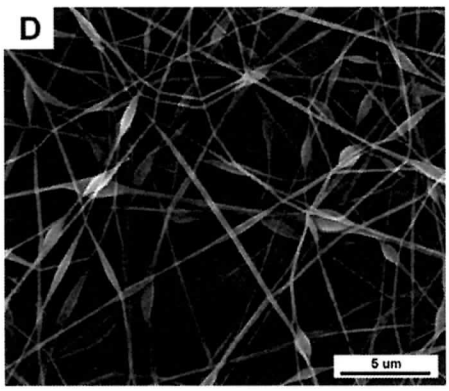
D
5 um

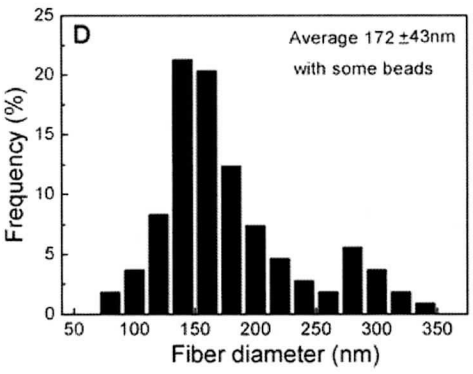
D
Average 172 ±43nm
with some beads
Frequency (%)
Fiber diameter (nm)

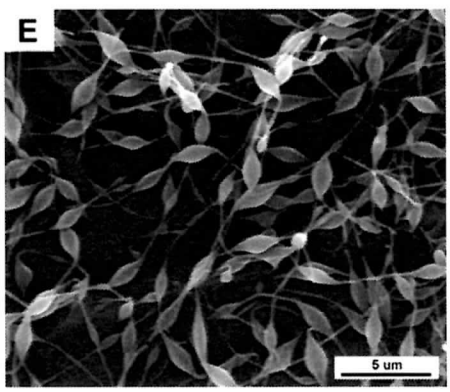
E
5 um

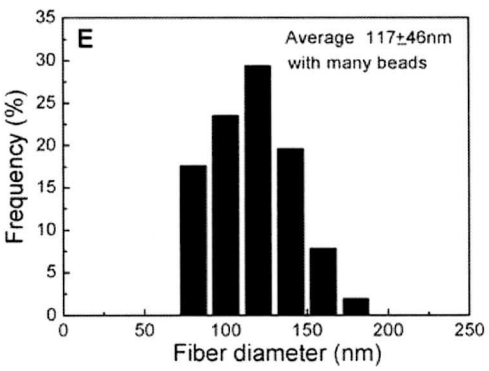
E
Average 117±46nm
with many beads
Frequency (%)
Fiber diameter (nm)

Figure 2.7 SEM image of FH-PVA nanofibers produced from solutions containing 0.1 M hydrazine monochloride (HMC) at various storage time: (A) Immediately after preparation; (B) 24 h storage; (C) 72 h storage; (D) 120 h storage; (E) 168 h storage.

2.4 Conclusions

We present a novel use of HMC for reducing the viscosity of FH-PVA. The viscosity of FH-PVA in aqueous solution decreased gradually with storage time in proportion to the amount of HMC present. This is opposite to the effect of ionic salts. In addition, after 7 days of storage, the viscosity of the FH-PVA test solutions decreased by 60% (related to the concentration of HMC) compared to those of the original solutions. These phenomena are related to the reconfiguration of hydrogen bonding in the solutions, confirmed by SAXS and ^{1}H NMR spectra observations. The morphology of FH-PVA electrospun fibers produced from solutions with different viscosities were investigated by SEM, and it was observed that the electrospun fibers became more uniform and the diameters became smaller as the concentration of HMC or the storage time increased. A beaded morphology resulted if the viscosity became too low. Therefore, the spinnability of FH-PVA aqueous solutions can be significantly improved using this method, and it is possible to readily produce ultrafine FH-PVA electrospun fibers with diameters below 200 nm.

References

[1] C. Shao, H. Kim, J. Gong, B. Ding, D. Lee and S. Park, *Mater Lett*, 57, 1579 (2003).

[2] M. Krumova, D. López, R. Benavente, C. Mijangos and JM. Peren, *Polymer*; 41, 9265 (2000).

[3] T. Okaya, *Polyvinyl alcohol: development,* John Wiley & Sons Ltd, UK: Chichester, pp.1–29 (1992).

[4] E. Chiellini, A. Corti, S. D'Antone and R. Solaro, *Prog. Polym Sci.*, 28, 963 (2003).

[5] C. C. DeMerlis and D. R. Schoneker, *Food Chem Toxicol*, 41, 319 (2003).

[6] S. H. Tan, R. Inai, M. Kotaki and S. Ramakrishna, *Polymer*, 46, 6128 (2005).

[7] K. H. Lee, O. Ohsawa, S. Lee, J. C. Park, K. W. Kim, H. Y. Kim, Y. Watanabe and I. S. Kim, *Seni Gakkaishi*, 64, 306 (2008).

[8] J. H. Park, B. S. Kim, Y. C. Yoo, M. S. Khil and H. Y. Kim, *J. Appl. Polym. Sci.*, 107, 2211 (2007).

[9] J. Doshi and D. H. Reneker, *J. Electrostat*, 35, 151 (1995).

[10] K. Wei, T. Ohta, B. S. Kim, K. H. Lee, MS. Khil, H. Y. Kim and I. S. Kim, *Polym. Adv Technol.*, 21, 746 (2010).

[11] J. M. Deitzel, J. Kleinmeyer, D. Harris and N. C. Beck Tan, *Polymer*, 42, 261 (2001).

[12] C. Chen, Y. H. Zhu, H. Bao, X. L. Yang and C. Z. Li, *Appl. Mater. Interfaces*, 2, 1499 (2010).

[13] B. E. B. Jensen, A. A. A. Smith, B. Fejerskov, A. Postma, P. Senn, E. Reimhult, M. Pla-Roca, L. Isa, D. S. Sutherland, B. Stadler and A. N. Zelikin, *Langmuir*, 27, 10216 (2011).

[14] A. D. Ossipov and J. Hilborn, *Macromolecules*, 39, 1709 (2006).

[15] A. D. Ossipov, S. Piskounova and J. Hilborn, *Macromolecules*, 41, 3971 (2008).

[16] F. Cavalieri, E. Chiessi, R. Villa, L. Vigano, N. Zaffaroni, M. F. Telling and G. Paradossi, *Biomacromolecules*, 9, 1967 (2008).

[17] S. I. Song and B. C. Kim, *Polymer*, 45, 2381 (2004).

[18] A. Koski, K. Yim and S. Shivkumar, *Mater. Lett.*, 58, 493 (2004).

[19] J. C. Park, T. Ito, KO. Kim, K. W. Kim, B. S. Kim, M. S. Khil, H. Y. Kim and I. S. Kim, *Polym. J.*, 42, 273 (2010).

[20] L. Yao, T. W. Haas, A. Guiseppi-Elie, G. L. Bowlin, D. G. Simpson and G. E. Wnek, *Chem Mater*, 15, 1860 (2003).

[21] C. X. Zhang, X. Y. Yuan, L. L. Wu, Y. Han and J. Sheng, *Euro Polym. J.*, 41, 423 (2005).

[22] W. W. Wang, Y. J. Zhu and M. L. Ruan, *J. Nanopart Res.*, 9, 419 (2007).

[23] B. Briscoe, P. Luckham and S. Zhu, *Polymer*, 41, 3851 (2000).

[24] C. Hara and M. Matsuo, *Polymer*, 36, 603 (1995).

[25] M. Komatsu, T. Inoue and K. Miyasaka, *J. Polym. Sci. Phys. Ed.*, 24, 303 (1986).

[26] M. Liu, R. Cheng and R. Qian, *J. Polym. Sci. Part B: Polym. Phys.*, 33, 1731 (1995).

[27] H. Fong, I. Chun and DH. Reneker, *Polymer*, 40, 4585 (1999).

[28] X. Zong, K. Kim, D. Fang, S. Ran, BS. Hsiao and B. Chu, *Polymer*, 43, 4403 (2002).

[29] E. Bianchi and G. Conio, *J. Phys. Chem.*, 71, 4563 (1967).

[30] H. E. Stanley. *Introduction to Phase Transitions and Critical Phenomena*, London: Oxford University Press, 1971, p.121.

[31] K. Nishikawa, Y. Kasahara and T. Ichioka, *J. Phys. Chem. B*, 106, 693 (2002).

[32] T. Fukasawa and T. Sato, *Phys. Chem. Phys.*, 13, 3187 (2011).

[33] G. I. Taylor, *Proc. Roy. Soc. A*, 280, 383 (1964).

[34] B. Adams and L. Lerner, *J. Am. Chem. Soc.*, 114, 4821 (1992).

[35] L, Poppe and H. Van Halbeek, *J. Am. Chem. Soc.*, 113, 361 (1991).

[36] L. Poppe, R. Stuike-Prill, R. B. Meyer and H. Van Halbeek, *J. Biomol. NMR*, 2, 109 (1992).

[37] R. Harris, T. J. Rutherford, M. J. Milton and S. W. Homans, *J. Biomol. NMR*, 9, 47 (1997).

[38] H. Van Halbeek and L. Poppe, *Magn. Reson. Chem.*, 30, 74 (1992).

[39] I. G. Loscertales, A. Barrero, I. Guerrero, R. Cortijo, M. Marquez and A. M. Gañán-Calvo, *Science*, 295, 1695 (2002).

[40] D. H. Reneker, A. L. Yarin, H. Fong and S. J. Koombhongse, *J. Appl. Phys.*, 87, 4531 (2000).

[41] A. L. Yarin, S. Koombhongse and D. H. Reneker, *J. Appl. Phys.*, 89, 3018 (2001).

[42] J. Zeleny, *Phys. Rev.*, 3, 69 (1914).

[43] W. J. Morton. *Method of dispersing fluids*, US Patent 705691, 1902.

[44] P. K. Baumgarten, *J. Coll. Interf. Sci.*, 36, 71 (1971).

[45] L. Larrondo and R. St. John Manley, *J. Polym. Sci.: Polym. Phys. Ed.*, 19, 909 (1981).

[46] J. Doshi and D. H. Reneker, *J.* Electrost., 35, 151 (1995).

[47] G. Srinivasan and D. H. Reneker, *Polym. Int.*, 36, 195 (1995)

CHAPTER THREE

Preparation of fully hydrolyzed ultra-high-molecular-weight polyvinyl alcohol nanofibers by viscosity control and improvement of fiber hot water resistance by annealing

3 Preparation of fully hydrolyzed ultra-high-molecular-weight polyvinyl alcohol nanofibers by viscosity control and improvement of fiber hot water resistance by annealing

Fully hydrolyzed ultra-high-molecular-weight polyvinyl alcohol (PVA) electrospun fibers with uniform diameters of about 200 nm were fabricated by reducing the viscosity of PVA in aqueous solution. A novel viscosity-modifier (hydrazine monochloride, HMC) gradually reduces the viscosity of PVA aqueous solution over a period of several days. This phenomenon is counter to the usual effect of ionic salt addition. After being stored for several days, the viscosity decreased by up to 60% compared to that of an equivalent pure PVA solution. Using HMC to control the viscosity of the PVA solution made it possible to fabricate ultrafine electrospun fibers. In addition, the hot water resistance of the fibers was obviously improved by annealing.

3.1 Introduction

Electrospinning is an inexpensive and relatively simple method to produce fibers with diameters in the nanometer range [1-5]. Polyvinyl alcohol (PVA) is one of the most popular polymers used for ultrafine electrospun fiber production. Nano-scale PVA fibers have several interesting characteristics, such as high surface area to mass ratio, significant possibilities for surface functionalization, and high mechanical performance due to an improvement in the molecular organization of the spun fiber. These properties make electrospun PVA fibers excellent candidates for many applications, such as filtration, reinforcing materials, wound dressings and drug releasing carriers [6-11].

Fully hydrolyzed ultra-high-molecular-weight PVA (FH-UHMW-PVA), with a degree of polymerization (DP) ≥ 8000), can be used to produce "super fibers" with high strength and high modulus due to the intrinsically high chemical stability, water resistance, and excellent physical and mechanical properties of the parent material. FH-UHMW-PVA nanofibers would therefore also have better properties than those produced from ordinary PVA. However, electrospinning nanofibers from FH-UHMW-PVA is extremely difficult due to the extremely high viscosity in solution, even at low concentrations [12-15], and the use FH-UHMW-PVA to fabricate ultra fine electrospun fibers has not yet been reported.

We have however, successfully fabricated electrospun FH-UHMW-PVA fibers with nominal diameters of 200 nm by controlling the solution viscosity. Hydrazine monochloride (HMC) is widely used in organic synthesis, but until now has not been used for reducing the viscosity of PVA [16]. The effect of HMC on the viscosity characteristics of the solutions was investigated and a reason for the change is proposed. Furthermore, parameters such as concentration and storage time were systematically examined and their effects on the morphology and diameter of electrospun FH-UHMW-PVA fibers are described. In addition, the solubility of the fibers, as shown by resistance to hot water was improved by annealing. It is now possible to produce ultrafine FH-UHMW-PVA electrospun fibers with excellent hot water resistance.

3.2 Experimental details

3.2.1 Materials

Samples of PVA with a degree of hydrolysis (DH) > 99 % and a degree of polymerization (DP) = 8000, and with DH > 99 % and DP = 1700 were kindly provided by Kuraray Co. Ltd, Tokyo, Japan. In this paper the abbreviation form, PVA-X-Y, is adopted to characterize polymer molecular weight and degree of hydrolysis. For example, PVA-80-99 represents a PVA with a DP of 8000 and a DH of 99 %.

As we known, PVA is produced industrially by hydrolysis of poly(vinyl acetate). Thus, DH of PVA is simply defined as the following:

$$DH = \frac{x}{x+y} \times 100\%$$

where x and y are the molar fractions of the hydroxyl and the acetate groups, respectively, specified in the following stoichiometric formula:

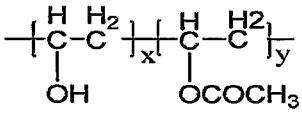

Hydrazine monochloride (HMC, or $N_2H_4 \cdot HCl$) and isopropanol (IPA) were obtained from Tokyo Chemical Industry Co., Ltd. All chemicals were of analytical grade and were used without further purification. De-ionized (DI) water was used as the solvent.

3.2.2 Preparation of PVA solutions

PVA-80-99 aqueous solution was prepared using the method described by Briscoe et al [17]. In brief, PVA powder was dispersed in distilled water at 25 °C for 2 h and this suspension was rapidly heated to above 95 °C and kept at this temperature with high speed stirring for about 3 hours. The solution was then cooled to room temperature. Various amounts of HMC were added to certain amounts of PVA solution to make solutions with HMC concentrations of 0.05 mol/L, 0.1 mol/L and 0.3 mol/L. These solutions were stirred for 2 hours to ensure homogenization and then put into a 40 °C water bath for several days. Viscosity, conductivity and surface tension were measured every 24 h at a temperature of 25 °C.

3.2.3 Electrospinning

The electrospinning experiments were performed at 25°C. The polymer solution was placed in a 12 mL syringe with a 0.8mm id needle, and the needle was connected to the high voltage power supply. A rotating cylinder wrapped with aluminum foil was used as a grounded collector. The applied voltage and the tip-to-collector distance (TCD) were fixed at 10 kV and 15 cm. The syringe pump flow rate

was set to 0.3 mL/h. Immediately before electrospinning, isopropanol (IPA) was added at 5wt% to the PVA solutions to slightly modify the surface tension [18].

3.2.4 Annealing and water resistance

Immediately after spinning, the electrospun fibers were dried at room temperature in a vacuum oven for 2 h. The annealing treatment was proceeded at 180 °C for 2 h. Then the samples were cooled down under nitrogen atmosphere before being removed from the oven. The annealed PVA fibers were immersed in DI water at 25 °C, 40°C and 60 °C for 3 days separately. The samples were then transferred into isopropyl alcohol for 5 min before loading in a chamber to complete the drying process under vacuum (0.002 MPa) for later SEM characterization.

3.2.5 Measurement

The rheological properties of the PVA-80-99 solutions were measured using a Rheologia-A300 controlled stress rheometer (ELQUEST) at 25 °C. A co-axial cylinder arrangement with a gap of 2.1mm was used to measure the apparent viscosities using the Steady Flow Viscosity Testing mode. Samples were tested after various storage times and a recycling-water bath was employed to ensure constant temperature surroundings. Apparent viscosities of different PVA solutions measured at a shear rate of 100 sec-1 were selected as reference viscosities.

Molecular weight measurements were performed on the Zetasizer Nano series (Malvern Instruments, UK) using a process called Static Light Scattering (SLS). All PVA solutions were tested under a series of concentrations under 0.1 wt%. The molecular weight was calculated through the modified Rayleigh equation [19] as follows:

$$\frac{KC}{R_\theta} = \frac{1}{M} + 2A_2C \tag{1}$$

R_θ: The Rayleigh ratio.

M: Sample molecular weight.

A_2: 2nd Virial Coefficient.

C : Concentration.

The conductivity of the solutions was measured using a conductivity meter (Model SC72 personal SC meter, Yokogawa Electric Corporation), and a tension meter (CBVP-Z, Kyowa Interface Science Co. Ltd, Saitama, Japan) using the Wilhelm plate method, was used to determine surface tension. The morphology of electrospun fibers was observed on a scanning electron microscope (SEM, Hitachi S-3000N) on samples sputtered with Palladium-Platinum.

Table 3.1 Molecular weight of PVA (SLS data)

	PVA molecular weight ($\times 10^3$)			
Concentration of HMC	0	0.05M	0.1M	0.3M
As-prepared	786	755	540	499
After 168 h	795	742	533	503

3.3 Results and discussion

3.3.1 Effect of HMC on the viscosity of PVA

PVA-80-99 is nearly completely hydrolyzed, and so a preparation temperature above 95 °C is required for the complete dissolution of the solid in an acceptable time. It is believed that both the inter- and intra-molecule hydrogen bonding in aqueous PVA solutions is disrupted by thermal energy during solution, but upon cooling the hydrogen bonds can re-form resulting in an increase in viscosity [20-22].

The viscosity of a PVA solution (η) depends on the molecular weight (Mw), concentration (c), degree of hydrolysis and the type of solvent. The dependence of zero shear viscosity on Mw in many polymers can be described by the Mark–Houwink equation:

$$[\eta] = K(M_w)^a$$

where "K" and "a" are the Mark-Houwink constants. Generally, the effects of Mw and c on solution viscosity can be modeled [23,24] as:

$$\eta = K(c\rho)^{\alpha}(M_w)^{\beta}$$

(α is empirical single-parameter and ρ is solution density)

According to the equation, the viscosity of the solution depends strongly on M_w and concentration. Furthermore, for fully hydrolyzed PVA aqueous solutions, there is inter- and intra chain hydrogen bonding between the polar hydroxyl groups in the PVA molecules, which will lead to a more rapid increase in viscosity. As shown in Fig. 1, the viscosity of a 6 wt. % PVA-17-99 solution is only 0.3 Pa·s, but the viscosity of PVA-80-99 is about 2 Pa·s, and the rate of increase of viscosity accelerates in proportion to concentration.

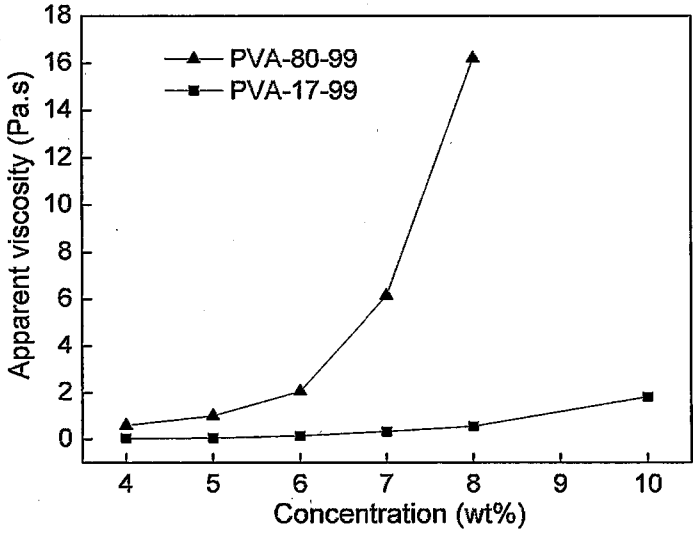

Figure 3.1 The change in apparent viscosity of PVA aqueous solutions with molecular weight and concentration at 25 °C (Shear rate: 100 1/sec).

Aqueous solutions of fully hydrolyzed PVA undergo a viscosity increase with time and may finally gel. It is reported that several additives, such as inorganic salts and organic compounds (Na_2SO_4, NaCl and KCl) will increase the viscosity, and a few such as NH_4SCN and IPA have a

distinct viscosity stabilizing effect [25]. However, we find that HMC has an unexpected effect on the viscosity of aqueous PVA, as can be seen in Fig. 2, where in the presence of HMC, the apparent viscosity of PVA in solution decreases gradually with storage time with final viscosities reduced by up to 60% depending on the amount of HMC. The addition of HMC may disrupt PVA chain inter- and intra-chain hydrogen bonding resulting in a decrease viscosity.

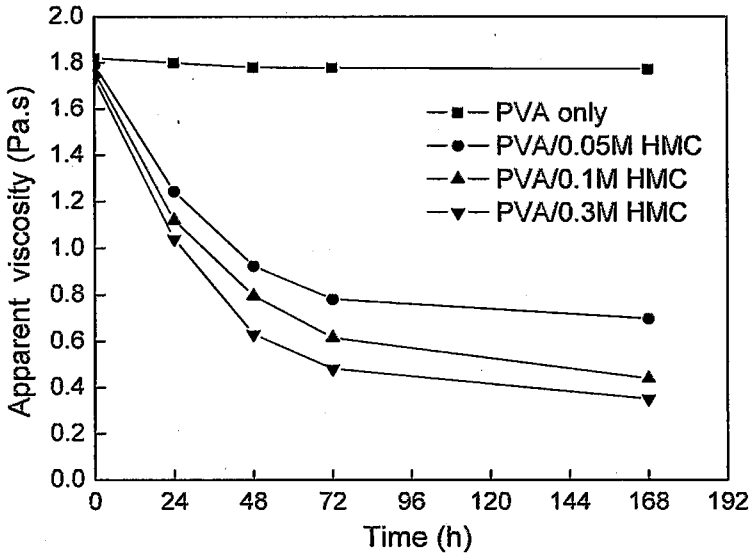

Figure 3.2 The variation of apparent viscosity of FH-UHMW-PVA aqueous solutions with varying amounts of HMC at 25 °C (Shear rate: 100 sec^{-1}).

Figure 3 shows the relationship between shear rate and apparent viscosity for different PVA solutions after 168 h. Clear shear thinning behavior is observed in the pure PVA-80-99 solution. This is due the ultra high molecular weight (causing more entanglements between the PVA chains) and the higher DH (causing more inter and intra chain hydrogen bonding in the solution) and hence a high degree of interaction between the PVA chains. This shear thinning behavior also indicates the presence of stronger polymer chain associations. In addition, after the viscosities had decreased, the PVA-80-99 solutions show almost no shear thinning. According to the SLS data as shown in Table 1, the molecular weights of our samples have almost no change although their viscosities greatly decreased. It is probable that the addition of HMC reduces inter- and intra-chain hydrogen bonding and thus

reduces the degree of interaction and entanglement between the molecular chains in PVA-80-99.

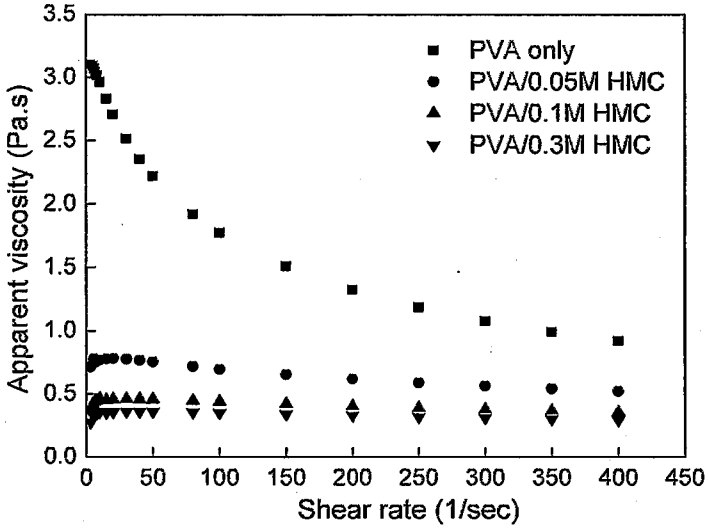

Figure 3.3 Relationship between apparent viscosity and shear rate for PVA aqueous solutions with varying concentrations of HMC at 25 °C (storage time: 168 h).

3.3.2 Electrical conductivity and surface tension

We have also examined electrical conductivity and surface tension, which are important factors in electrospinning [26]. As seen in Fig. 3, the surface tension was slightly reduced by adding HMC while the conductivities increased sharply in proportion with the concentration of HMC. However, both the surface tension and conductivity changed very little during the period of storage although during the same period the viscosity decreased greatly.

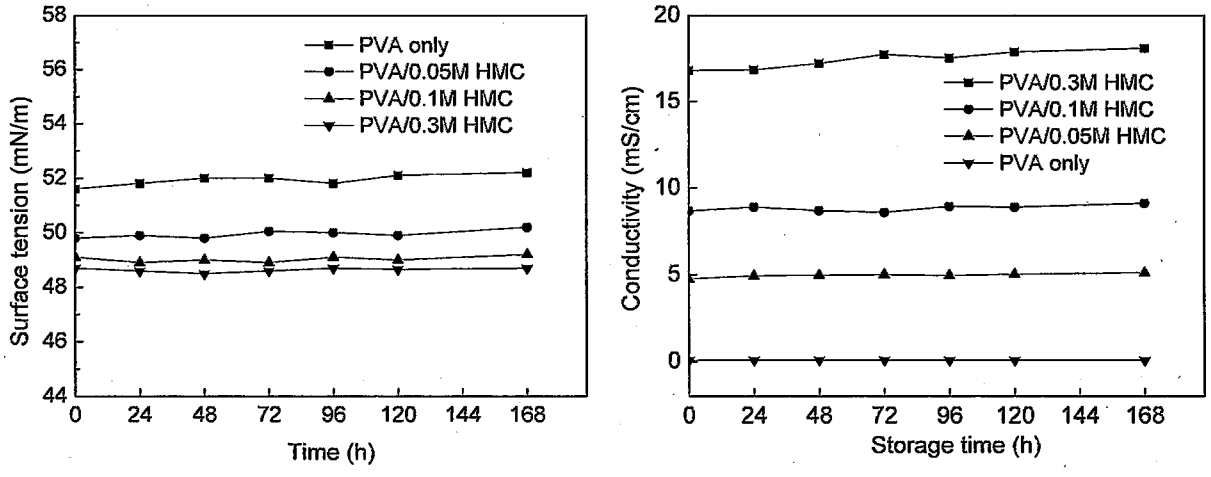

(a) (b)

Figure 3.4 Surface tension (a) and conductivity (b) of PVA in aqueous solution with different concentrations of HMC and varying storage time at 25 °C.

3.3.3 Electrospinnability

The fundamental processes in electrospinning are related to solution viscosity and surface tension; these properties also significantly affect the morphology and diameter of the fibers [27-31]. It is very different to fabricate electrospun fibers using FH-UHMW-PVA because of the extremely high solution viscosity, even at low concentration: viscosity is the critical factor in electrospinning of FH-UHMW-PVA.

We proposed the use of a special additive, HMC, to reduce the viscosity of PVA-80-99 solutions and thence to electrospin fibers. Electrospun PVA-80-99 fibers fabricated from solutions with different viscosities, controlled by a combination of HMC addition and aging are shown in Fig. 5. From the pure PVA control solution (Fig. 5a), long threads with irregular thick structures were formed from the high surface tension and viscosity precursor solutions. However, in the presence of HMC, the diameters of electrospun fibers are significantly decreased (when the concentration of HMC is above 0.3M and after 168 h) and fibers with diameter of 200-250 nm could be fabricated. This is a combined effect due to the decrease of surface tension and the increase in conductivity, and the decrease in viscosity. Control of all these factors is required to get regular morphology ultrafine fibers.

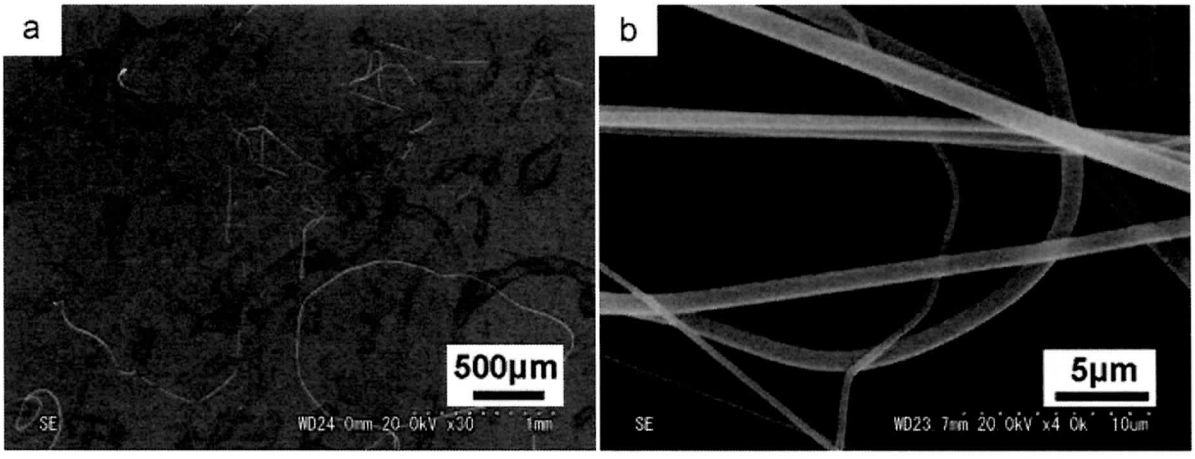

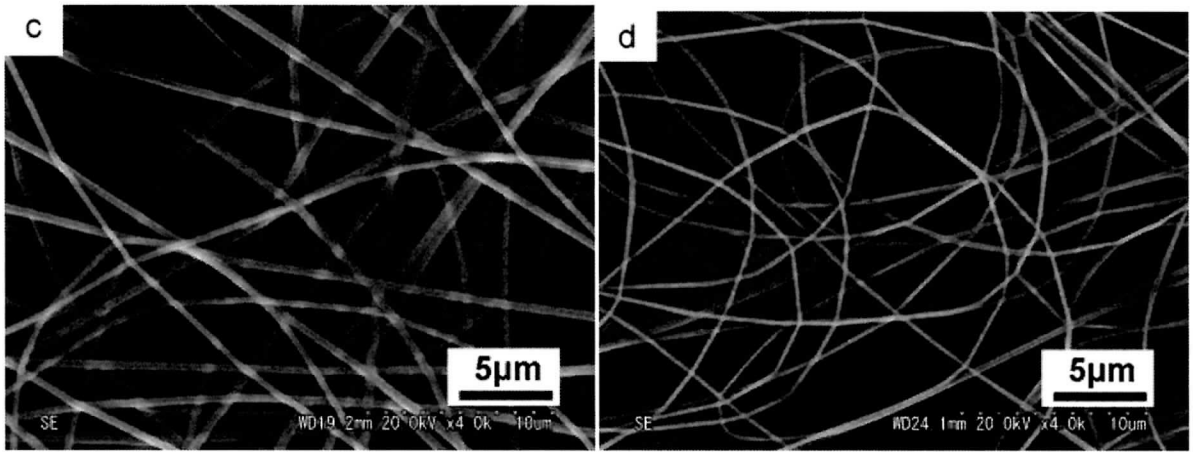

Figure 3.5 SEM images of electrospun PVA-80-99 fibers produced from different solutions: (a) PVA only; (b) PVA/0.05M HMC; (c) PVA/0.1M HMC; (d) PVA/0.3M HMC). (Storage time: 168 h)

To reveal the relationship between viscosity, fiber diameter and morphology, PVA-80-99 solution with 0.3M HMC was selected as a model solution since its surface tension and conductivity remained virtually constant (shown in Fig. 6), even as the viscosity gradually decreased during the storage period: electrospun fibers from this solution are shown in Fig. 6. Initially, both the conductivity and viscosity are high and it is difficult to form a stable jet and only some spotty deposition was observed on the aluminum foil target (Fig. 6a). After several days of storage, the solution viscosity decreased, and uniform electrospun fibers could be fabricated. All the results indicate that viscosity is a predominant factor affecting fiber diameter. Electrospun PVA-80-99 fibers with diameter down to about 200 nm can be fabricated by this method of controlling viscosity.

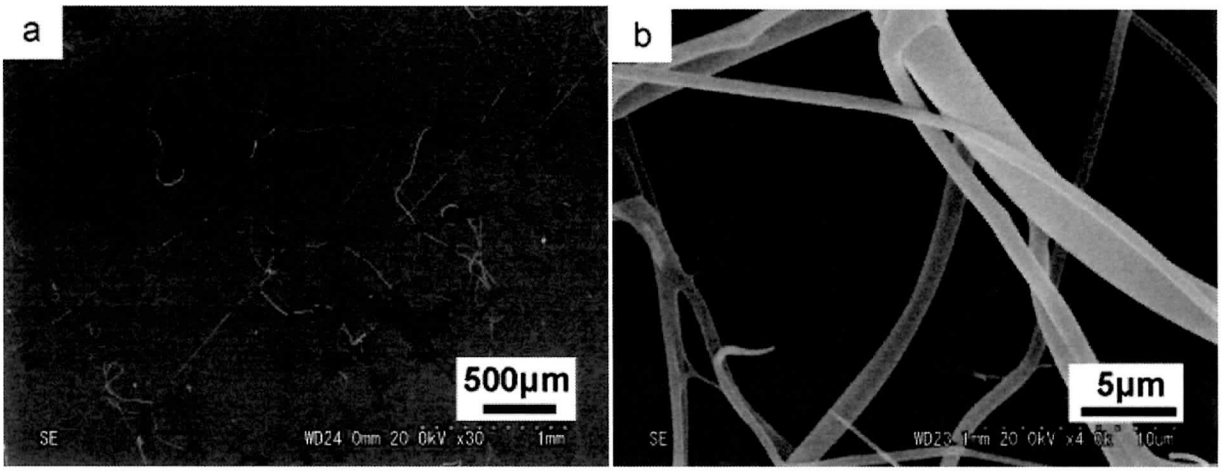

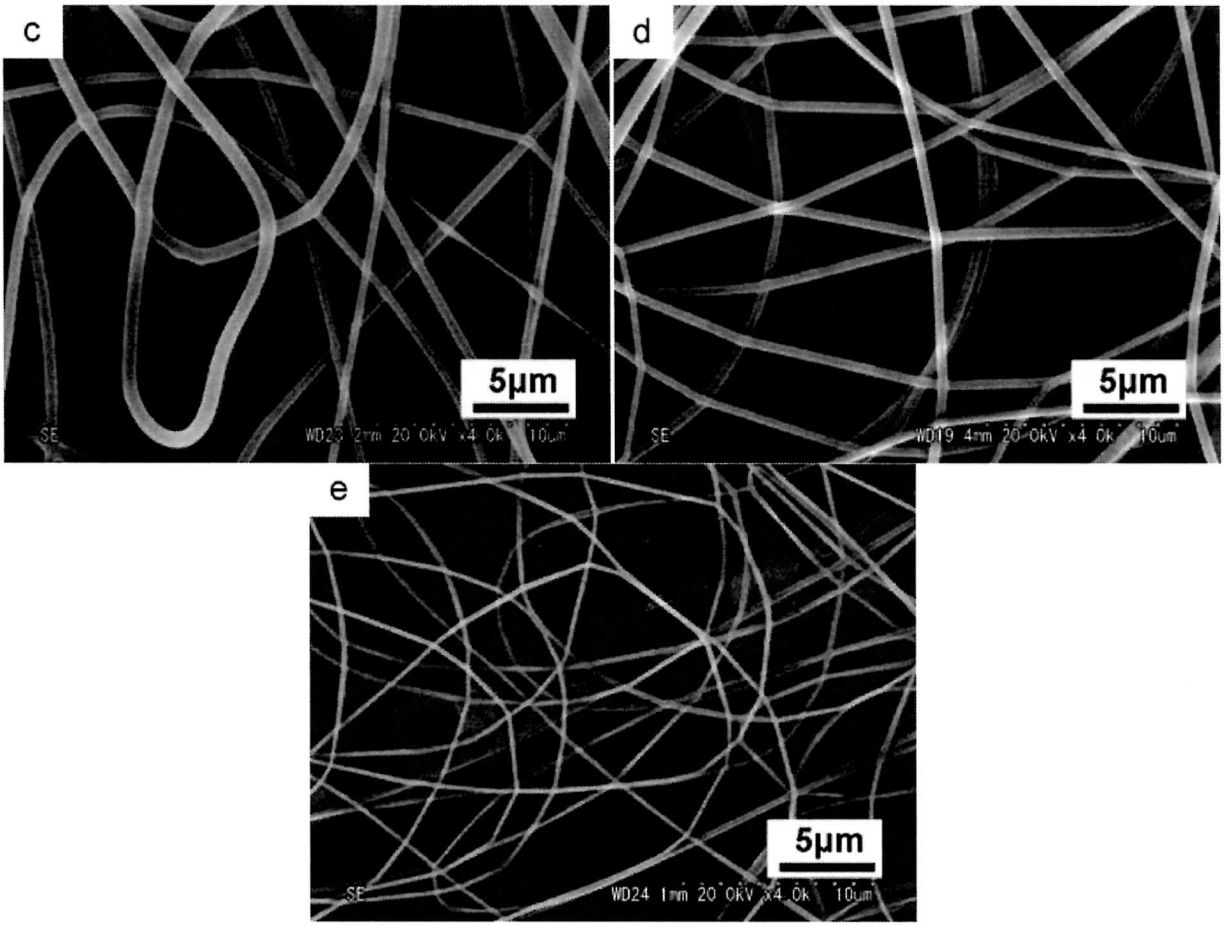

Figure 3.6 SEM images of PVA-80-99 nanofibers produced from solutions containing 0.3M HMC at various storage times: (a) Immediately after preparation; (b) 24 h storage; (c) 72 h storage; (d) 120 h storage; (e) 168 h storage.

3.3.4 Stabilization of PVA fibers against dissolution

The biggest drawback of electrospun PVA nanofibers, and a significant limit to their practical application, is the poor stability in water of the material [32,33]. When an electrospun PVA mat is immersed in water, the mat instantaneously shrinks and the unique nanofibrous structure is lost by dissolution into the aqueous environment. As shown in Fig. 6, the as-spun PVA-17-99 fibers display very poor stability in water (the left side of SEM image of Fig. 7a). After immersion in DI water for 1 min, the fiber structure has completely disappeared and a film with no porosity has formed. However, if ultra high molecular PVA, PVA-80-99 is subjected to the same treatment, the fiber structure still can be seen

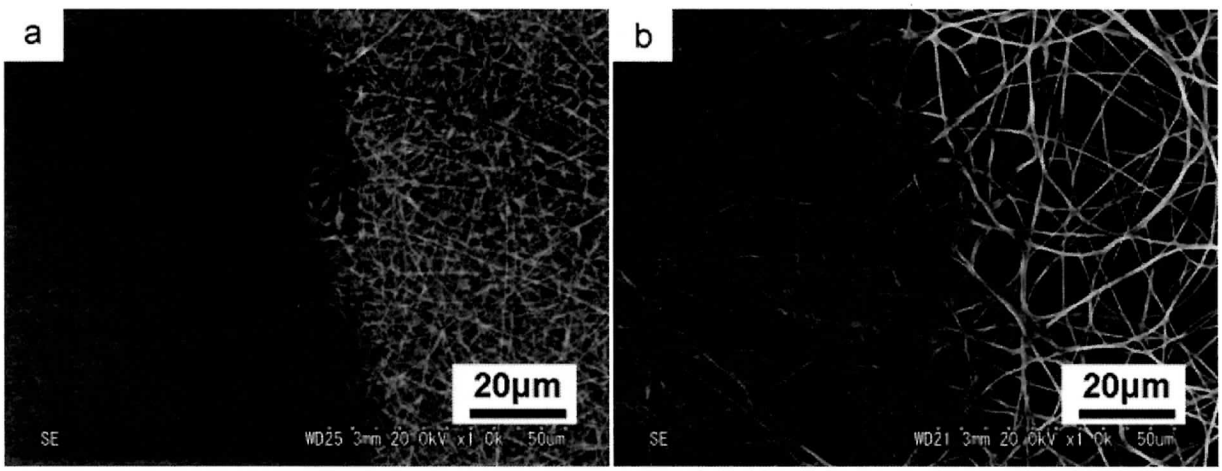

Figure 3.7 SEM images of PVA fibers after immersed in 25°C DI water for 1min (a) PVA-17-99 (b) PVA-80-99

To improve the water resistance of PVA nanofibers, most researchers have concentrated on chemical cross-linking by a variety of substances including glutaraldehyde, acetaldehyde, or formaldehyde [34,35]. The process of annealing is an alternative physical treatment to increase the stability of PVA nanofibers [36]. Electrospun PVA-80-99 nanofibers were annealed at 180 °C in a nitrogen atmosphere. This treatment improves the stability of the PVA-80-99 nanofibers, and also has the beneficial effect of eliminating any vestige of HMC that might still be present. The treated fibers were immersed in water at different temperatures for several days to test the water resistance. As seen in Fig. 8, after 3 d, there was almost no change for samples immersed at temperatures up to 40 °C, and even at 60 °C there is still a significant fibrous character (Fig. 8d).

It is believed that annealing increases the degree of crystallinity, and hence the number of physical cross-links in electrospun PVA fibers. This may occur by removal of bound water within the fibers allowing PVA-water hydrogen bonding to be replaced by intermolecular polymer hydrogen bonding and also increasing the degree of crystallization.

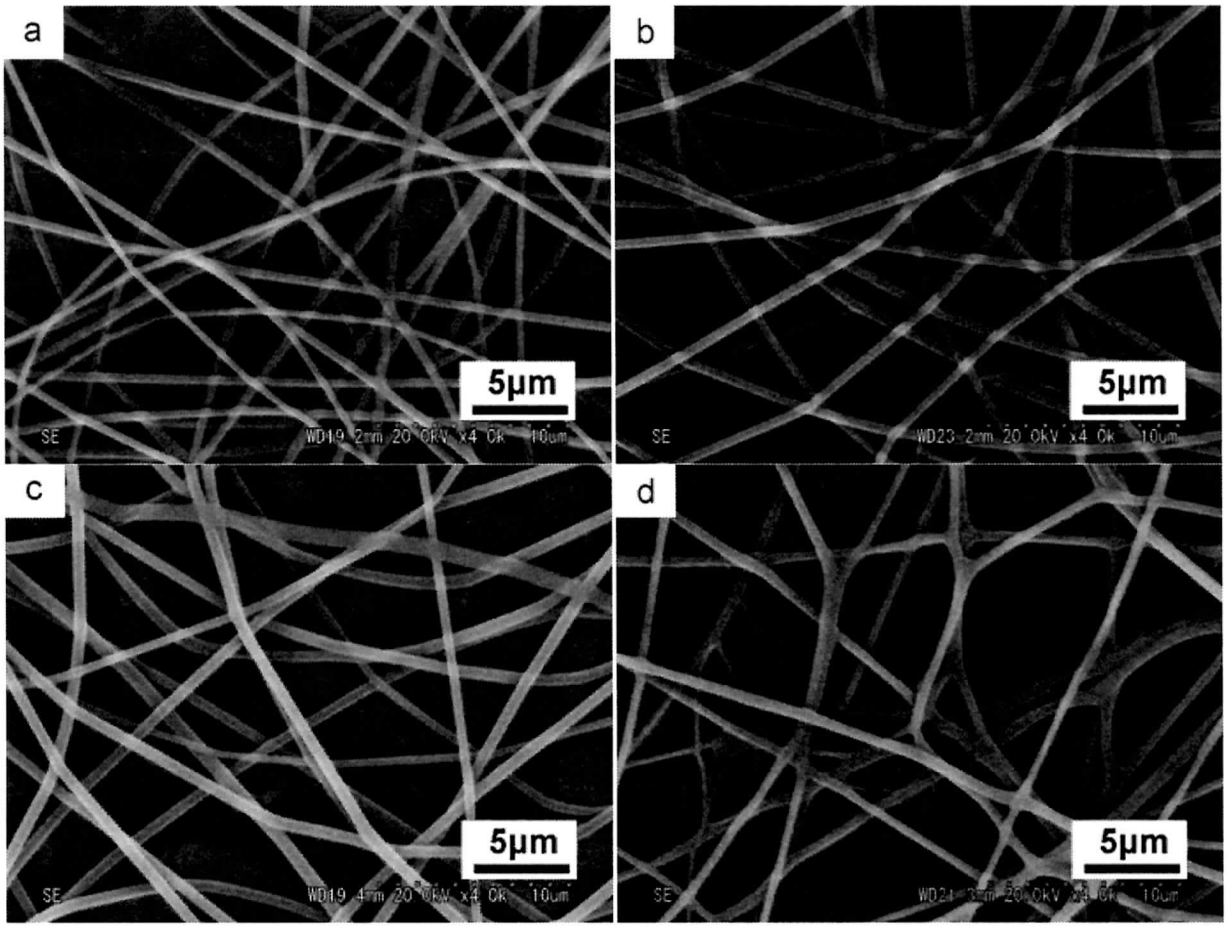

Figure 3.8 SEM images of PVA-80-99 fibers with 2 h of 180 °C annealing treatment after (a) annealing; (b) immersed in 25 °C DI water for 3 days; (c) immersed in 40 °C DI water for 3 days; (d) immersed in 60 °C DI water for 3 days.

3.4 Conclusions

We present the novel use of HMC to reduce the viscosity of fully hydrolyzed UHMW PVA. The viscosity of PVA-80-99 in aqueous solution is decreased gradually with time in proportion to the amount of HMC present; this is opposite to the effect of the addition of ionic salts. After 7 days of storage, the viscosity of PVA-80-99 solutions had decreased by about 60% (related to the concentration of HMC) compared to those of the original solutions. These phenomena are related to the reconfiguration of hydrogen bonding in the solutions. The morphology of PVA-80-99 electrospun fibers produced from solutions with different viscosities were investigated by SEM, and it was

observed that the electrospun fibers became more uniform and the diameters became smaller as the concentration of HMC or the storage time increased. As a result, the spinnability of fully hydrolyzed UHMW PVA can be significantly improved by using this method, making it possible to readily produce ultrafine fully hydrolyzed UHMW PVA electrospun fibers with diameters about 200 nanometers. Furthermore, by simple annealing treatment, the electrospun fibers can remains their structure even in 60 °C water.

Reference

[1] S. H. Tan, R. Inai, M. Kotaki, S. Ramakrishna, Polymer, 46, 6128 (2005).

[2] K. H. Lee, O. Ohsawa, S. Lee, J. C. Park, K. W. Kim, H. Y. Kim, Y. Watanabe, I. S. Kim, Sen'i Gakkaishi, 64, 306 (2008).

[3] J. H. Park, B. S. Kim, Y. C. Yoo, M. S. Khil, H. Y. Kim, J. Appl. Polym. Sci., 107, 2211 (2007).

[4] J. Doshi, D. H. Reneker, J. Electrostat., 35, 151 (1995).

[5] K. Wei, T. Ohta, B. S. Kim, K. H. Lee, M. S. Khil, H. Y. Kim, I. S. Kim, Polym. Adv.Technol., 21, 746 (2010).

[6] J. M. Deitzel, J. Kleinmeyer, D. Harris, N. C. Beck Tan, Polymer, 42, 261 (2001).

[7] C. Chen, Y. H. Zhu, H. Bao, X. L. Yang, C. Z. Li, Appl. Mate. Interfaces, 2, 1499 (2010).

[8] B. E. B. Jensen, A. A. A. Smith, B. Fejerskov, A. Postma, P. Senn, E. Reimhult, M. Pla-Roca, L. Isa, D. S. Sutherland, B. Stadler, A. N. Zelikin, Langmuir, 27, 10216 (2011).

[9] A. D. Ossipov, J. Hilborn, Macromolecules, 39, 1709 (2006).

[10] D. A. Ossipov, S. Piskounova, J. Hilborn, Macromolecules, 41, 3971 (2008).

[11] F. Cavalieri, E. Chiessi, R. Villa, L. Vigano, N. Zaffaroni, M. F. Telling, G. Paradossi, Biomacromolecules, 9, 1967 (2008).

[12] S. I. Song, B. C. Kim, Polymer, 45, 2381 (2004).

[13] A. Koski, K. Yim, S. Shivkumar, Mater. Lett., 58, 493 (2004).

[14] W. S. Lyoo, S. J. Lee, J. H. Kim, S. K. Noh, B. C. Ji, B. C. Kim, J. Appl. Polym. Sci., 93, 41 (2004).

[15] H. M. Ji, H. W. Lee, M. R. Karim, I. W. Cheong, E. A. Bae, T. H. Kim, M. S. Islam, B. C. Ji, J. H. Yeum, Collo. Polym. Sci., 287, 751 (2009).

[16] W. W. Wang, Y. J. Zhu, M. L. Ruan, J. Nanopart. Res., 9, 419 (2007).

[17] B. Briscoe, P. Luckham, S. Zhu, Polymer, 41, 3851 (2000).

[18] A. Saluja, A. V. Badkar, D. L. Zeng, S. Nema and D. S. Kalonia, Biophysical Journal 92, 234 (2007).

[19] C. Hara, M. Matsuo, Polymer, 36, 603 (1995).

[20] M. Komatsu, T. Inoue, K. Miyasaka, J. Polym. Sci. Phys. Ed., 24, 303 (1986).

[21] M. Liu, R. Cheng, R. Qian, J. Polym. Sci. Part B: Polym. Phys., 33, 1731 (1995).

[22] P. Hong, C. Chou, C. He, Polymer, 42, 6105 (2001).

[23] J. C. J. F. Tacx, H. M. Schoffeleers, A. G. M. Brands, L. Teuwen, Polymer, 41, 947 (2000).

[24] R. P. A. Hartman, D. J. Brunner, D. M. A. Camelot, J. C. M. Marijnissen, and B. Scarlett, Journal of Aerosol Science, 31, 65 (2000).

[25] C. A. Finch, Poly(vinyl alcohol) Development, Wiley, Chichester, UK, 1992.

[26] L. Yao, T. W. Haas, A. Guiseppi-Elie, G. L. Bowlin, D. G. Simpson, G. E. Wnek, Chem. Mater., 15, 1860 (2003).

[27] J. Zeleny, Physical Review, 3, 69 (1914).

[28] W. J. Morton, US Patent 705691, (1902).

[29] P. K. Baumgarten, J. Collo. Inter. Sci., 36, 71 (1971).

[30] L. Larrondo, R. St. John Manley, J. Polym. Sci.: Polym. Phys., 19, 909 (1981).

[31] J. Doshi, D. H. Reneker, J. Electrost., 35, 151 (1995).

[32] V. S. Praptowidodo, J. Mol. Struct., 739, 207 (2005).

[33] L. B. Carvalho, A. M. Araujo, A. M. P. Almeida, W. M. Azevedo, Sens. Actuators B Chem., 35, 427 (1996).

[34] S. Kurihara, S. Sakamaki, S. Mogi, T. Ogata, T. Nonaka, Polymer, 37, 1123 (1996).

[35] L. Gao, C. J. Seliskar, Chem. Mater., 10, 2481 (1998).

[36] K. K. H. Wong, M. Z. Allmang, W. K. Wan, J. Mater. Sci., 45, 2456 (2010).

CHAPTER FOUR

Preparation of magnetic polyvinyl alcohol composite nanofibers with homogenously dispersed nanoparticles and high water resistance

4 Preparation of magnetic polyvinyl alcohol composite nanofibers with homogenously dispersed nanoparticles and high water resistance

Magnetic nanoparticles (MNPs)/polymer composite nanofibers were prepared via electrospinning of polyacrylic acid (PAA)/polyvinyl alcohol (PVA) aqueous solutions with homogenously dispersed magnetite Fe_3O_4 nanoparticles (NPs). Experiment results showed that the diameters of Fe_3O_4 NPs were in a range of 10 nm to 40 nm under all of our synthesis conditions; and Fe_3O_4 NPs can homogenously disperse in PVA composite nanofibers when they were stabilized by PAA; the crystallinity of PAA/PVA nanofibers increased along with the increase in Fe_3O_4 NPs content. The magnetic property of Fe_3O_4 NPs/PAA/PVA composite nanofibers was also investigated and the results showed that the composite nanofibers show a soft ferromagnetic behavior which is the same as Fe_3O_4 at room temperature. In addition, the water resistance of Fe_3O_4 NPs/PAA/PVA composite nanofibers was dramatically enhanced by heat treatment. Therefore, in our process to preparing magnetic Fe_3O_4 NPs/PVA composite nanofibers, PAA acts not only as a dispersant but also as a cross-linking agent.

4.1 Introduction

Polymer magnetic nanocomposite systems have many potential applications in various fields. Thus, interest in the design and controlled preparation of these composite materials with magnetic property continues to increase.[1−4] One of the most useful magnetic materials may be magnetic

fiber, which is used for applications such as magnetic paper, health-care cloth, magnetic filters, electromagnetic wave adsorbents, and various other applications because of their high forming abilities.[5–7] Traditionally, magnetic fibers have been produced by coating magnetite nanoparticles (MNPs) on the surface of the fibers.[8–10] However, the magnetism of these products is not high enough for magnetic application because there may be not enough amounts of MNPs coated on the surface. Furthermore, the magnetism would weaken as a result of the losses of MNPs after post treatments. To obtain a magnetic fiber with higher magnetism and higher stability, some researchers tried to incorporate the MNPs into a polymeric fiber matrix directly.[11–14] Nevertheless, one of the main challenges is the ability to deliver well-dispersed nanoparticles with the desired composition as well as the prevention of aggregation.[15–17] Surfactants can be used to resolve the issue and prepare homogeneous MNPs/polymer composite system, but their use will unavoidably sacrifice part of the mechanical property of the composite fibers.

Electrospinning is a relatively simple and inexpensive method to produce fibers with a diameter ranging from a few micrometers to a few nanometers.[18–21] Due to their large surface areas and small sizes in comparison with conventional textiles, electrospun nonwoven mats have become excellent candidates for applications in filtration, biomedical films, and scaffolds for tissue engineering.[22–25] This novel fiber-spinning technique provides the capacity to produce ultrafine magnetic composite fibers a using mixture of various polymers and magnetic nanoparticles.[26–30]

Polyvinyl alcohol (PVA) is one of the most popular polymers used for electrospun composite fiber production due to its thermostability, excellent biocompatibility and high mechanical performance.[31–35] However, its applications are limited by its high hydrophilicity, through which it dissolves immediately on contact with water. Therefore, PVA nanofibers have usually been modified by either chemical or physical cross-linking to improve their water resistance and mechanical properties.[36]

This paper describes the fabrication of MNPs/PAA/PVA composite nanofibers with homogeneous dispersion of Fe_3O_4 NPs and high water resistance. In our experiments, polyacrylic acid (PAA) was used as a polymer surfactant[37, 38] to stabilize Fe_3O_4 NPs aqueous suspension and facilitate their dispersal in PVA solutions, due to PAA could provide electrostatic and steric repulsion against particle aggregation. Furthermore, PAA was also used as a cross-linking agent to enhance the water resistance of the magnetic composite nanofibers through heat treatment.[39] This method provides a simple and convenient process to prepare homogenous NPs/PVA composite system with high stability and can greatly improve the practical application of NPs/PVA composite.

4.2 Experimental details

4.2.1 Materials

PVA HC with a degree of hydrolysis (DH) = 99.9 mol% and degree of polymerization (DP) =1700 was kindly provided by Kuraray Co. Ltd, Tokyo, Japan. PAA (M_W=5000), Iron (II) sulfate heptahydrate ($FeSO_4 \cdot 7H_2O$), iron (III) chloride anhydrous ($FeCl_3$), ethanol, HCl solution and ammonia solution (28% NH_3 in water) were purchased from Wako Pure Chemical Industries, Ltd., Japan. All chemicals were of chemical grade and were used without further purification. Distilled water was used as the solvent.

4.2.2 Preparation of Magnetic Fe_3O_4 NPs

Magnetic Fe_3O_4 NPs were prepared by coprecipitating Fe^{2+} and Fe^{3+} ions in aqueous ammonia solution.[40] Next, 200 mL of a mixture of $FeCl_3$ (0.01 mol/L) and $FeSO_4$ (0.006 mol/L) at pH 2 was prepared under N_2. Then, NH_4OH aqueous solution (5 mol/L) was dropped into it with violent stirring until the pH of the solution rose to 10. The resulting precipitate was stirred for 30 min. After triple washes with deionized water and ethanol the precipitates were re-suspended in 100 mL deionized water. The pure magnetic NPs were isolated from the solution by a magnet bar and dried in

vacuum oven at 40 °C for 48 h.

4.2.3 Preparation of Fe_3O_4 NPs/PVA/ and Fe_3O_4 NPs/PAA/PVA suspension

1.5 g Fe_3O_4 NPs were dispersed in 50 mL distilled water and 50 mL (5 wt%) PAA aqueous solution respectively, then both suspensions was treated by ultrasonic mixing for 30 min to get two kinds of 3 wt% Fe_3O_4 NPs suspension for reserve. PVA chips were dissolved in distilled water in a static rotary mixer (500 rpm) at 25 °C for 1 h and then rapidly heated to 95 °C and this temperature was maintained with high-speed stirring (1000 rpm) for 2 h to obtain a 30 wt% PVA solution. Varying amounts of 3 wt% Fe_3O_4 NPs suspension, PAA solution and water were then added to the as-prepared PVA solution to adjust the Fe_3O_4 NPs concentration in the PVA to 5, 10, and 15 wt% (weight of solid PVA content) while maintaining the PVA concentration at 8 wt% (PVA/PAA = 2:1) in each composite suspension with high speed stirring. Finally, two kinds of suspension were obtained: PVA/Fe_3O_4 NPs and PVA/PAA/Fe_3O_4 NPs.

4.2.4 Electrospinning

The electrospinning setup (Kato Tech, Kyoto, Japan) used in this study consists of a syringe with a flat-end metal needle (1.20 mm × 38 mm), a syringe pump for controlling the feeding rate, a grounded cylindrical stainless steel mandrel, and a high-voltage direct current (DC) power supply. For the electrospinning procedure, the suspensions were loaded into a syringe coupled with nozzles and electrospun under a high DC voltage of 10 kV, with a distance from the needle tip to the collector of 15 cm and a feeding speed of 0.5 mL/h.

4.2.5 Annealing treatment and water resistance test

Immediately after spinning, the electrospun fibers were dried at room temperature in a vacuum oven for 24 h, and then the temperature was raised and maintained at 80 °C for 2 h. The samples were allowed another 2 h to cool down before being removed from the oven. The nanofibers were immersed in 25 °C water for several days separately. The samples were then transferred into

isopropyl alcohol for 10 min before loading in a chamber to complete the drying process under vacuum (0.002 MPa) for later SEM characterization.

4.2.6 Characterization

Our samples were imaged with a field emission scanning electron microscopy (FE-SEM, Hitachi S-5000, and 10 kV, sputtered with Palladium-Platinum), scanning electron microscope (SEM, Hitachi S-3000N, and 20 kV, sputtered with Palladium-Platinum) and transmission electron microscopy (TEM, JEM-1010, and 10 kV). Thermo-gravimetrical analysis (TGA) was performed on a Rigaku Thermo Plus TG8120 apparatus (Rigaku Denki, Japan) under air atmosphere at 5 °C /min in a temperature range of 30 °C to 850 °C. The magnetic NPs and composite nanofibers were examined with an X-ray diffraction (XRD) pattern obtained using a Rigaku RINT-2550 at a voltage of 40 kV and a current of 40 mA with Cu KR radiation (λ = 1.5406 A °), in the 2θ range from 3° to 90° at a scanning step of 2°/min. Magnetic measurements were performed on a commercial superconducting quantum interference device (SQUID) magnetometer (Quantum Design, MPMS). Hysteresis loops were measured at 300 K in a magnetic field in the range of -10 kOe to10 kOe.

Table 4.1 The diameters of synthesized Fe_3O_4 NPs under all of our experiment conditions

Fe_3O_4 NPs Samples	Concentration of Fe^{2+} and Fe^{3+} (mol/L)	Concentration of $NH_3 \cdot H_2O$ (mol/L)	Synthesis Temperature (°C)	Mean Diameters (nm)
a	0.0225	0.25	60	14.4
b	0.0375	0.25	60	25.3
c	0.05	0.25	60	37.6
d	0.0225	0.5	60	19.7
e	0.0225	1.0	60	28.3
f	0.0225	0.25	40	18.3
g	0.0225	0.25	50	16.6

4.3 Results and discussions

4.3.1 Characterization of Magnetic Fe_3O_4 NPs

Figure 1 illustrates the FE-SEM images (a) and TEM images (b) of the magnetic NPs, and we can see that the diameters of nanoparticles are monodispersed in the range of 10 nm to 20 nm. More detailed structural information of the products was provided by the high resolution TEM (HRTEM) analysis, which shows the HRTEM image taken from an individual NP structure. Clear lattice fringes are observed in HRTEM image, indicating that crystalline particles formed in the hydrothermal process. Moreover, the measured spacing of the crystallographic planes is about 0.483 nm, which is close to that of the (111) lattice planes of magnetite crystals, and 0.298 nm which is close to that of (220) lattice planes of magnetite crystals.[41, 42]

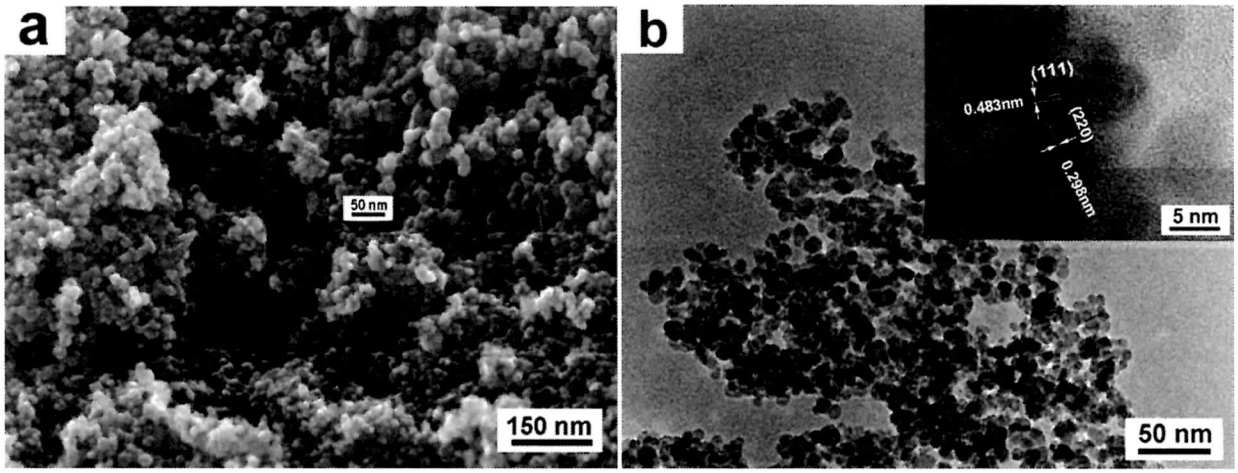

Figure 4.1 FE-SEM and TEM image of Fe_3O_4 NPs synthesized by coprecipitation method. (inserts are high-resolution images)

XRD was used to further characterize the magnetic NPs. As shown in Figure 2, the XRD patterns of the as-obtained magnetic NPs are in good agreement with those of the pure Fe_3O_4 (Magnetite, JCPDS No. 64-8075). In addition, the weight of magnetic NPs samples increased and their colors were change form black to red during the TGA, which further proved the synthesized magnetic NPs were Fe_3O_4 (Figure 3). The intensity of the XRD pattern of the magnetic NPs also clearly increased along

with the increase in synthesis temperatures, indicating that temperature has a positive influence on Fe_3O_4 NPs crystallinity. The effect of synthesis temperature, ferric ion concentration and $NH_3 \cdot H_2O$ on the NPs diameters was investigated. And the results are shown in Table 1. The diameters of synthesized Fe_3O_4 NPs under all of our experiment conditions is no bigger than 40 nm and sample (a) with the smallest diameter was chosen as a filler for preparation of magnetic composite nanofibers.

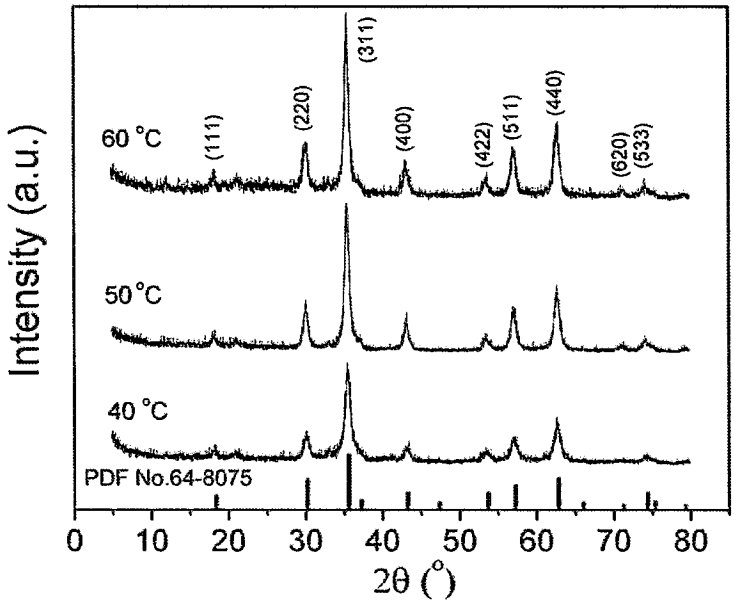

Figure 4.2 XRD patterns of magnetic NPs synthesized at different temperatures.

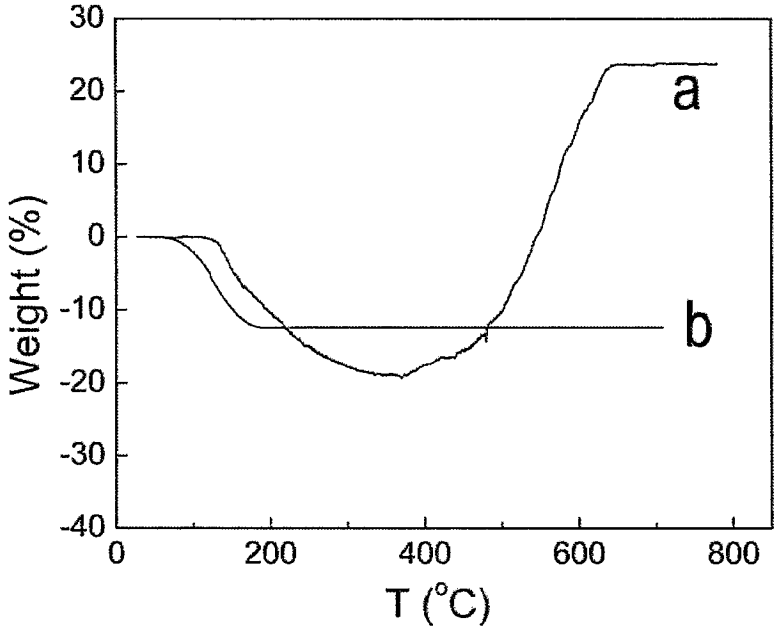

Figure 4.3 TGA of ferric oxide NPs (a. Fe_3O_4; b. Fe_2O_3).

4.3.2 Characterization of Magnetic Fe_3O_4 NPs/PAA/PVA composite nanofibers

The preparation of magnetic nanoparticles/polymer composite systems has been intensively pursued because of these systems' broad applications, including magnetic storage media, ferrofluids, magnetic resonance imaging, and magnetically guided drug delivery. However, one of the main challenges facing almost all of these applications is the ability of the composite systems to deliver well-dispersed nanoparticles with the desired composition, structure, and uniformity as well as the prevention of aggregation. The principal cause of aggregation is the short-range forces-van der Waals attraction between the two particles.[43] To counteract these attractive interactions and promote stability, equally short-range repulsive forces are required. These are enforced either by electrostatic repulsion between the particles or by coating the particles with organic long-chain molecules.

For fully hydrolyzed PVA aqueous solution, the viscosity is very high even in low concentration (< 10 wt%), therefore, it is extremely difficult to prepare homogeneously dispersed NPs/PVA composite materials. In our experiments, PAA was used as a polymer surfactant to stabilize NPs aqueous suspension, which could provide electrostatic and steric repulsion against particle aggregation. As seen in Figure 4a and b, Fe_3O_4 NPs randomly formed irregular aggregation in PVA electrospun nanofibers (diameter is about 250 nm), which will cause heterogeneity of magnetism distribution in the magnetic nanofibers mat. But Fe_3O_4 NPs, which were formed prior to dispersal in the PAA solution, can homogenously disperse in PVA composite nanofibers (Figure 4c and d).

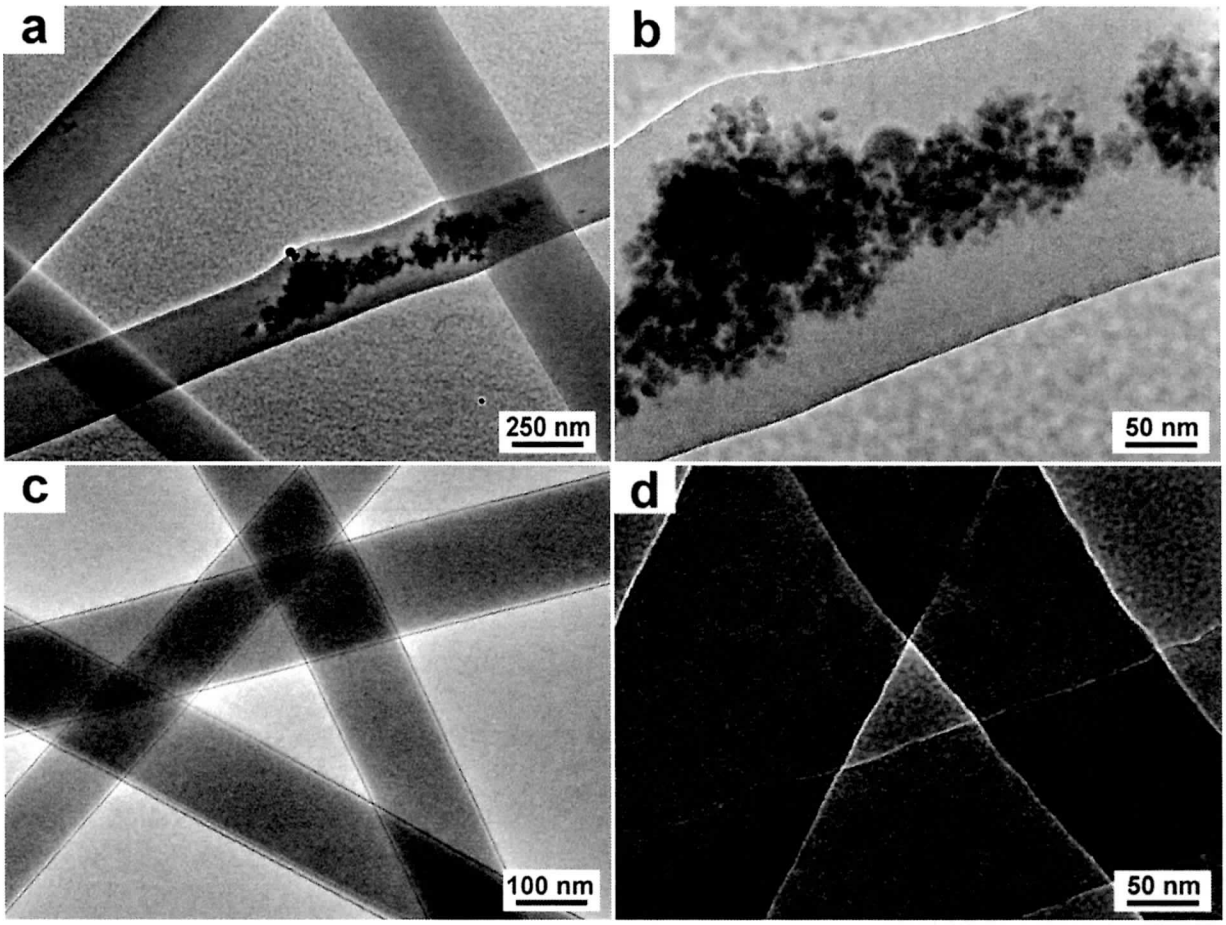

Figure 4.4 TEM images of Fe_3O_4 NPs/polymer composite nanofibers. (a and b: Fe_3O_4 NPs /PVA composite nanofibers; c and d: Fe_3O_4 NPs /PAA/PVA composite nanofibers).

The XRD pattern of Fe_3O_4 NPs/PAA/PVA composite nanofibers revealed the characteristic peaks of both the Fe_3O_4 and the PVA as shown in figure 5. A wide peak was observed at 19.4°, which is in agreement with the XRD peak of the crystalline pure PVA nanofibers, while the other peaks are identical to Fe_3O_4 NPs. The intensity of the peak at 19.4° became stronger along with the content of Fe_3O_4 NPs, which indicated that the existence of Fe_3O_4 NPs facilitated the crystallization of polymer.

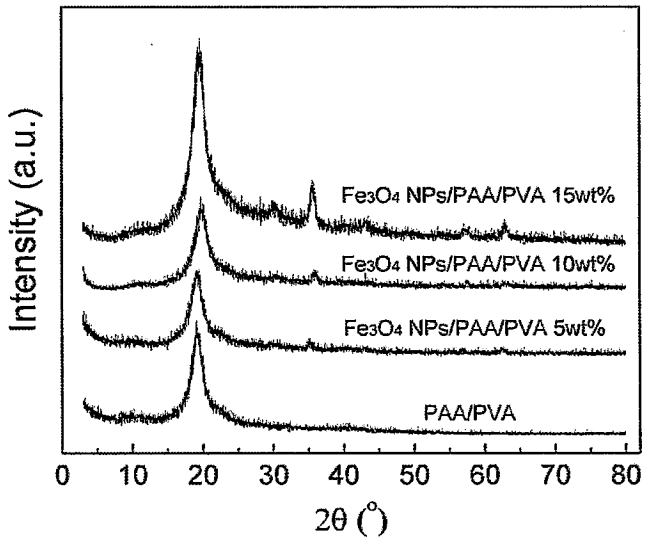

Figure 4. 5 XRD patterns for the Fe_3O_4/polymer nanofibers mat.

The TGA curve for PAA/PVA nanofibers and Fe_3O_4 NPs/PAA/PVA nanofibers are shown in Figure 6. The figure shows the weight loss before 200 °C resulted from the evaporation of bonded water in PAA/PVA.

Table 4.2 Content of Fe_3O_4 in magnetic nanofibers and the saturation magnetization

Fe_3O_4/Polymer (wt%)		Saturation magnetization (emu/g)
Preparation content	Fact content (calculated basing on TG data)	
5	3.94	1.72
10	8.47	3.17
15	14.23	6.77

PAA/PVA nanofibers decomposed in the temperature range of about 200 °C to 500 °C while Fe_3O_4 NPs/PAA/PVA nanofibers decomposed in the temperature range of about 300 °C to 450 °C, this result is in agreement with reference.[44, 45] The remnant in TGA is believed to be Fe_2O_3 and

which is also confirmed by XRD patterns and the color of NPs. Therefore the fact content of Fe_3O_4 NPs in Fe_3O_4 NPs/PAA/PVA composite nanofibers was calculated on the basis of the TGA data using the following formulation:

$$\alpha = \frac{m_r \times \frac{W_{Fe_3O_4}}{W_{Fe_2O_3}}}{W_f} \times 100 \quad (1)$$

where α is the content of Fe_3O_4 NPs (wt%); m_r is the remnant weight; w_f is the weight of composite nanofibers; and w_{Fe2O3} and w_{Fe3O4} are molecular weight of Fe_2O_3 and Fe_3O_4 respectively. The results are listed in Table 2.

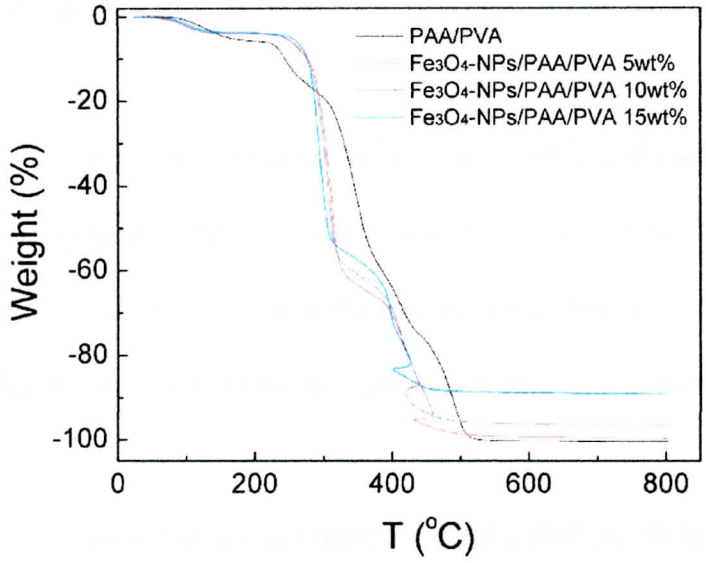

Figure 4.6 TGA of PAA/PVA nanofibers and Fe_3O_4 NPs/PAA/PVA nanofibers.

As a magnetic material, the magnetic property of the Fe_3O_4/polymer nanofiber nonwoven is important to its applications. The magnetization curves at 25 °C of the Fe_3O_4/polymer nanofiber nonwoven are shown in Figure 7a. The results in Table 2 show that the magnetic nanofiber nonwoven has saturation magnetization of 1.72 emu/g to 6.77 emu/g, which is lower than that of the corresponding bulk (92 emu/g) resulting from the existence of polymer. [46]

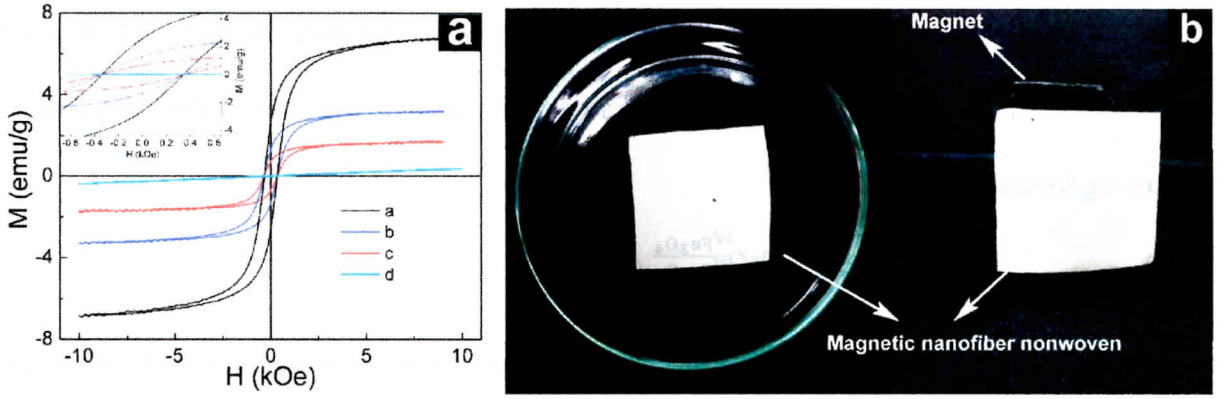

Figure 4.7(a) Hysteresis loops of the polymer/Fe_3O_4 hybrids measured at 25 °C and (b) the attraction of polymer/Fe_3O_4 on a magnet. (The weight rate of Fe_3O_4-NPs/polymer in Fe_3O_4-NPs/PAA/PVA nanofiber nonwoven: a. 14.23 wt%; b. 8.47 wt%; c. 3.94 wt%; d. PVA/PAA only)

The coercivity is also about 300 Oe at 25 °C (see the inset of Figure 7a). Therefore, the products show a soft ferromagnetic behavior, which is the same as Fe_3O_4. The magnetism of the products was demonstrated by holding a commercial magnet close to the sample as shown in Figure 7b. The magnetic nanofiber nonwoven was attracted to the magnetite, indicating that the nanofiber nonwoven had strong magnetism.

4.3.3 Water resistance of Fe_3O_4 NPs/PAA/PVA composite nanofibers

The biggest drawback of electrospun PVA nanofibers, and a significant limit to their practical application, is the poor stability in water of the material.[47, 48] To improve the water resistance of PVA nanofibers, most researchers have concentrated on chemical cross-linking by a variety of substances including glutaraldehyde, acetaldehyde, or formaldehyde.[49, 50] In our study, PAA was used not only as a dispersing agent for Fe_3O_4 NPs, but also as a cross-linking agent to enhance the water resistance of PVA composite nanofibers. Figure 8 shows SEM images of Fe_3O_4 NPs/polymer composite nanofibers after being immersed in water for several days. The Fe_3O_4 NPs/PVA nanofibers quickly swelled and the unique nanofibrous structure is lost by dissolution into water. However, the Fe_3O_4 NPs/PAA/PVA nanofibers only swelled and maintained their fibrous structures after being in

contact with water for 1 d. Chemical cross-linking between PVA and PAA was proved to occur through an ester formation between the –OH groups in PVA and the –COOH groups in PAA during heat treatment at 100 °C for 1 h, which prevented the dissolution of PVA composite nanofibers.[39]

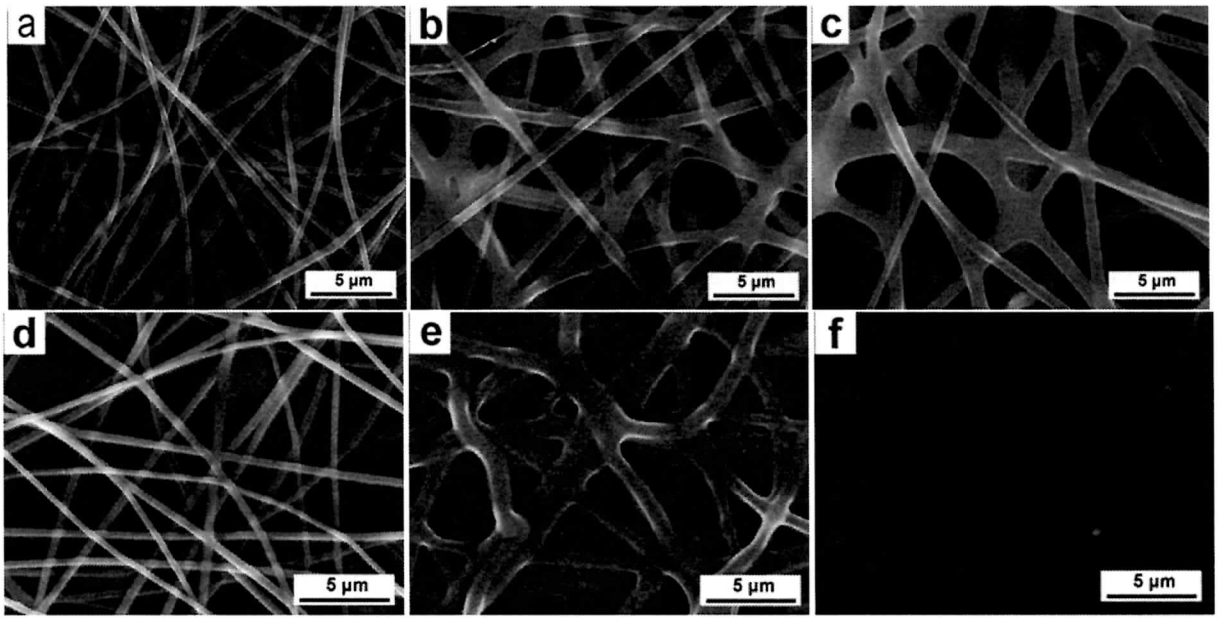

Figure 4.8 SEM images of Fe_3O_4/polymer nanofibers after contact with water for different periods, followed by vacuum drying. (a) Fe_3O_4 NPs/PAA/PVA nanofibers, immediately after annealing; (b) Fe_3O_4 NPs/PAA/PVA nanofibers, contact with water for 1 h (c) Fe_3O_4 NPs/PAA/PVA nanofibers, contact with water for 1 d; (d) Fe_3O_4 NPs/PVA nanofibers, immediately after annealing; (e) Fe_3O_4 NPs/PVA nanofibers, contact with water for 1 h (f) Fe_3O_4 NPs/PVA nanofibers, contact with water for 1 d.

4.4 Conclusions

Fe_3O_4 NPs/PAA/PVA composite nanofibers were prepared via the electrospinning of PAA/PVA aqueous solutions with magnetite Fe_3O_4 NPs which were homogenously dispersed by PAA. Experiment results showed that the diameters of Fe_3O_4 NPs were in a range of 10 nm to 40 nm under our experimental conditions; Fe_3O_4 NPs stabilized by PAA can homogenously dispersed in PVA composite nanofibers; the crystallinity of PAA/PVA nanofibers increased along with the increase in

Fe_3O_4 NPs content. The magnetic property of Fe_3O_4 NPs/PAA/PVA composite nanofibers was also investigated and the results showed that the composite nanofibers show a strong magnetism and soft ferromagnetic behavior which is the same as Fe_3O_4 at room temperature. In addition, the water resistance of Fe_3O_4 NPs/PAA/PVA composite nanofibers was enhanced by heat treatment. As a result, in our process to preparing magnetic Fe_3O_4 NPs/PVA composite nanofibers, PAA acts not only as a dispersant but also as a cross-linking agent. This method provides a simple and convenient process to prepare homogenous NPs/PVA composite system with high stability and can greatly improve the practical application of NPs/PVA composite.

Reference

[1] S. M. Lebedev, o. S. Gefle, S. N. Tkachenko, *J Electrostat,* 68, 122 (2010).

[2] E. M. A. Jamal, P. A. Joy, P. Kurian, M. R. Anantharaman, *Mater Chem Phys,* 121, 154 (2010).

[3] J. R. Liu, M. Itoh, T. Horikawa, K. Machida, S. Sugimoto, T. Maeda. *J Appl Phys,* 98, 254305/1 (2005).

[4] H. Lee, E. Lee, D. K. Kim, N. K. Jang, Y. Y. Jeong, S. Jon, *J Am Chem Soc,* 128, 7383 (2006).

[5] F. Caruso, M. Spasova, A. Susha, M. Giersig, R. A. Caruso, *Chem Mater,* 13, 109 (2001).

[6] F. Caruso, A. S. Susha, M. Giersig, H. Mohwald, *Adv Mater,* 11, 950 (1999).

[7] E. L. Bizdoaca, M. Spasova, M. Farle, M. Hilgendorff, F. Caruso, *J Magn Magn Mater,* 240, 44 (2002).

[8] L. Raymond, J. F. Revol, D. H. Ryan. R. H. Marchessault, *Chem Mater,* 6, 249 (1994).

[9] E. L. Mayes, F. Vollrath, S. Mann. *Adv Mater,* 10, 801 (1998).

[10] H. Peniche, A. Osorio, N. Acosta, A. de la Campa, C. Peniche, *J Appl Polym Sci,* 98, 651 (2005).

[11] X. Liu, Y. Guan, Z. Ma, H. Liu, *Langmuir,* 20, 102782 (2004).

[12] H. Shang, W. S. Chang, S. Kan, S. A. Majetich, G. U. Lee, *Langmuir,* 22, 2516 (2006).

[13] J. Ramos, A. Millan, F. Palacio, *Polymer,* 41, 8461 (2000).

[14] D. Rabelo, E. C. D Lima, D. P. Barbosa, V. J. Silva, O. Silva, R. B. Azevedo, L. P. Silva, A. P. Lemos, p. C. Morais, *J Magn Magn Mater,* 252, 13 (2002).

[15] C. Chouly, D. Pouliquen, I. Lucet, J. J. Jeune, P. Jallet, *J Microencapsul,* 13, 245 (1996).

[16] K. Thode, M. Luck, W. Schroder, W. Semmler, T. Blunk, R. H. Muller, M. Kresse, *J Drug Target,* 5, 35 (1997).

[17] S. Mahapatra, N. Pramanik, S. K. Ghosh, P. Pramanik, *Nanosci Nanotechnol* 6, 823 (2006).

[18] S. H. Tan, R. Inai, M. Kotaki, S. Ramakrishna. *Polymer,* 46, 6218 (2005).

[19] K. H. Lee, O. Ohsawa, S. Lee, J. C. Park, K. W. Kim, H. Y. Kim, Y. Watanabe & I.S. Kim, *Sen'i Gakkaishi,* 64, 306 (2008).

[20] J. H. Park, B. S. Kim, Y. C. Yoo, M. S. Khil, & H. Y. Kim, *J Appl Polym Sci,* 107, 2211 (2007).

[21] K. Wei, T. Ohta, B. S. Kim, K. H. Lee, M. S. Khil, H. Y. Kim & I. S. Kim, *Polym Adv Technol* 21, 746 (2010).

[22] P. Gibson, H. Schreuder-Gibson, D. Rivin, *Colloid Surf A,* 187-188, 469(2001).

[23] D. H. Reneker, A. L. Yarin, *Polymer,* 49, 2387 (2008).

[24] X. H. Zong, K. Kim, D. F. Fang, S. F. Ran, B. S. Hsiao, B. Chu, *Polymer,* 43, 4403 (2002).

[25] K. Kim, M. Yu, X. H. Zong, J. Chiu, D. F. Fang, Y. S. Seo, B. S. Hsiao, B. Chu, M. Hadjiargyrou, *Biomaterials* 24, 4977 (2003).

[26] T. Song, Y. Z. Zhang, T. J. Zhou, C. T. Lim, S. Ramakrishna, B. Liu. *Chem Phys Lett,* 415, 317 (2005).

[27] S. T. Tan, J. H. Wendorff, C. P. ietzonka, Z. H. Jia, G. Q. Wang. *Chemphyschem,* 6, 1461 (2005).

[28] V. S. Pavan Kumar, V. Jagadeesh Babu, G. K. Raghuraman, R. Dhamodharan, T. S. Natarajan. *J Appl Phys,* 101, 114717 (2007).

[29] Q. Xiao, X. K. Tan, L. L. Ji, L. Xue, *Synth Met,* 157, 784 (2007).

[30] A. Wang, H. Singh, T. A. Hatton, G. C. Rutledge, *Polymer,* 45, 5505 (2004).

[31] J. M. Deitzel, J. Kleinmeyer, D. Harris, N. B. Tan, *Polymer,* 42, 261 (2001).

[32] C. Chen, Y. H. Zhu, H. Bao, X. L. Yang, C. Z. Li, *Appl Mate Interfaces,* 2, 1499 (2010).

[33] E. B. Bettina, J. A. A. A. Smith, B. Fejerskov, A. Postma, P. Senn, E. Reimhult, M. Pla-Roca, L. Isa, D. S. Sutherland, B. Stadler, A. N. Zelikin, *Langmuir,* 27, 10216 (2011).

[34] A. D. Ossipov, S. Piskounova, J. Hilborn, *Macromolecules,* 41, 3971 (2008).

[35] F. Cavalieri, E. Chiessi, R. Villa, L. Vigano, N. Zaffaroni, M. F. Telling, G. Paradossi, *Biomacromolecules,* 9, 1967 (2008).

[36] C. K. Kim, B. S. Kim, F. A. Sheikh, U. S. Lee, M. S. Khil & H. Y. Kim, *Macromolecules* 40, 4823 (2007).

[37] C. L. Lin, C. F. Lee, W. Y. Chiu., *J Colloid Interface Sci,* 291, 441 (2005).

[38] Y. H. Ma, S. Y. Wu, T. Wu, Y. J. Chang, M. Y. Hua, J. P. Chen, *Biomaterials* 30, 3343 (2009).

[39] J. C. Park, T. Ito, K. O. Kim, K. W. Kim, B. S. Kim, M. S. Khil, H. Y. Kim and I. S. Kim, *Polymer Journal,* 42, 273 (2010).

[40] R. S. Molday, Magnetic iron-dextran microspheres. US Patent 4452773, 1984.

[41] T. H. Kim, E. Y. Jang, N. J. Lee, D. J. Choi, K. J. Lee, J. T. Jang, J. S. Choi, S. H. Moon and J. W. Cheon, *Nano Lett*, 9, 2229 82009).

[42] H. Yu, M. Chen, P. M. Rice, S. X. Wang, R. L. White and SH. D. Sun, *Nano Lett,* 5, 379 (2005).

[43] H. C. Hamaker *Physica,* 4, 1058 (1937).

[44] K. Chrissafis, D. Bikiaris. *Thermochimica Acta,* 523, 1 (2011).

[45] D. Bikiaris, *Thermochimica Acta,* 523, 25 (2011).

[46] D. H. Han, J. P. Wang, H. L. Luo. *J Magn Magn Mater,* 136, 176 (1994).

[47] V. S. Praptowidodo, *J Mol Struct*, 739, 207 (2005).

[48] J. L. B. Carvalho, A. M. Araujo, A. M. P Almeida, W. M. Azevedo WM. *Sens Actuators B Chem,*

36, 427 (1996).

[49] S. Kurihara, S. Sakamaki S, S. Mogi, T. Ogata, T. Nonaka, *Polymer,* 37, 1123 (1996).

[50] L. Gao, C. J. Seliskar, *Chem Mater,* 10, 2481 (1998).

CHAPTER FIVE

Fabrication of high-strength aligned multi-walled carbon nanotubes/polyvinyl alcohol composite nanofibers by electrospinning

5 Fabrication of high-strength aligned multi-walled carbon nanotubes/polyvinyl alcohol composite nanofibers by electrospinning

High-strength uniaxially-aligned electrospun nanofibers were prepared from PVA reinforced by modified hydrophilic multi-walled carbon nanotubes (MWCNTs). In order to get a homogeneous spinning solution, a one-step process using ammonium persulfate (APS) as oxidant was employed to fabricate water-soluble MWCNTs, and then they were dispersed in a 10 wt% PVA aqueous solution. We utilized this macroscopically homogeneous dispersion to produce nanofibers mat by electrospinning with an ultra-high-speed rotating cylinder as a collector. SEM image shows that the aligned degree of the fibers increases along with the increase in rotating speed. When the speed is up to 2000 rpm, the electrospun nanofibers are nearly uniaxially aligned. The tensile test results suggest that a small amount of MWCNTs dramatically enhanced the tensile strength of PVA fibers.

5.1 Introduction

Electrospinning has been viewed as a simple and versatile method for fabricating ultrafine fibers with diameters being in sub-micrometer down to nanometer range.[1-5] PVA is one of the most popular polymers used for ultrafine electrospun fiber production. Nano-scale PVA fibers have several interesting characteristics, such as high surface area to mass ratio, significant possibilities for surface functionalization, and high mechanical performance due to an improvement in the molecular organization of the spun fiber. These properties make electrospun PVA fibers excellent candidates for many applications, such as filtration, reinforcing materials, wound dressings, tissue scaffolding, and

drug releasing carriers.[6-11] However, one of the biggest problems that limit the application of electrospun PVA nanofibers is the weakness in strength due to the as-spun fibers are often collected as randomly oriented structure in the form of non-woven mats.

A practical and convenient method to overcome this issue is to fabricate aligned electrospun PVA nanofibers. To the best of our knowledge, five techniques for fabricating aligned fibers have been proposed: they are a rotating drum collector technique, an auxiliary electrode and electrical field technique, a spinning thin wheel with a sharp edge technique, a frame collector technique, and a multiple field technique.[12-16] In these methods, rotating collector technique is simple and convenient; furthermore, there have been many products on the basis of this technology.

Another practical method to improve the strength of electrospun PVA nanofibers is to produce composite nanofibers. Carbon nanotubes (CNTs) as an excellent reinforcement for nanocomposites have already been the object of numerous research efforts. CNT/PVA composite fibers have attracted more and more interest for many years. Unfortunately, CNTs have a tendency to aggregate together into bundles, which makes the handling and processing very problematic. Up until now, many efforts have been made to prepare hydrophilic CNTs [17-25] and numerous modification methods for CNTs have already been reported.

In ours study, we use the one-step process using ammonium persulfate (APS) as oxidant to prepare water-soluble multi-walled carbon nanotubes (MWCNTs), which is a low-cost, eco-friendly, facile method without the need for organic solvents and acids. Then the APS treated MWCNTs were mixed with PVA solution to prepare homogenous MWCNTs/PVA aqueous solutions. The solutions were undergone electrospinning using electrospinning equipment with an ultra-high-speed rotating cylinder as a collector to fabricate aligned electrospun nanofibers. With excellent mechanic properties, this kind of MWCNTs composite has potential applications in many different fields.

5.2 Experimental details

5.2.1 Materials

PVA HC with a degree of hydrolysis (DH) = 99.9 mol% and degree of polymerization (DP) =1700 was kindly provided by Kuraray Co. Ltd, Tokyo, Japan. Multi-walled carbon nanotubes with a diameter of 20-30 nm, ammonium persulfate (APS) and ammonia solution (28% NH_3 in water) were purchased from Wako Pure Chemical Industries Ltd., Japan. All chemicals were used without further purification.

5.2.2 One-step reaction for preparing water-soluble MWCNTs

Water-soluble MWCNTs was prepared using the method of one-step reaction described by Zhang et al. [26] 20 mg original MWCNTs and 100 ml deionized water were added to a flask and dispersed with the aid of an ultrasonic water bath for 60 min at room temperature. Then 0.5 g APS was added to the flask and the pH of the reaction system was adjusted to about 12 by adding concentrated NH_4OH solution. The flask equipped with a reflux condenser and a magnetic stir bar was kept at 90° C with vigorous mixing for 2 h, and then cooled down to room temperature naturally. The contents of the flask were carefully diluted with water and dispersed with ultrasonic water bath, followed by a centrifugation process at 4000 rpm for 10 min. The centrifugation process was expected to separate the catalyst and bundled MWCNTs from the solution. The supernatant solution was collected and filtered through a hydrophilic polytetrafluoroethylene membrane (45 mm/0.2 mm, from Millipore) and washed with distilled water. Finally, the products were dried in vacuum oven for 24 h at 80 °C.

5.2.3 Preparation of MWCNTs/PVA solution

10 mg APS treated MWCNTs NPs were dispersed in 10 mL distilled water, then the suspension was treated by ultrasonic mixing for 30 min to get a 0.1 wt% MWCNTs suspension for reserve. PVA chips were dissolved in distilled water in a static rotary mixer (500 rpm) at 25 °C for 1 h and then rapidly heated to 95 °C and this temperature was maintained with high-speed stirring (1000 rpm) for 2

h to obtain a 30 wt% PVA solution. Varying amounts of 0.1 wt% MWCNTs suspension, deionized water were then added to the as-prepared PVA solution to adjust the MWCNTs concentration in the PVA to 0.05, 0.1, 0.2, 0.3 and 0.5 wt% (MWCNTs/PVA) while maintaining the PVA concentration at 10 wt% in each composite suspension with high speed stirring. Finally, homogenous PVA/MWCNTs/PVA mixed solutions were obtained.

5.2.4 Electrospinning

The electrospinning setup (MECC-NANO-01a, MECC CO., LTD, Japan, as seen in Figure 1) used in this study is consists of a syringe with a flat-end metal needle (1.20 mm × 38 mm), a syringe pump for controlling the feeding rate, a grounded cylindrical stainless steel mandrel, and a high-voltage direct current (DC) power supply. For the electrospinning procedure, the solutions were loaded into a syringe coupled with nozzles and electrospun under a high DC voltage of 10 kV, with a distance from the needle tip to the collector of 15 cm and a feeding speed of 0.4 mL/h.

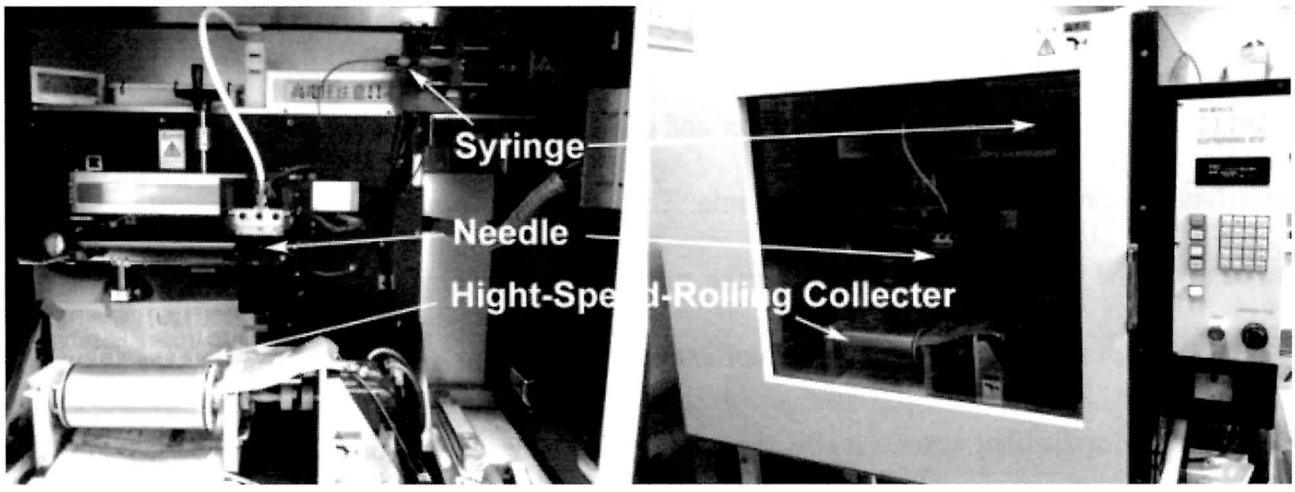

Figure 5.1 Electrospinning equipment with high-speed- rolling collector.

5.2.4 Measurements

Scanning electron microscopy (SEM) was conducted with a Hitachi Hitachi S-3000N instrument after sputter coating the samples with platinum.

Tensile testing was performed with an A & D Tensilon RTC-1250A at room temperature with a 50 N load cell, gauge length 10 mm and crosshead speed 20 mm/min. The sizes of nonwoven samples were 5mm(W)×10mm(L)×0.05mm(T). The experimental results were evaluated as the averages of at least 20 measurements.

5.3 Results and discussion

5.3.1 Hydrophilic modification of MWCNTs

The APS-treated MWCNTs exhibit obvious improvement of water solubility, which can be readily observed by visual inspection as shown in Figure 2, while the original MWCNTs start aggregating and precipitate rapidly after sonication; the treated nanotubes form stable suspensions without visible aggregation and precipitation even after 30 days. The highest MWCNTs concentration of stable nanotubes solution is around 1.4 mg/mL according to the literature methods [27]. Our data indicate that the solubility and stability of treated nanotubes are strongly improved.

In order to further support the enhanced dispersion property of treated nanotubes in water, optical microscope analysis of original SWNTs and treated SWNTs was carried out. Figure 3 shows optical microscope image of different suspension systems. Each was prepared by homogenization for 10 min.

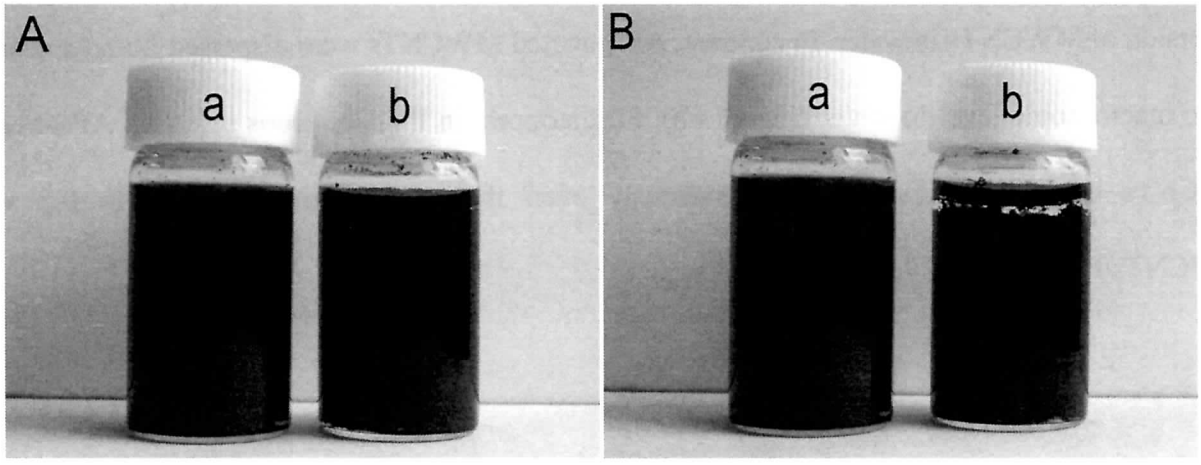

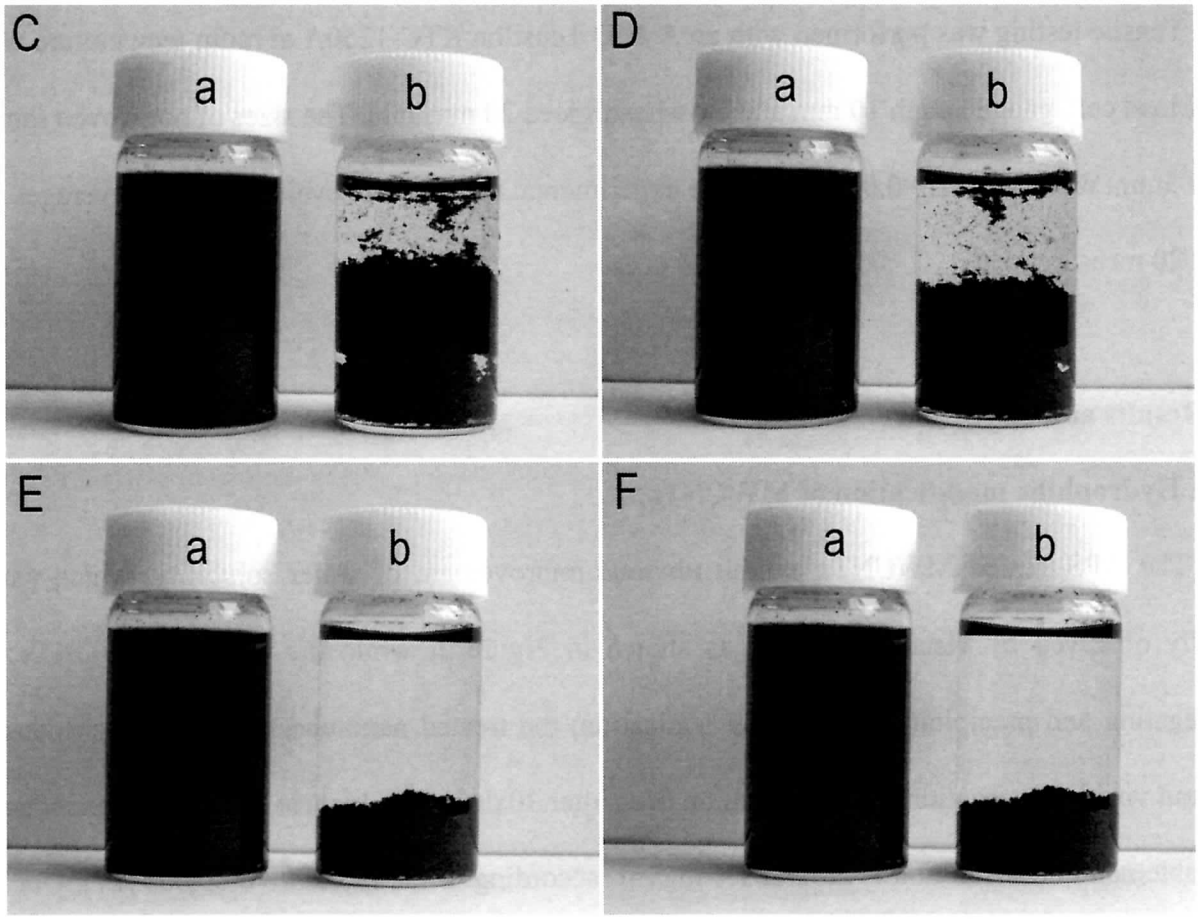

Figure 5.2 Optical photographs of (a) original MWCNTs and (b) APS-treated MWCNTs in water. (A) Immediately after sonication; (B) after 1 min; (C) after 5 min; (D) after 1 h; (E) after 1 day; and (F) after 30 days.

For original MWCNTs (Figure 3a), only aggregations can be observed, which indicate poor dispersion of MWCNTs in water. In contrast, APS-treated MWCNTs were dispersed homogeneously at the macroscopic level in water (Figure 3b). Furthermore, in PVA aqueous solution, APS-treated MWCNTs could also disperse homogeneously even the concentration was up to 0.5 wt% (MWCNTs/PVA) (Figure 3c and d).

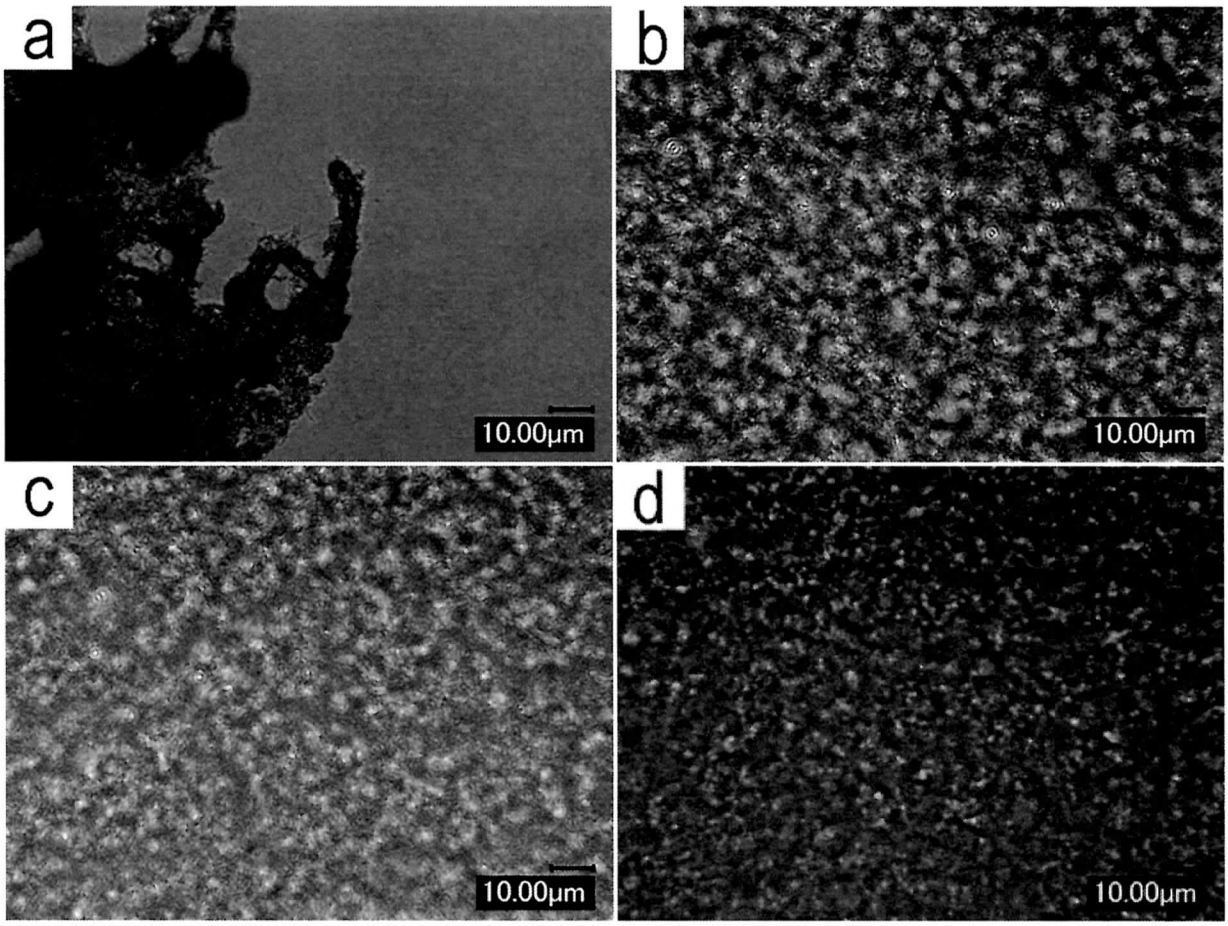

Figure 5.3 Optical microscope images of (a) original MWCNTs in water; (b) APS-treated MWCNTs in water (0.01 wt%); (c) APS-treated MWCNTs/PVA mixed suspension (MWCNTs/PVA = 0.05 wt%); (d) APS-treated MWCNTs/PVA mixed suspension (MWCNTs/PVA = 0.5 wt%).

5.3.2 Aligned MWCNTs/PVA nanofibers by electrospinning

One of the biggest problems that limit the application of electrospun nanofibers is the weakness in strength. A practical method to deal this issue is to fabricate aligned nanofiber. In our study, we use the rotating collector technique during electrospinning process, which is simple and convenient to prepare aligned electrospun nanofibers. SEM images of our samples were shown in Figure 4. From Figure 4 a to d, rolling speed of the collector increased from 0 rpm to 2000 rpm and we can see clearly that the fibers aligned gradually along by the rolling direction during this process. Especially when the speed became 2000 rpm, the fibers were almost uniaxially-aligned and the average included angle

between each fiber is only about 10 degree.

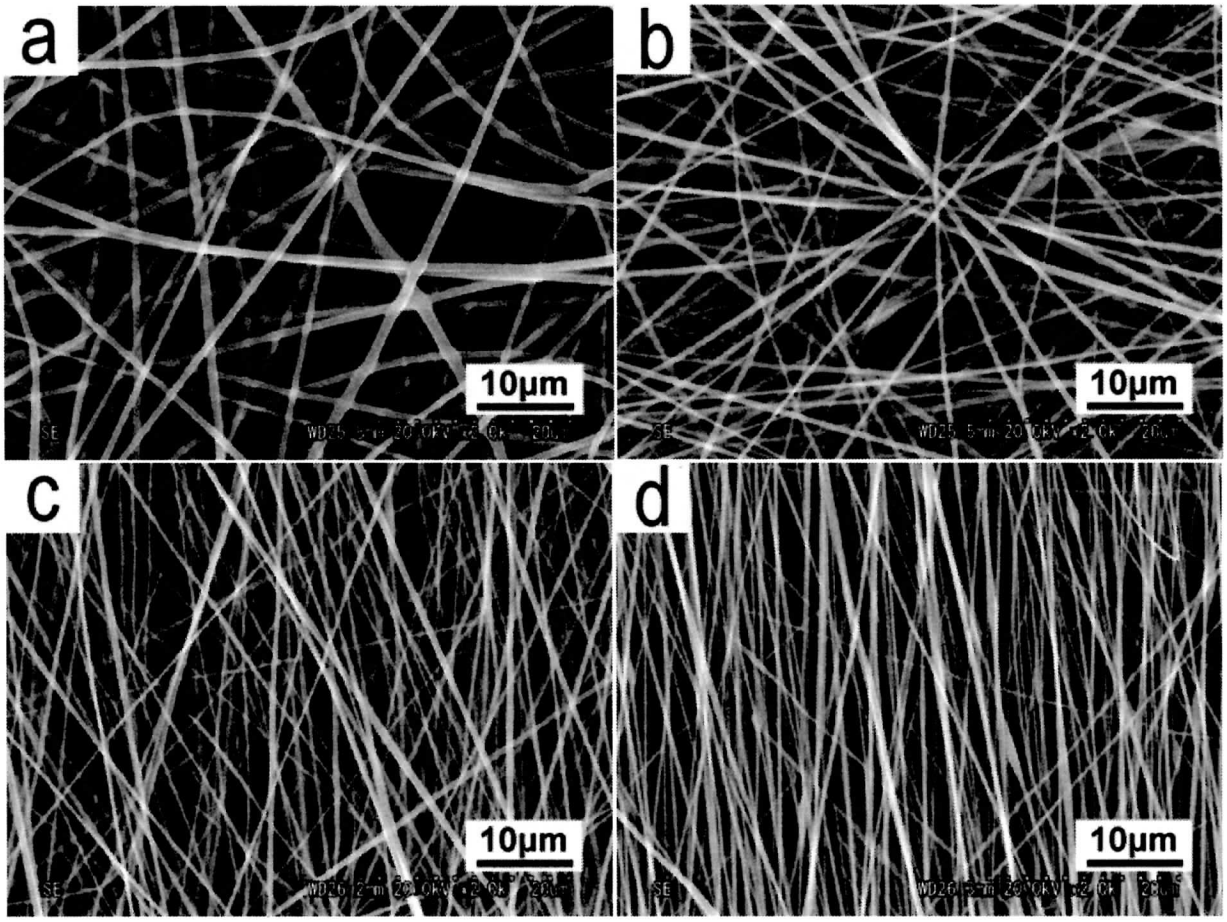

Figure 5.4 SEM images of APS-treated MWCNTs/PVA electrospun fibers (MWCNTs/PVA = 0.1 wt%). The rolling speeds of collector are (a) 0 rpm; (b) 500 rpm; (c) 1000 rpm; (d) 2000 rpm.

5.3.3 Tensile strength of MWCNTs/PVA nanofibers

Tensile stress-strain curves of neat PVA and APS-treated MWCNTs/PVA nanofiber nonwoven are presented in Figure 5. The neat PVA stress–strain curve exhibits an obvious nonlinear region starting at about 0.6 MPa, which likely corresponds to the micro cracks and partial damage of molecular chains during the large elongation process. The ultimate strain of neat PVA is about 220%. However, the nonlinear region in the stress–strain curves of APS-treated MWCNTs/PVA nanofiber nonwoven decreases rapidly with the increment of MWCNTs content.

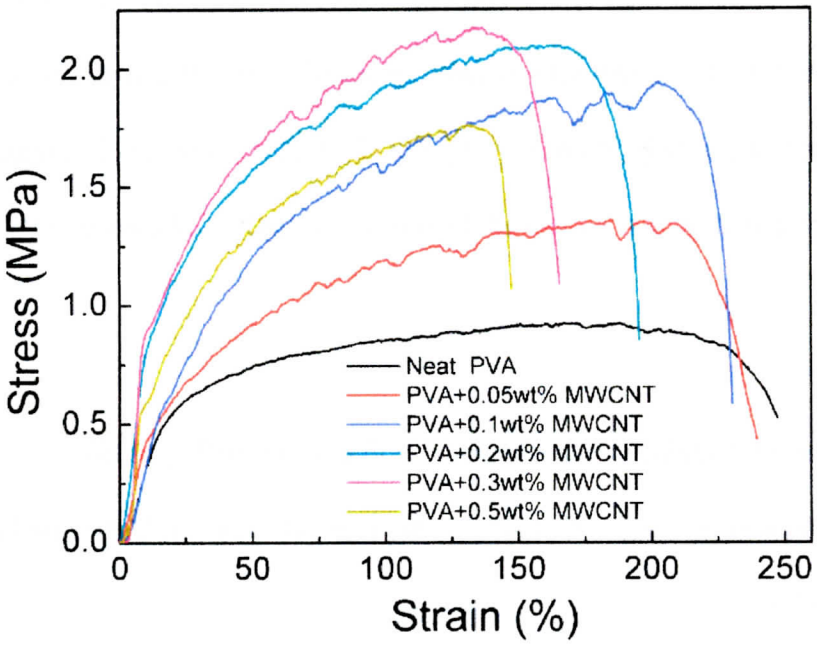

Figure 5.5 Stress-strain curves of neat PVA and MWCNTs/PVA electrospinning nanofiber nonwoven mat (prepared condition: collector rotating speed = 2000 rpm).

Tensile strength of the APS-treated MWCNTs/PVA nanofiber nonwoven has a relative moderate enhancement until the MWCNTs loading up to 0.3 wt%, improvement from 0.8 MPa to 2.3 MPa. However, a sudden decrease happens at 0.5 wt% loading that may result from not only the increase of the probability of MWCNTs agglomeration, which is inevitable at such a high concentration, but also the considerable decrease of plastic range in nanocomposites.

5.4 Conclusions

In our study, aligned electrospun composite MWCNTs/PVA nanofibers were prepared. In order to get a homogeneous spinning solution, a one-step process using APS as oxidant was employed to fabricate water-soluble MWCNTs, and then they were dispersed in a 10 wt% PVA aqueous solution. We utilized this macroscopically homogeneous dispersion to produce nanofibers mat by

electrospinning with an ultra-high-speed rotating collector. SEM image shows that the aligned degree increases along with the increase in rotating speed. When the speed is up to 2000 rpm, the electrospun nanofibers are nearly uniaxially aligned. The tensile test results suggest that only small amount of MWCNTs could greatly enhanced the tensile strength of electrospun PVA nanofibers.

Reference

[1] S. H. Tan, R. Inai, M. Kotaki, S. Ramakrishna, *Polymer*, 46, 6128 (2005).

[2] K. H. Lee, O. Ohsawa, S. Lee, J. C. Park, K. W. Kim, H. Y. Kim, Y. Watanabe, I. S. Kim, *Sen'i Gakkaishi*, 64, 306 (2008).

[3] J. H. Park, B. S. Kim, Y. C. Yoo, M. S. Khil, H. Y. Kim, *J. Appl. Polym. Sci.*, 107, 2211 (2007).

[4] J. Doshi, D. H. Reneker, *J. Electrostat.*, 35, 151 (1995).

[5] K. Wei, T. Ohta, B. S. Kim, K. H. Lee, M. S. Khil, H. Y. Kim, I. S. Kim, Polym. Adv.Technol., 21, 746 (2010).

[6] J. M. Deitzel, J. Kleinmeyer, D. Harris and N. C. Beck Tan, *Polymer,* 42, 261(2001).

[7] C. Chen, Y. H. Zhu, H. Bao, X. L. Yang and C. Z. Li, *Appl Mater Interfaces,* 2, 1499 (2010).

[8] B. E. B. Jensen, A. A. A. Smith, B. Fejerskov, A. Postma, P. Senn, E. Reimhult, M. Pla-Roca, L. Isa, D. S. Sutherland, B. Stadler and A. N. Zelikin, *Langmuir*, 27, 10216 (2011).

[9] A. D. Ossipov and J. Hilborn, *Macromolecules*, 39, 1709 (2006).

[10] A. D. Ossipov, S. Piskounova and J. Hilborn, *Macromolecules*, 41, 3971 (2008).

[11] F. Cavalieri, E. Chiessi, R. Villa, L. Vigano, N. Zaffaroni, M. F. Telling and G. Paradossi, *Biomacromolecules*, 9, 1967 (2008).

[12] A.Bornat, US Patent 4689186, 1987.

[13] J. P .Berry , US Patent 4965110, 1990.

[14] A. Theron, E. Zussman, and A. L. Y arin, Nanotechnology, 12, 384 (2001).

[15] R. Dersch, T. Liu, A. K. Schaper , A. Greiner , and J. H. W endorff, *J. Polym. Sci.-A: Polym. Chem.*, 41, 545 (2003).

[16] J. M. Deitzel, J. Kleinme yer, J. K. Hirv onen, and T. N. C. Beck, Polymer, 42, 8163 (2001).

[17] K. Nobusawa, A. Ikeda, J. Kikuchi, S. Kawano, N. Fujita, S. Shinkai, Angew, *Chem. Int. Ed.*, 47, 4577 (2008).

[18] C. Hu, Z. Chen, A. Shen, X. Shen, J. Li, S. Hu, *Carbon*, 44, 428(2006).

[19] F. Liang, J. M. Beach, P. K. Rai, W. Guo, R. H. Hauge, M. Pasquali, R. E. Smalley, W. E. Billups, *Chem. Mater.*, 18, 1520 (2006).

[20] J. L. Hudson, H. Jian, A. D. Leonard, J. J. Stephenson, J. M. Tour, *Chem. Mater.*, 18, 2766 (2006).

[21] J. J. Stephenson, J. L. Hudson, S. Azad, J. M. Tour, *Chem. Mater.*, 18, 374 (2006).

[22] J. Chattopadhyay, F. J. Cortez, S. Chakraborty, N. K. H. Slater, W. E. Billups, *Chem. Mater.*, 18, 5864 (2006).

[23] B. Jia, L. Gao, *J. Phys. Chem. B*, 111, 5337 (2007).

[24] M. N. Tchoul, W. T. Ford, G. lolli, D. E. Resasco, S. Arepalli, *Chem. Mater.*, 19, 5765 (2007).

[25] A. G. Osorio, I. C. L. Silveira, V. L. Bueno, C. P. Bergmann, *Appl. Surf. Sci.*, 255, 2485 (2008).

[26] L. Zhang, Q. Q. Ni, Y. Q. Fu, T. Natsuki, *App. Surf. Sci.*, 255, 7095 (2009).

[27] J. Zou, L. Liu, H. Chen, S. I. Khondaker, R. D. McCullough, Q. Huo, L. Zhai, *Adv. Mater.*, 20, 2055 (2008).

CHAPTER SIX

Conclusions

6 Conclusions

This thesis has investigated the preparation and application of functional PVA nanofibers by electrospinning.

In order to improve the spinnability of PVA and get ultrafine PVA nanofibers, we use a novel viscosity-modifier (HMC) to reduced the viscosity of PVA aqueous solution and readily fabricated FH-PVA electrospun fibers with uniform diameters of less than 200 nm and ultra-high-molecular-weight PVA electrospun fibers with uniform diameters of about 200 nm; in order to the water resistance and homogeneity of PVA composite nanofibers, we prepared a magnetic PVA composite nanofibers with homogenously dispersed nanoparticles and high water resistance based on polyacrylic acid (PAA) stabilized Fe_3O_4 nanoparticles (NPs); in order to overcome the weakness in strength of PVA nanofibers, we fabricated high-strength uniaxially-aligned PVA composite nanofibers by electrospinning with an ultra-high-speed rotating cylinder as a collector, using modified hydrophilic multi-walled carbon nanotubes (MWCNTs) as a reinforcement filler.

In chapter 1, I reviewed references and provided brief summary of electrospinning technology and the application of PVA electrospun nanofibers.

In chapter 2, we present a novel use of HMC for reducing the viscosity of FH-PVA. The viscosity of FH-PVA in aqueous solution decreased gradually with storage time in proportion to the amount of HMC present, this is opposite to the effect of ionic salts. In addition, after 7 days of storage, the viscosity of the FH-PVA test solutions decreased by 60% (related to the concentration of HMC)

compared to those of the original solutions. These phenomena are related to the reconfiguration of hydrogen bonding in the solutions, confirmed by SAXS and ^{1}H NMR spectra observations. The morphology of FH-PVA electrospun fibers produced from solutions with different viscosities were investigated by SEM, and it was observed that the electrospun fibers became more uniform and the diameters became smaller as the concentration of HMC or the storage time increased. A beaded morphology resulted if the viscosity became too low. Therefore, the spinnability of FH-PVA aqueous solutions can be significantly improved using this method, and it is possible to readily produce ultrafine FH-PVA electrospun fibers with diameters below 200 nanometers.

In chapter 3, we present the novel use of HMC to reduce the viscosity of fully hydrolyzed UHMW PVA. The viscosity of PVA-80-99 in aqueous solution is decreased gradually with time in proportion to the amount of HMC present; this is opposite to the effect of the addition of ionic salts. After 7 days of storage, the viscosities of PVA-80-99 solutions had decreased by about 60% (related to the concentration of HMC) compared to those of the original solutions. These phenomena are related to the reconfiguration of hydrogen bonding in the solutions. The morphology of PVA-80-99 electrospun fibers produced from solutions with different viscosities were investigated by SEM, and it was observed that the electrospun fibers became more uniform and the diameters became smaller as the concentration of HMC or the storage time increased. As a result, the spinnability of fully hydrolyzed UHMW PVA can be significantly improved by using this method, making it possible to readily produce ultrafine fully hydrolyzed UHMW PVA electrospun fibers with diameters about 200 nanometers. Furthermore, by simple annealing treatment, the electrospun fibers can remains their structure even in 60 °C water.

In chapter 4, Fe_3O_4 NPs/PAA/PVA composite nanofibers were prepared via the electrospinning of PAA/PVA aqueous solutions with magnetite Fe_3O_4 NPs which were homogenously dispersed by PAA. Experiment results showed that the diameters of Fe_3O_4 NPs were in a range of 10 nm to 40 nm

under our experimental conditions; Fe_3O_4 NPs stabilized by PAA can homogenously dispersed in PVA composite nanofibers; the crystallinity of PAA/PVA nanofibers increased along with the increase in Fe_3O_4 NPs content. The magnetic property of Fe_3O_4 NPs/PAA/PVA composite nanofibers was also investigated and the results showed that the composite nanofibers show a strong magnetism and soft ferromagnetic behavior which is the same as Fe_3O_4 at room temperature. In addition, the water resistance of Fe_3O_4 NPs/PAA/PVA composite nanofibers was enhanced by heat treatment. As a result, in our process to preparing magnetic Fe_3O_4 NPs/PVA composite nanofibers, PAA acts not only as a dispersant but also as a cross-linking agent. This method provides a simple and convenient process to prepare homogenous NPs/PVA composite system with high stability and can greatly improve the practical application of NPs/PVA composite.

In chapter 5, we prepared high-strength uniaxially-aligned electrospun nanofibers from PVA reinforced by water-soluble multi-walled carbon nanotubes (MWNTs). In order to get a homogeneous spinning solution, a one-step process using ammonium persulfate (APS) as oxidant was employed to fabricate water-soluble MWNTs, and then they were dispersed in a 10 wt% PVA aqueous solution. We utilized this macroscopically homogeneous dispersion to produce nanofibers mat by electrospinning with an ultra-high-speed rotating cylinder (500 rpm to 3000rpm) as a collector. SEM image shows that the aligned degree increases along with the increase in rotating speed. When the speed is up to 3000 rpm, the electrospun nanofibers are nearly uniaxially aligned. The tensile test results suggest that a small amount of MWNTs dramatically enhanced the tensile strength of PVA fibers. The results of mechanical properties and Raman spectra for the MWNT/PVA nanofibers suggest the relatively good interfacial adhesion of the nanotubes and PVA that improves the load transfer from the polymer matrix to the reinforcing phase. In addition, mechanical properties and thermal behavior of the fiber tow were also investigated.

List of publications

Fan Liu, Tomohiro Nishikawa, Wataru Shimizu, Takaaki Sato, Hisanao Usami, Shigetoshi Amiya, Qing-Qing Ni and Yasushi Murakami, Preparation of fully hydrolyzed polyvinyl alcohol electrospun nanofibers with diameters of sub-200 nm by viscosity control, *Textile Research Journal.* (In pressing)

Fan Liu, Tomohiro Nishikawa, Shigetoshi Amiya, Qing-Qing Ni, Yasushi Murakami, Preparation of Fully Hydrolyzed Ultra-High-Molecular-Weight Polyvinyl Alcohol Nanofibers by Viscosity Control and Improvement of Fiber Hot Water Resistance by Annealing, *Sen'i Gakkaishi* (*Journal of the Society of Fiber Science and Technology, Japan*). 68, (2012)49-54.

Fan Liu, Qing-Qing Ni and Yasushi Murakami, Preparation of Magnetic Polyvinyl alcohol Composite Nanofibers with Homogenously Dispersed Nanoparticles and High Water Resistance. *Textile Research Journal.* (In pressing)

Acknowledgments

It is my pleasure to write this message and express my gratitude to all those who have directly or indirectly contributed to the creation of this thesis. First of all I would like to thank my supervisor Prof. Qing-Qing Ni and vice-supervisor Prof. Yasushi Murakami for giving me the opportunity to study in this group and for always keeping me motivated and supporting me with a lot of useful advice.

I am particularly grateful to Prof. Hisanao Usami, Prof. Yasuo Gotoh and Prof. Jianhui Qiu for accepting to be a co-referee of this thesis and for the discussion and helpful suggestions and comments.

I would like to express my sincere thanks to Global COE of Shinshu University for financial support.

I thank Mr. Mitsuo Ueno, Dr. Li Zhang, Dr. Takaaki Sato, Prof. Hitoshi Fujimatsu, Ms. Miho Nakamura, and Ms. Etsuko Adachi in Shinshu University for sharing their extensive knowledge of experimental equipment and offering their guidance, and valuable insight to my study.

Thanks also go to my group mats (Mr. Wataru Shimizu, Dr. Masami Kobayashi, Ms. Masue Shiraka, Ms. Megumi Kuramochi, Mr. Jyunsuke Hokka, Mr. Yusuke Gozu, Mr. Takahiro Enoki, Mr. Mituyoshi Nakano, Mr. Takuhiro Kumagai, Mr. Tatsuya Ogikubo, Mr. He Ma, Mr. Shunsuke Hattori, Mr. Kazuya Yumoto) of their general advice and input on various things related to research, as well as things not related.

Special thanks to Prof. Wenxing Chen, Prof. Yaqin Fu, Dr. Yuyuan Yao, and Dr. Wangyang Lv at Zhejinang Sci-Tech University (Hangzhou, Zhejiang).

I also want to express my thanks to the oversea students Ms. Xianhua Zhang, Mr. Yi Wang, Mr. Jinxing Shi, Mr. Xudong Jin, Mr. Yaofeng Zhu, Mr. Junfeng Zhang, Mr. Jian Zhou, Mr. Guangyu

Zhang, Ms. Xiaowen Lei, Ms. Yan Wang and Ms. Jiayi Yu, Mr. Zhongwei Lei et al., who gave me many different helps and encourage me to finish this work in my depressed periods.

Finally, I dedicate this work to my family; I am grateful for being able to say that I have a great family that has always set a good example and provide me with unlimited support.